

**AN EXPLORATION OF THE
ELECTROPHYSIOLOGICAL PROPERTIES
AND ION TRANSPORT ACROSS THE ISOLATED
PERFUSED SEMINIFEROUS TUBULE OF THE RAT**



by

David W Fisher

UNIVERSITY *of the*
WESTERN CAPE

Dissertation presented for the degree of
Doctor of Philosophy
Department of Physiological Sciences
Faculty of Natural Sciences
University of the Western Cape

Promoter: Prof. G van der Horst Ph.D., Ph.D.

CONTENTS

<i>Abstract</i>	<i>i</i>
<i>General Introduction</i>	<i>iv</i>
<i>Chapter One: Review: The Seminiferous tubule</i>	<i>1</i>
<i>1.1 Introduction</i>	<i>1</i>
<i>1.2 The Anatomical Aspects</i>	<i>1</i>
<i>1.3 The Inter Tubular Organization of the Testis</i>	<i>3</i>
<i>1.4 Cycle of the Seminiferous Epithelium</i>	<i>6</i>
<i>1.5 The Epithelium of the Seminiferous Tubules</i>	<i>8</i>
<i>1.6 The blood-Testis Barrier</i>	<i>10</i>
<i>1.6.1 Anatomical Location of the Blood-testis Barrier</i>	<i>10</i>
<i>1.6.2 Establishment of the Blood-testis Barrier</i>	<i>12</i>
<i>1.6.3 Role of the Blood-testis Barrier</i>	<i>13</i>
<i>1.6.4 The Initiation of the Blood-Testis Barrier</i>	<i>14</i>
<i>1.7 The Seminiferous Tubular Fluid</i>	<i>16</i>
<i>1.7.1 Introduction</i>	<i>16</i>
<i>1.7.2 The Initiation of Fluid Secretion</i>	<i>16</i>
<i>1.7.3 The Flow of Seminiferous Tubular Fluid</i>	<i>17</i>
<i>1.7.4 The Composition of Seminiferous Tubular Fluid</i>	<i>18</i>
<i>1.7.5 Osmolality and pH of the Seminiferous Tubular fluid</i>	<i>19</i>
<i>1.7.6 Androgen Transport into Seminiferous Tubules</i>	<i>20</i>
<i>1.7.7 The Amino Acids of the Seminiferous Tubular Fluid</i>	<i>21</i>
<i>1.7.8 Endocrine Effects on Fluid Secretion</i>	<i>21</i>
<i>1.7.9 Temperature and Fluid Secretion</i>	<i>22</i>

	Contents
1.8 The Effects of Temperature on the Testis	23
1.8.1 Introduction	23
1.8.2 The Effect of Temperature on Some Substances Entering the Tubule	23
1.8.3 Cryptorchidism	24
1.8.4 Cell types Damaged by Heat	24
1.8.5 Effect of Heat on Androgen Production	25
1.8.6 Temperature Conclusion	25
1.9 Electrophysiology of the Seminiferous Tubule	26
1.9.1 Introduction	26
1.9.2 General background	27
1.9.3 Electrophysiological Effects of FSH	28
1.9.4 Ouabain	31
1.9.5 Dinitrophenol and Glucose Deprivation	31
1.9.6 High Potassium Concentration	32
1.10 Conclusion	33
1.11 The aims of the study	34
Chapter 2: METHODS AND MATERIALS	36
2.1 Animals Treatment	36
2.2 Dissection and Transfer of Tubules	36
2.3 Aeration and Temperature Regulation During Perfusion	37
2.4 The Perfusate Reservoir	38
2.5 Perfusion Apparatus	38
2.6 The Agar Probe	39
2.7 the Oil-gap Technique	40
2.8 the Electrical Measurements During Perfusion	42
2.9 Cable Analysis	44
2.10 Composition of Solutions	46
2.11 Statistical Analysis	47

CHAPTER 3:	<i>Effects of experimental techniques on the morphology of rat seminiferous tubules</i>	49
3.1	<i>Introduction</i>	49
3.2	<i>Materials And Methods</i>	52
	<i>3.2.1 The Experimental Design</i>	52
	<i>Perfused tubules</i>	52
	<i>'Non perfused' tubules</i>	53
	<i>3.2.2 Transfer Procedures</i>	54
	<i>3.2.3 Processing Protocol for Perfused Seminiferous Tubules</i>	54
3.3	<i>Results</i>	57
	<i>3.3.1 Effects of Perfusate Height on Perfusion Rates</i>	57
	<i>3.3.2. Effects Perfusate Flow on the Morphology of the Germinal Epithelium</i>	59
	<i>3.3.2.1 Controls</i>	59
	<i>3.3.2.2 Effects of High Perfusate Flow Rates on Tubular Morphology</i>	60
	<i>3.3.2.3 Effects of Low Perfusate Flow Rates on Tubular Morphology</i>	62
	<i>3.3.2.4 Effects of Oil-gap Technique on Tubular Morphology</i>	63
	<i>3.3.2.5 Effects of the Agar Probe on Tubular Morphology</i>	64
	<i>3.3.2.6 Effects of Micro Perfusion Pipette on Tubular Morphology</i>	64
3.4	<i>Discussion</i>	65
	<i>3.4.1 Perfusing Technique and Morphology</i>	67
	<i>3.4.1.1 The Relationship Between the Perfusate Height and Perfusate Rate</i>	67
	<i>3.4.1.2 Effects of Perfusate Rates</i>	68
	<i>3.4.2 Alternative Methods</i>	70
	<i>3.4.2.1 The Agar Probe</i>	70
	<i>3.4.2.2 The Micro Perfusion Pipette</i>	70

3.4.2.3 <i>The Oil-gap Method</i>	72
3.5 <i>Summary and Conclusion: The best method?</i>	72
CHAPTER 4: Electrophysiological Results	75
4.1 <i>Introduction</i>	75
4.2 <i>Transepithelial potentials:</i>	
<i>A comparison of techniques in morphology study</i>	75
4.3 <i>Equilibration Time</i>	77
4.4 <i>Effects of bath temperature on V_t</i>	79
4.5 <i>Oil-gap experiments</i>	83
4.5.1 <i>Effects of High potassium Ringers</i>	83
4.5.2 <i>Effects of Low Chloride Ringers</i>	84
4.5.3 <i>Effects of Furosemide and Bumetanide</i>	86
4.5.4 <i>Effects of $BaCl_2$</i>	88
4.6 <i>Agar-probe Experiments</i>	89
4.6.1 <i>Effects of Low Chloride Ringers</i>	89
4.6.2 <i>Effects of Furosemide</i>	91
4.6.3 <i>Effects of $BaCl_2$</i>	92
4.6.4 <i>Effects of DNP</i>	92
4.7 <i>Perfusion Experiments</i>	94
4.7.1 <i>Introduction</i>	94
4.7.2 <i>Control cable parameters</i>	95
4.7.3 <i>Induced Changes In V_o and Cable Parameters</i>	97
4.7.3.1 <i>Effects of High potassium Ringers</i>	97
4.7.3.2 <i>Effects of $BaCl_2$</i>	97
4.7.3.3 <i>Effects of Low Chloride Concentration</i>	101
4.7.3.4 <i>Effects of Furosemide</i>	103
4.7.3.5 <i>Effects of 2',4'-DNP</i>	105
4.8 <i>Conclusion</i>	107

	Contents
CHAPTER 5: Discussion	108
5.1 Introduction	108
5.2 The equivalent electrical circuit	108
5.3 Perfusion rates, Morphology and Transtubular Potentials	112
5.4 The Equilibration Time	114
5.5 Effects of Bath Temperature on V_t	115
5.6 Oil-gap experiments	116
5.6.1 The Effect of Increased Bath Potassium	118
5.6.2 Effects of $BaCl_2$	119
5.6.3 Effects of Low Chloride Ringers	120
5.6.4 The Effects of Furosemide and Bumetanide	120
5.7 Agar-probe Experiments	121
5.7.1 Effects of Low Chloride Ringers	122
5.7.2 Effects of Furosemide on V_t	122
5.7.3 Effects of $BaCl_2$ on V_t	123
5.7.4 Effects of DNP on V_t	123
5.8 Electrophysiology of Isolated Perfused Seminiferous Tubules	124
5.8.1 Validation of Cable Analysis	124
5.8.2 Controls	126
5.8.3 The Effects of High Potassium Ringers	129
5.8.4 The Effects of $BaCl_2$	131
5.8.5 The Effects of Low Chloride Concentration	132
5.8.6 Effects of Furosemide	133
5.8.7 Effects of 2',4'-DNP	133
5.9 General Conclusion	134
References	137
Appendix A	158
Appendix B	159

Abstract

AN EXPLORATION OF THE ELECTROPHYSIOLOGICAL PROPERTIES AND ION TRANSPORT ACROSS THE ISOLATED PERFUSED SEMINIFEROUS TUBULE OF THE RAT

A knowledge of the transport of ions is fundamental to the understanding of the 'blood-testis' barrier and the transport of fluid across the seminiferous tubule. This is the first study which has investigated the isolated perfused seminiferous tubule of the rat to measure the transepithelial potential (V_t) according to the technique of Burg, *et. al.* (1966). It has simultaneously used cable analysis to determine the transepithelial resistance. In an attempt to find additional confirmation of the V_t measured via the perfusion technique, a further two techniques, the 'oil-gap' technique (O'Donnell and Maddrell, 1984) as well as with the 'agar probe' technique developed during the current study, were used to record V_t .

Initially, after performing experiments using the above mentioned techniques, the tubules were studied morphologically to establish whether or not damage had occurred to the germinal epithelium. The study established that only low perfusion rates prevented damage to the germinal epithelium. High perfusion rates resulted in the germinal epithelium breaking down and subsequently the resultant cellular debris and spermatids

Abstract

were washed out of the tubule. The surrounding myoid layer appeared intact irrespective of the perfusion rates. The morphology of tubules exposed to the 'oil-gap' and 'agar probe' techniques did not differ from the control study.

The current study endorsed the prevalent view that seminiferous tubules had a transepithelial potential (V_t) of 4-6 mV, the lumen being negative relative to the bathing medium. The transepithelial resistance (R_t) was found to be 4.4 ± 0.87 kOhm.cm (specific transepithelial resistance: 53.97 ± 10.7 ohm.cm²). The average virtual short-circuit current (SCCv) for the epithelium of the seminiferous tubule was -1.69 ± 10.1 μ Amps/cm.

Increasing the external concentration of K^+ 10 fold produced no statistically significant changes in the V_t , but simultaneously decreased the R_t ($P < 0.00001$). The introduction of the K^+ channel blocker, barium, to the bathing medium also failed to produce significant changes to V_t , but increased R_t slightly ($P < 0.0001$) while simultaneously decreasing the SCCv. The results seem to suggest that the serosal membrane of the seminiferous tubule may be permeable to barium. Barium appears to subsequently effect the apical membranes by possibly blocking K^+ channels, resulting in the increased R_t and decreased SCCv.

The study endorsed the view that chloride was co-transported with cations across the seminiferous epithelium. Decreasing the external chloride concentration from 111 mM to 2 mM resulted in the V_t decreasing ($P < 0.00001$), while R_t increased ($P < 0.00001$). The increased R_t is indicative of a decrease in the transepithelial conductance (G_t), a

Abstract

response which was supported by the decrease in SCC_v ($P < 0.00001$). These results were further supported by the effects of furosemide and bumetanide (inhibitors of Na-Cl co-transport) both of which resulted in V_t responses which mimicked the V_t response brought about by decreasing the external chloride concentration.

Treatment of the seminiferous tubules with the metabolic inhibitor, 2',4'-Dinitrophenol (DNP) resulted in the V_t decreasing to close to zero. However, this failed to effect any of the cable parameters with the exception of the input resistance which decreased significantly ($P < 0.0002$). This supports the reports in the literature that DNP decreased the intracellular potential by 16 mV (Cuthbert and Wong, 1975) and abolished fluid secretion in isolated seminiferous tubules (Cheung, *et. al.*, 1976).

The current study provides a useful tool for future investigations involving transepithelial ionic transport and in addition has ascertained valuable electrophysiological properties for the seminiferous tubule of the rat.

General Introduction

The **seminiferous tubules** found in the testis houses the germinal epithelium from which spermatozoa are produced. It is generally accepted that the epithelium of the seminiferous tubule with its surrounding myoid layer forms the basis of the 'blood-testis' barrier and secretes a unique luminal fluid which is essential for the process of spermatogenesis. Although much research has been carried out on the seminiferous tubules, little is known of the mechanisms that govern the transepithelial transport in the three dimensional tubule. Thus far the only studies which shed some light on transepithelial transport involved the movement of radio-active ions and molecules into isolated tubules and across monolayers of culture cells.

The first part of the study determines the feasibility in **isolating** and **perfusing** the seminiferous tubule according to the established perfusion technique in renal research (Burg, *et. al.*, 1966). The study was extended by investigating the **transepithelial potentials** of seminiferous tubule using two addition techniques, viz., the '**oil-gap**' technique (O'Donnell and Maddrell, 1984), used primarily to investigate transepithelial potentials in Malpighian tubules, and the '**agar probe**' technique designed during the course of this study. In addition, all tubules used during this part of the study were subsequently subjected to morphological scrutiny to ensure that the germinal epithelium was not damaged.

In order to understand more precisely the cellular mechanisms of ion transport in the

General Introduction

transepithelial potentials and resistances. In the past only transepithelial potentials in seminiferous tubules have been measured using microelectrode techniques. Furthermore, although the 'oil-gap' technique is prone to errors (see chapter 5), it has been used in this study to measure transepithelial potentials as an additional affirmation to the potentials recorded in the other techniques used in the current study. The agar probe technique and the perfusion techniques employed in this study avoid these errors. However, the agar probe technique is at a disadvantage to the perfusion technique in not being able to measure transepithelial potentials simultaneously with transepithelial resistances.

This valuable perfusion technique was employed for the first time in the current study to investigate mechanisms of ion transport on the isolated seminiferous tubule and therefore comparative information in the literature is non-existent. Isolated perfusion has the added benefit of facilitating the use of **cable analysis** to measure the resistances across the transepithelial membrane of the seminiferous tubule. In addition, it was convenient to use the afore mentioned electrophysiological data to model the transport of ions across the seminiferous tubule with the aid of a simple equivalent electrical circuit.

As the understanding of germinal epithelium is central to appreciating the processes involved in the regulation of transepithelial transport mechanisms, this dissertation begins with chapter 1 reviewing the literature on the seminiferous tubule of the rat, presenting a background to the subject and establishing what electrophysiological data has hitherto been reported. Chapter 2 thereafter reports in detail on the techniques and methods employed to obtain the data experimentally. Chapter 3 reports on the methods and results

General Introduction

employed to obtain the data experimentally. Chapter 3 reports on the methods and results of the morphological study carried out after the tubules were exposed the different techniques. These morphological data are also discussed at length in this chapter. Chapter 4 records all the statistically manipulated electrophysiological data, while in chapter 5 this data is discussed. This is followed by a listing of all the references used in the current dissertation and appendix A and B.



CHAPTER 1

Review: The Seminiferous tubule

1.1 Introduction

The testis is central to the male reproductive system. It is the organ in which haploid germ cells (i.e. cells with half the number of chromosomes) are formed by a process called spermatogenesis and it is the site of androgen (eg. testosterone) production. The purpose of this review is to present a brief overview on the testis, the current views and research on the germinal epithelium as a physiologically functional barrier, i.e. the “blood-testis” barrier. This review will emphasize the electrophysiological properties of the seminiferous tubules and cell cultured epithelium, but an in depth discussion of spermatogenesis will not be given here. Specific attention will be devoted to the rat ‘blood-testis’ barrier.

1.2 The Anatomical Aspects

Spermatogenesis takes place in the convoluted seminiferous tubules which houses the germinal epithelium. In the rat there are approximately 12 metres of tubules per gram of testis, with a surface area of approximately 120 cm²/g (Wing and Christensen, 1982). The number of tubules per testis varies from one species to the next. Rats have about 30 tubules per testis, with each tubule about 1 metre long (Clermont and Huckins, 1961),

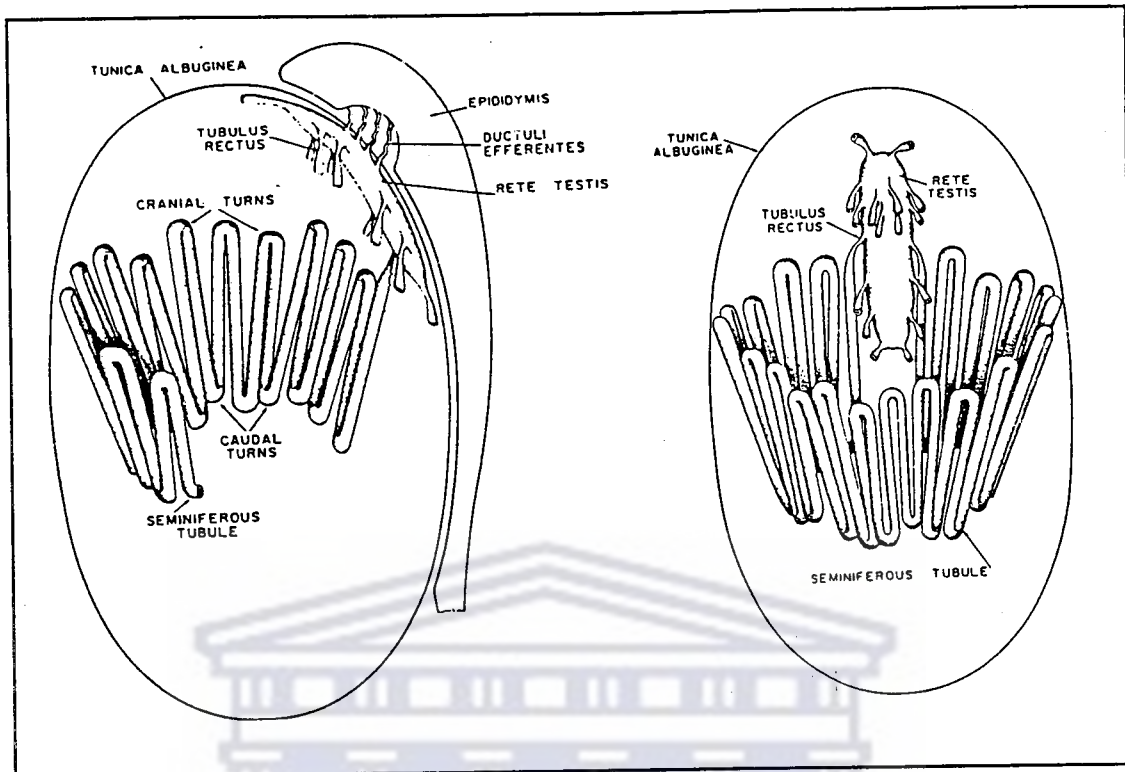


Figure 1.1: A diagram of the anatomy of an individual seminiferous tubule and the rete testis of the rat. Left: Only one part of the tubule is shown, and only some of the junctions of the seminiferous tubules with the rete testis are depicted (taken from Clermont and Huckins, 1961).

but there may be as few as 5 tubules in some of the dasyurid marsupials (Woolley, 1975). In humans one to four tubules is found in each of the approximate 300 lobules (Setchell and Brooks, 1988). In mature rats the average lumen diameter is 50 μm . However, this value almost doubles in areas where the spermatozoa are about to be released (Wing and Christensen, 1982). Eusebi and colleagues (1983) found that the lumen diameter of the isolated rat seminiferous tubule to range between 36 and 45 μm . The variability in lumen size has been shown to be a function of the particular stage in the spermatogenic cycle (see section 1.4) (Wing and Christensen, 1982). In the testis, these tubules (see figure 1.1) are usually a two ended loop, opening at both ends via short tubuli (tubuli recti) into the rete testis. Spermatozoa subsequently pass by way of the efferent ducts into the epididymis. The seminiferous tubules are not penetrated by blood, lymph vessels or

nerves. These are confined to the spaces between the closely packed seminiferous tubules together with small hormone (androgens) producing groups of cells, the Leydig cells (Setchell and Brooks, 1988). The seminiferous tubules and interstitial tissue are in turn encased in a spherical, tough fibrous capsule known as the tunica albuginea.

1.3 The Inter Tubular Organization of the Testis

The interstitial tissue is a loose connective tissue containing blood, lymph vessels, mast cells and macrophages and islands of peritubular endocrine cells which secrete testosterone, called Leydig cells. In rodents the interstitial tissue is very sparse with large lymphatic sinusoids and the Leydig cells are clustered around the blood capillaries

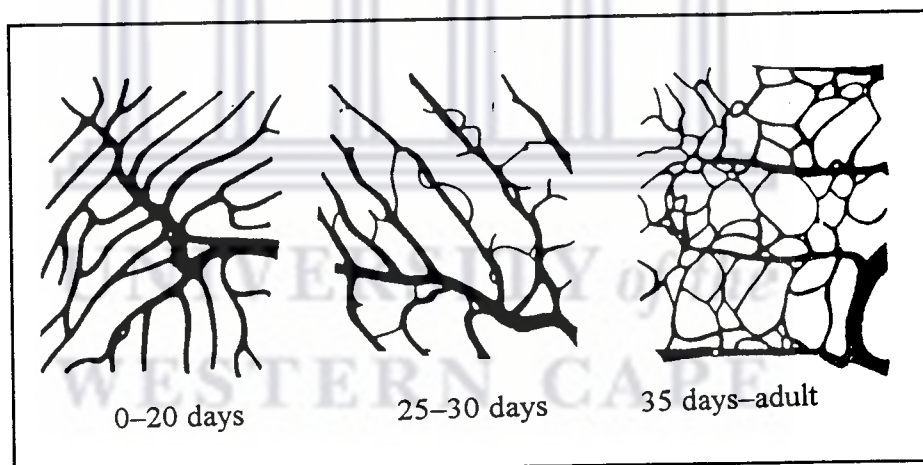


Figure 1.2: The vascular anatomy around the seminiferous tubules of rats of different ages as seen from the surface of the testis. Note how the capillaries lying at right angles to the tubules are not present in the young rats but develop only at puberty. (Reproduced from Kormano, 1967).

(Setchell, 1978). The capillaries of the testis seem to be orientated either parallel to the tubules and larger vessels in the interstitial spaces (Zwickelcapillaren) or at right angles to the tubules (Quercapillaren) (see figure 1.2) (Setchell, 1978). This capillary

Chapter 1: Review: The Seminiferous Tubule

organization only develops at puberty and its significance is not known. This capillary arrangement might have the effect of carrying testosterone from the Leydig cells first round the seminiferous tubules and then to the systemic circulation (Setchell and Waites, 1975).

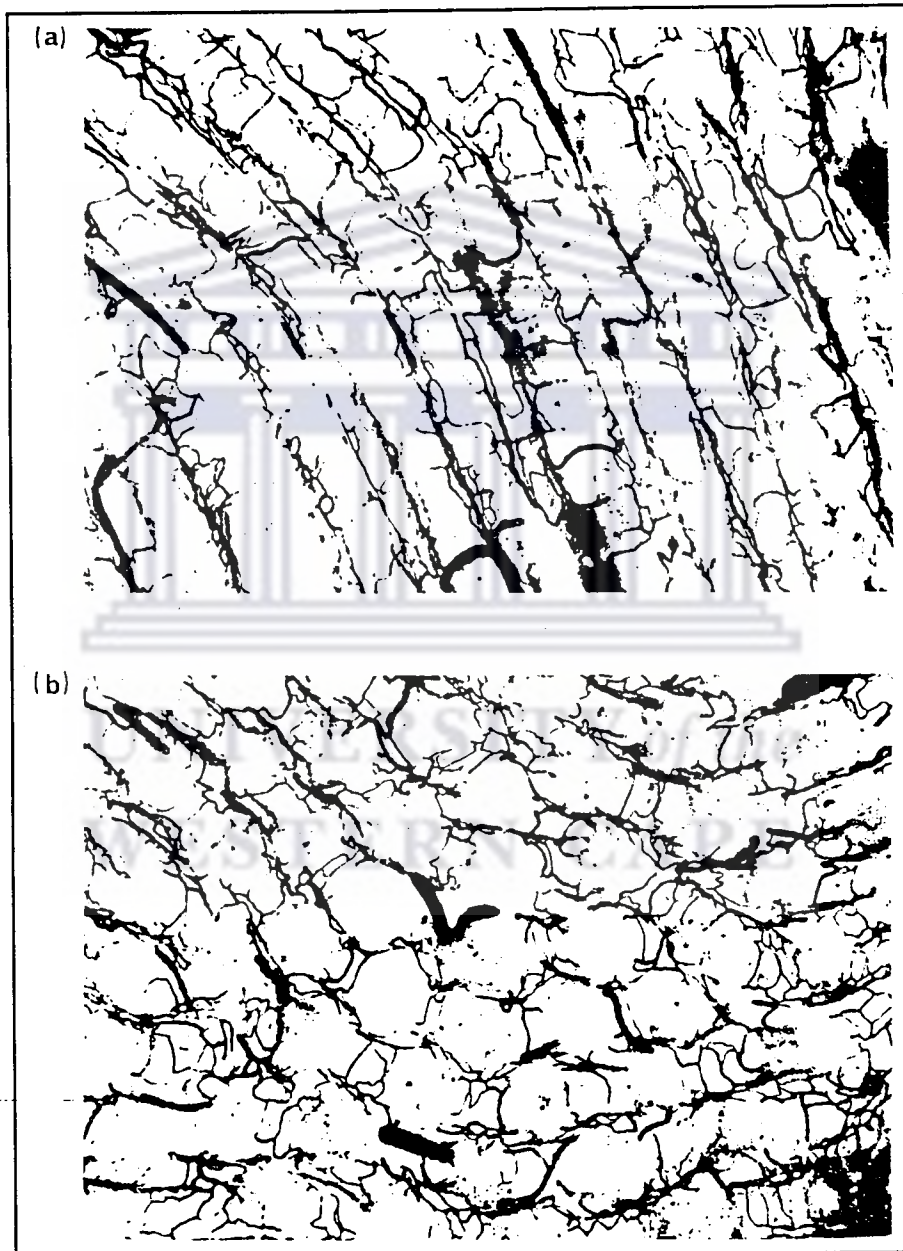


Figure 1.3: Photographs of thick sections (300 μm) of a rat testis, (a) cut approximately parallel with the seminiferous tubules, and (b) cut at approximately right angles to the tubules. Note that some capillaries lie parallel to the tubules in the interstitial spaces, while others run around the walls at right angles to the length of the tubule (Taken from Setchell, 1978).

Chapter 1: Review: The Seminiferous Tubule

The capillaries and other blood vessels, lymph vessels and nerves of the testis never enter the seminiferous tubules but are confined to the interstitial spaces in between the seminiferous tubules (see figure 1.3). Thus, for a substance to pass from the bloodstream into the lumen of the tubules, it must cross the capillary wall, and then either penetrate the wall of the tubules or enter the rete testis and approach the tubular cells from their luminal surfaces (Setchell and Waites, 1975). The capillary wall is, therefore, the first

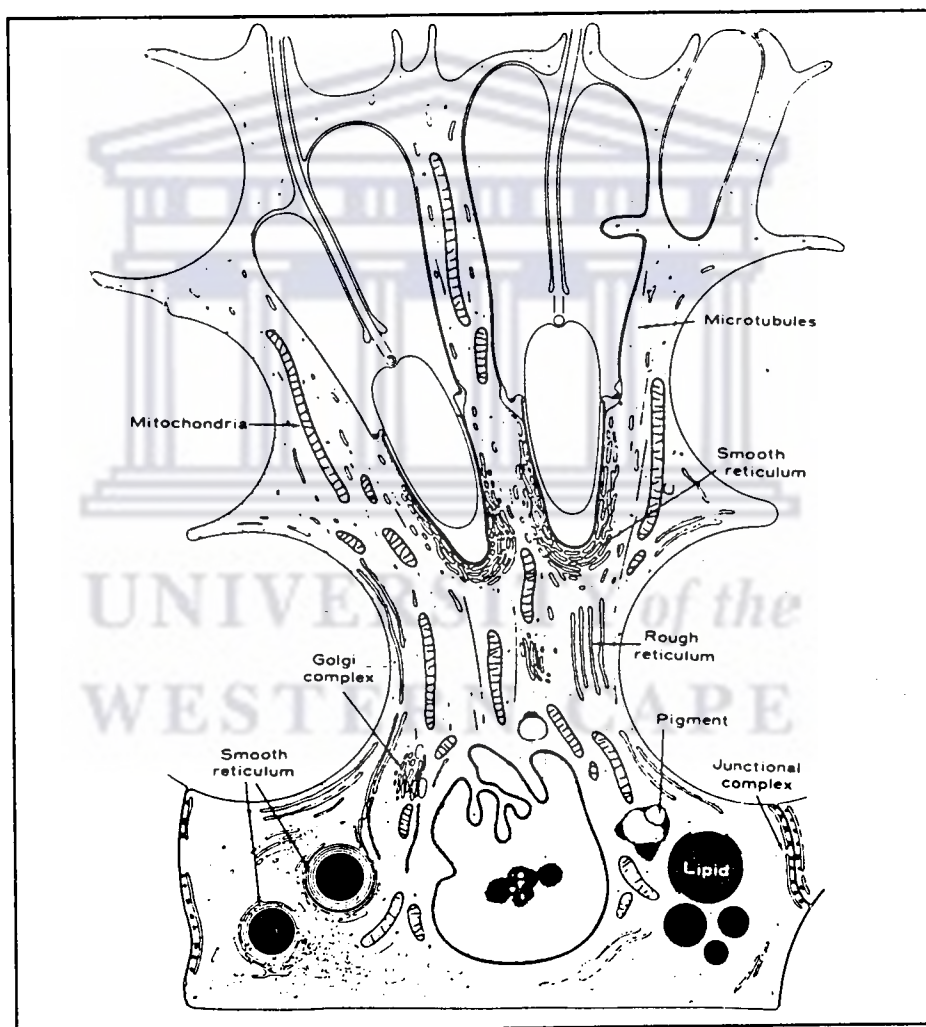


Figure 1.4: Diagram showing some details of the structure of a Sertoli cell. Note the lobulated nucleus with its prominent nucleolus, the junctional complexes between this cell and adjacent Sertoli cells, and the prominent smooth endoplasmic reticulum associated principally with lipid droplets and the acrosome region of the later spermatids (taken from Fawcett, 1975).

barrier which substances must cross in order to leave the bloodstream.

Recent studies on the brain-blood barrier have shown that the tight junctions between the capillary endothelial cells are key cellular components of this barrier. This is not the case in the testis. Electron microscopic examination of these vessels offers no evidence of extensive tight junctions that would retard or prevent the escape of large molecules from the blood stream (Fawcett, *et. al.*, 1970). Furthermore, permeability studies provided abundant evidence of a high degree of permeability of the interstitial capillaries and venules (Lindner, 1963).

In eutherian mammals, the testicular arterioles and capillaries with scrotal testes have an elongated coiling artery which is surrounded by multiple veins of the pampiniform plexus (Setchell, 1978). This arrangement of the blood vessels plays an important role in the temperature regulation of the testes (see section 1.7).

1.4 Cycle of the Seminiferous Epithelium

Spermatogenesis has been divided into cellular associations (groups), called 'stages' in the cycle of the seminiferous epithelium. It is customary to designate the stages by a Roman numeral (e.g., Stage VII)(Leblond and Clermont, 1952). Each stage consists of the associated seminiferous epithelial cells that are found at a particular point in time during the overall process of spermatogenesis. In the rat, histologic sections of the testis reveal that cross-sections of the seminiferous tubules contain a uniform epithelium consisting of only one of the fourteen stages of the cycle. The stages are repeated in consecutive order along the length of the seminiferous tubules, which forms the "wave

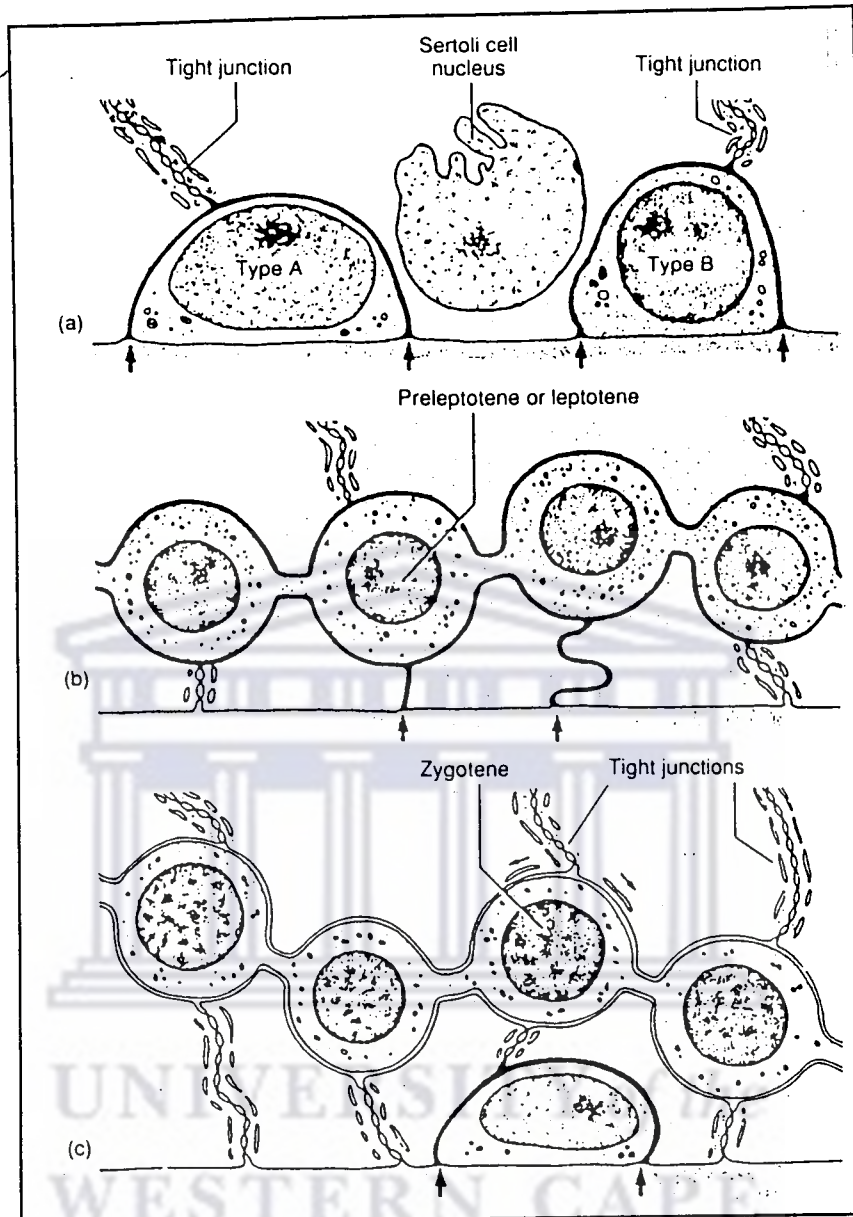


Figure 1.5: The upward migration of germ cells from the basal aspect of the seminiferous epithelium towards the lumen. In each diagram, tracer entry into the intercellular spaces is shown by large arrows. (a) Entry of tracers into the seminiferous epithelium is prevented by the occluding inter-Sertoli tight junctions. (b) Preleptotene and leptotene primary spermatogonia are displaced above the basal lamina. Tight junctions are seen below, above, or both below and above these forms of cells, and consequently tracers are able to surround the interconnected cells via cytoplasmic bridges. Tight junctions above the germ cells prevent further passage of tracers into the seminiferous epithelium. (c) When leptotene primary spermatocytes enter the zygotene phase of meiotic prophase, tracers do not surround zygotene spermatocytes, because tight junctions are formed beneath these cells. Dissociation of inter-Sertoli cell junctions into hemijunctions has been suggested and is indicated by small arrows. Taken from Kretser and Kerr, 1988.

of spermatogenesis." It is clear from the literature that many of the activities and responses of segments of seminiferous tubules are dependent on the particular stage.

1.5 The Epithelium of the Seminiferous Tubule

The seminiferous tubules of most species are made up of two main cellular layers separated by the acellular basement membrane. The inner cellular layer, which lines the lumen of the seminiferous tubule, forms the germinal epithelium and consists of two types of cells: the germ cells and the Sertoli cells. Inside the tubules the only cells abutting on the basement membrane are spermatogonia and Sertoli cells. All other germinal cells, spermatocytes, spermatids, and developing spermatozoa are sandwiched between pairs of Sertoli cells or embedded in their luminal surfaces (Setchell and Waites, 1975). Pairs of Sertoli cells are joined above the spermatogonia but below the spermatocytes by specialised junctions (see figure 1.4). These junctions divide the intercellular spaces into a "basal" compartment and an "adluminal" compartment (Dym and Fawcett, 1970). These junctions form a major component of the blood-testis barrier. (see figure 1.5).

Surrounding the seminiferous tubules is a lamina propria, which is made up of the basement membrane of the germinal epithelium, the layer of myoid cells which are simple squamous in shape and the outer glycoprotein coating (Dym and Fawcett, 1970; Davidoff, *et. al.*, 1990). These peritubular, contractile myoid cells are closely attached to each other in a polygonal manner and contain large quantities of bundled actin filaments. These bundles of actin filaments are arranged at right angles to each other in the myoid cell and in relation to the longitudinal axis of the tubule, suggesting that

Chapter 1: Review: The Seminiferous Tubule

contraction may occur in different directions (Clermont, 1958, Maekawa, *et. al.*, 1994). Isolated tubules from rats more than 15 days old contract spontaneously *in vitro* (Kormano and Hovatta, 1972) and respond to oxytocin (Niemi and Kormano, 1965). This contractility persists for approximately 3 weeks in cultured fragments from adult rats (Kormano and Hovatta, 1972). The response of the tubules to oxytocin was also stage-dependent, with the peptide producing the largest increases in contractile activity at stages VII-VIII and having no effect at stages IV-V (Harris and Nicholson, 1998). Myoid cells have been grown in culture and under these conditions secrete a number of proteoglycans and extracellular matrix. This is especially pronounced when grown in coculture with Sertoli cells (Skinner and Fritz, 1985).

The myoid cells are generally hexagonally organised into a flattened tube (Vogl and Soucy, 1985) that forms a continuous layer around the seminiferous tubule. Myoid cells are held together at their boundaries by junctions. Dym and Fawcett (1970) showed that lanthanum (used as an electron opaque marker) introduced intravascularly moved freely into the interstitial tissue but was largely prevented from reaching the germinal epithelium by intercellular tight junctions between the myoid cells. Where lanthanum gained access to the base of the germinal epithelium it permeated the intercellular space between the spermatogonia and the surrounding Sertoli cells before being stopped by focal tight junctions on the Sertoli-Sertoli cell interface. Thus, in rodents, the myoid layer also forms the primary barrier to substances wanting to penetrate the seminiferous tubules, while the long narrow bands of tight junctions that collectively form a continuous barrier above the spermatogonia and between Sertoli cells constitutes a secondary barrier to the passage of materials into the testicular fluid. In the rat the intact lamina propria is of paramount importance for the maintenance of spermatogenesis as it not only forms part of the

blood-testis barrier, but is the origin of many paracrine factors impacting the maturation of sperm (Raychoudhury, *et. al.*, 1993).

In primates, the situation is different. In human beings and monkeys, the myoid cells do not form tight junctions with each other and therefore in the latter species offer little or no resistance to the entry of electron opaque markers. The Sertoli-Sertoli cell junctions in this species act as the only barrier to penetration but it appears to be just as effective as the dual barrier in rodents. Similar results have been reported in the fowl (Setchell and Waites, 1975).

1.6 The Blood-Testis Barrier

1.6.1 Anatomical Location of the Blood-testis Barrier

In the rodent, the blood-testis barrier resides partially in the peritubular contractile layer of myoid cells of the seminiferous tubules (Dym and Fawcett, 1970). In all other species it resides more specifically in the junctional complexes between the Sertoli cells (Nicander, 1967; Dym and Fawcett, 1970; de Kretser and Kerr, 1988). Tight, gap and adhering junctions have been shown between Sertoli cells and germ cells (see figure 1.6) (Pelletier and Byers, 1992). These complexes are found in the basal portion of the Sertoli cell and they divide the seminiferous epithelium of the mammals into two compartments, a basal compartment and an adluminal compartment (Fawcett, 1975).

It should be clear from the above discussion that the term “blood-testis” barrier is really a misnomer. It should, more precisely, be called a “blood-seminiferous tubule” barrier

as the Leydig cells and in many species the peritubular myoid cells do not form part of this barrier. However, for the sake of continuity, the term “blood-testis” barrier will be used in this review.

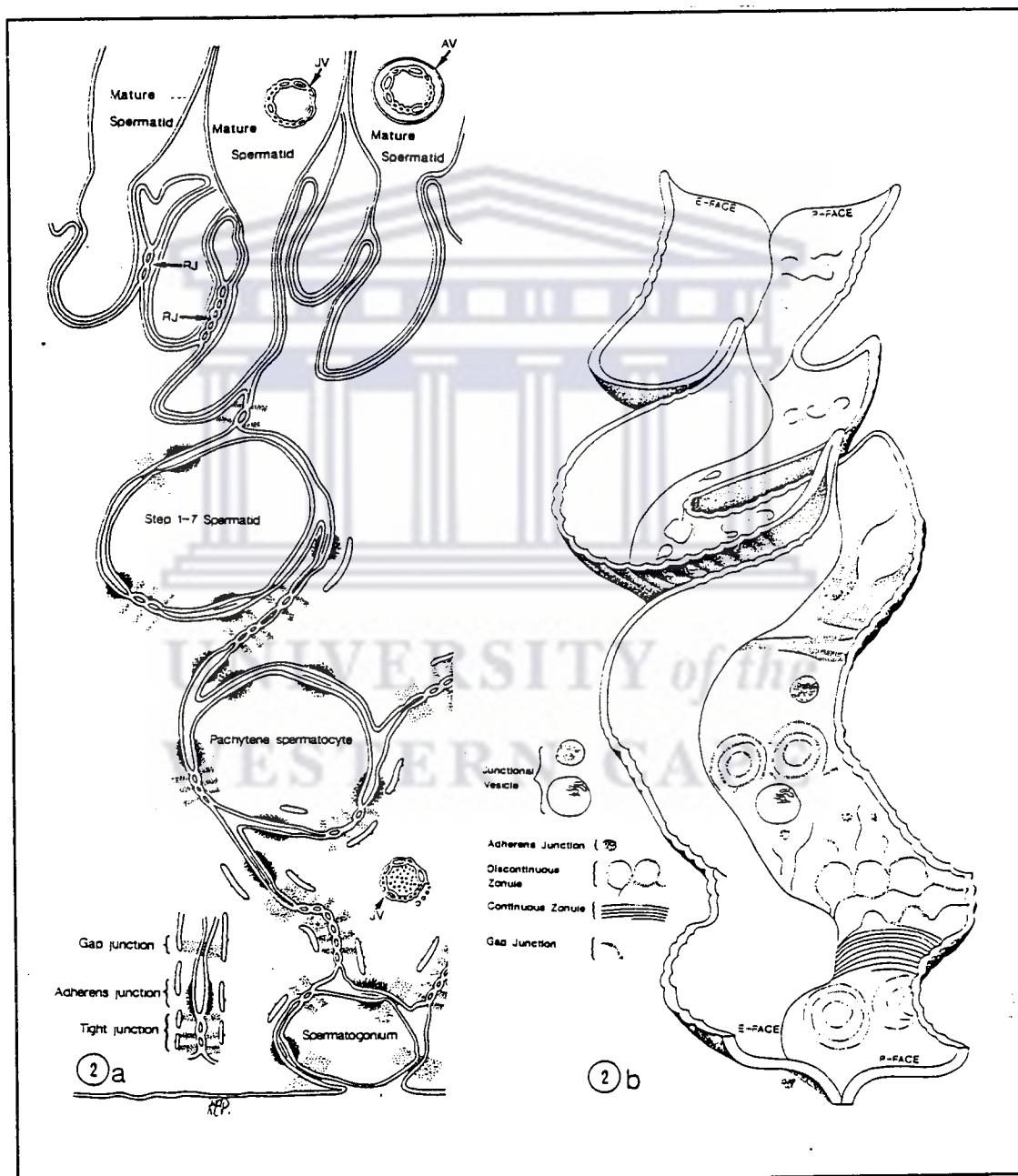


Figure 1.6: Diagrams illustrating the distribution of various types of Sertoli-Sertoli cell junctions and Sertoli-germ cell junctions. a: JV, junctional vesicles; AV, autophagic vesicle containing a junctional vesicle. b: Freeze-fracture replicas of 2 adjacent Sertoli cells. (Taken from Pelletier and Byers, 1992).

Chapter 1: Review: The Seminiferous Tubule

The concept of a blood-testis barrier emerged from observation of acridine dyes and other substances being injected intravascularly and from being excluded from the seminiferous tubules (de Bruyn, *et. al.*, 1950; Kormano, 1967, 1968; Setchell and Waites, 1975; Waites and Gladwell, 1982 and de Kretser and Kerr, 1988). Waites and Setchell (1969) have demonstrated that when substances of varying molecular size are introduced into the bloodstream, they appear rapidly in the testicular lymph but not in the fluid of the cannulated testis.

Substances from the extratubular compartment which use the route of intercellular spaces have direct access to the basal portion of Sertoli cells, to spermatogonia and to early prophase spermatocytes (see figure 1.5). The inter-Sertoli cells specialized junctions prevent direct access to other layers of the seminiferous epithelium. Once the inter-Sertoli cells tight junctions are formed, they are resistant to perfusion of hyperosmotic solutions which dissociate junctions in other epithelia (Gilula, *et. al.*, 1976) and to other deleterious substances (Fawcett, 1975; Waites and Gladwell, 1982). It must be emphasized, as was shown by germ cell-depleted busulfan-treated rats, that barrier competence does not depend on the number of inter-Sertoli cell tight junctions but rather on the special arrangement of these as a belt parallel to the basal membrane (Cavicchia and Sacherdote, 1991).

1.6.2 Establishment of the Blood-testis Barrier

According to Vitale, *et. al.* (1973) who used the exclusion of lanthanum and peroxidase as a permeability test, the blood-testis barrier is established between 16 - 19 days in the rat. Sun and Gondos (1986) demonstrated that the blood-testis barrier in the rabbit is

functional between the 9th and 10th postnatal week. In both species the appearance of the barrier is associated with the first division of meiosis. In the case of the rat the establishment of an efficient barrier takes place simultaneously with the appearance of zygotene-pachytene spermatocytes and seems to be dependent on those, rather than directly on the age of the animal (Cavicchia and Sacherdote, 1991). The functional barrier to water soluble markers is established later and more progressively than the barrier to electron-opaque markers (Setchell, *et. al.*, 1988). This may indicate that functions of the blood-testis barrier come sequentially into operation during the development of the spermatogenic process.

1.6.3 Role of the Blood-testis Barrier

Several major roles have been assigned to the blood-testis barrier: promotion of cohesion and cytoarchitecture of the epithelium; the constitution of a physiochemical microenvironment required for the completion of the meiotic process; spermiogenesis, and the prevention of contact between surface antigens specific to late prophase primary spermatocytes and spermatids; and the immune system (Fawcett, 1975; Waites and Gladwell, 1982; de Kretser and Kerr, 1988).

In all mammalian species studied thus far, as well as birds, reptiles, fish, amphibians, insects and nematodes, it has been demonstrated that a morphological blood-testis barrier isolates the testicular compartment where meiosis and spermiogenesis occur (Szollosi and Marcaillou, 1977; Bergmann, *et. al.*, 1984; de Kretser and Kerr, 1988; Jégou, 1992). This suggests that the blood-testis barrier is crucial for the normal progression of spermatogenesis.

Chapter 1: Review: The Seminiferous Tubule

Another role for the barrier is to ensure that the body's immunological system does not recognize the haploid germ cells as self, as an animal can be immunized against its own spermatozoa (Setchell, 1979).

The barrier also regulates the movement of substances of endocrinological importance both into and out of the seminiferous tubules. FSH is prevented from entering the lumen of the seminiferous tubule. The barrier is responsible for the hundred fold higher concentration of inhibin in the rete testis fluid of sheep than in the testicular lymph (Setchell, 1979). Also, as the inter-Sertoli junctions are formed at puberty in the rat, there is a decreased concentration of androgen-binding protein in the serum of rats from 18 to 60 days (Gunsalus, *et. al.*, 1978).

Lastly, the barrier probably plays an important role in the exclusion of potentially toxic substances from entering the seminiferous fluid.

1.6.4 The Initiation of the Blood-Testis Barrier

One is tempted to speculate whether the organisation of the barrier is as a result of some signal from zygotene-pachytene spermatocytes to the Sertoli cells to start the rearrangement of competent inter-Sertoli tight junctions. This view is supported by studies on busulfan treated rats (Camatini, *et. al.*, 1980, 1981). These studies indicate that in the case of germ cell aplasia the blood-testis barrier is not preserved. Also, pachytene cells, co-cultured with Sertoli cells, liberate peptides into the medium promoting protein synthesis in Sertoli cells (Djakiew and Dym, 1988). This supports the view that the developing germ cells play a role in the initiation of the blood-testis barrier.

However, it seems pertinent to mention that many studies show that Sertoli cells in culture (*in vitro*) and in the absence of germ cells are able to assemble competent junction devices (Hadley, *et al.*, 1985; Byers, *et al.*, 1986; Djakiew, *et al.*, 1986; Dym, *et al.*, 1988; Cavicchia and Sacerdote, 1991).

Furthermore, seminiferous tubules exposed to x-irradiation before birth were shown to be devoid of germ cells. It is generally believed that Sertoli-Sertoli junctions are necessary to maintain the K^+ gradient observed in seminiferous tubular fluid (Setchell and Waites, 1975). These tubules produced functional junctions between Sertoli cells before the age of 30 days and were able to produce a tubular fluid having Na^+ and K^+ concentrations of 136.3 and 39.7 mM, respectively (Tindale, *et al.*, 1975; Muffly, *et al.*, 1985). These values were almost identical to the mean concentrations reported by Jenkins and colleagues (1980) of 135.44 and 39.77 mM for Na^+ and K^+ , respectively, in tubular fluid of normal rats. In the rats treated with busulfan during pregnancy, there was a K^+ concentration of 4.6 mM in the seminiferous tubular fluid which did not differ significantly from plasma values (Levine and Marsh, 1975). In their criticism of this study, Muffley, *et al.* (1985), pointed out that the effects of busulfan was not uniform throughout the testis as these tubules still contained numerous germ cells whereas the effects of x-irradiation had a far more uniform effect. Furthermore, it was not known whether busulfan had damaged the Sertoli cells and had disrupted Sertoli-Sertoli cell junctions. In addition, the effects of busulfan on the hormonal regulation of the testis was not known.

1.7 The Seminiferous Tubular Fluid

1.7.1 Introduction

Testicular fluid was first described by de Graaf (1668, English translation by Jocelyn and Setchell, 1972) as ‘the breath of life, joined with more subtle part of the blood in the seminal tubules....’. Since then it has become clear that the Sertoli cells are responsible for the secretion of fluid, proteins, a few peptides and steroids into the lumen of the seminiferous tubules. In fact, the secretion of fluid by the apical surfaces of the Sertoli cells into the centre of the maturing seminiferous tubules is probably responsible for the development of the lumen (Fawcett, 1975). The role of this fluid from this point onwards seems to be essentially two fold: firstly, to provide a specialized microenvironment for the nutrition of the maturing germ cells and released spermatozoa, and secondly, for the transport of the newly released spermatozoa from the seminiferous tubules to the rete testis and subsequently to the *caput epididymidis*.

1.7.2 The Initiation of Fluid Secretion

There is no direct evidence for Sertoli cells forming luminal fluid, but experiments in which germ cells were destroyed following injections of busulphan *in utero* or irradiation to destroy germ cells, seminiferous tubules consisting only of Sertoli cells still continued to produce luminal fluid (Setchell and Brooks, 1988). Paracellular back-flow of fluid is prevented by a barrier of occluding junctions (component of the blood-testis barrier)

between the Sertoli cells (Dym and Fawcett, 1970). The barrier starts to develop around 15 days, approximately the same time the first germ cells are entering the meiotic phase of prophase. At this time the clearest exclusion of electron dense tracer molecules (lanthanum) are found in those parts of the tubule where the germ cells have reached the pachytene stage of meiosis (Bergmann and Dierichs, 1983).

Jégou *et. al.* (1983) established experimentally that fluid secretion begins at 16 to 19 days of age in the rat and the rate of fluid secretion increases until days 70-80, after which it plateaus.

1.7.3 The Flow of Seminiferous Tubular Fluid

Fluid secretion begins just after puberty in the rat, before the first spermatozoa are released, and increases to reach adult rates at approximately 30 days at 15 $\mu\text{l/g}$ of testis (Setchell; 1970). This evidence was reinforced by a separate study which showed that at 10 days of age no lumina had developed in any of the seminiferous tubules. However, by 30 days all of the tubules had developed lumina (Russell, *et. al.*, 1989). It was calculated a single seminiferous tubules secretes between 0.5 and 1 $\mu\text{l}/\text{hour}$ (Setchell, *et. al.*, 1978).

The flow of fluid within the lumina of tubules may be due to fluid pressure that built up as a result of the continuous secretion by Sertoli cells and/or to the contractions of the peritubular myoid cells causing periodic constriction of the seminiferous tubules (Russell,

et. al., 1989). The third contributing factor may be the contraction of the tunica albuginea resulting in intra testicular pressure which could possibly assist in moving fluid and spermatozoa out of the testis (Setchell, 1978).

1.7.4 The Composition of Seminiferous Tubular Fluid

"One of the most compelling pieces of evidence for the existence of a blood-testis barrier is the difference in composition between blood plasma and testicular lymph when compared with the fluid inside the rete testis and seminiferous tubules" (Setchell and Waites, 1975). Fluid from individual seminiferous tubules has been collected using micropuncture and various catherization techniques (Henning and Young, 1971; Setchell,

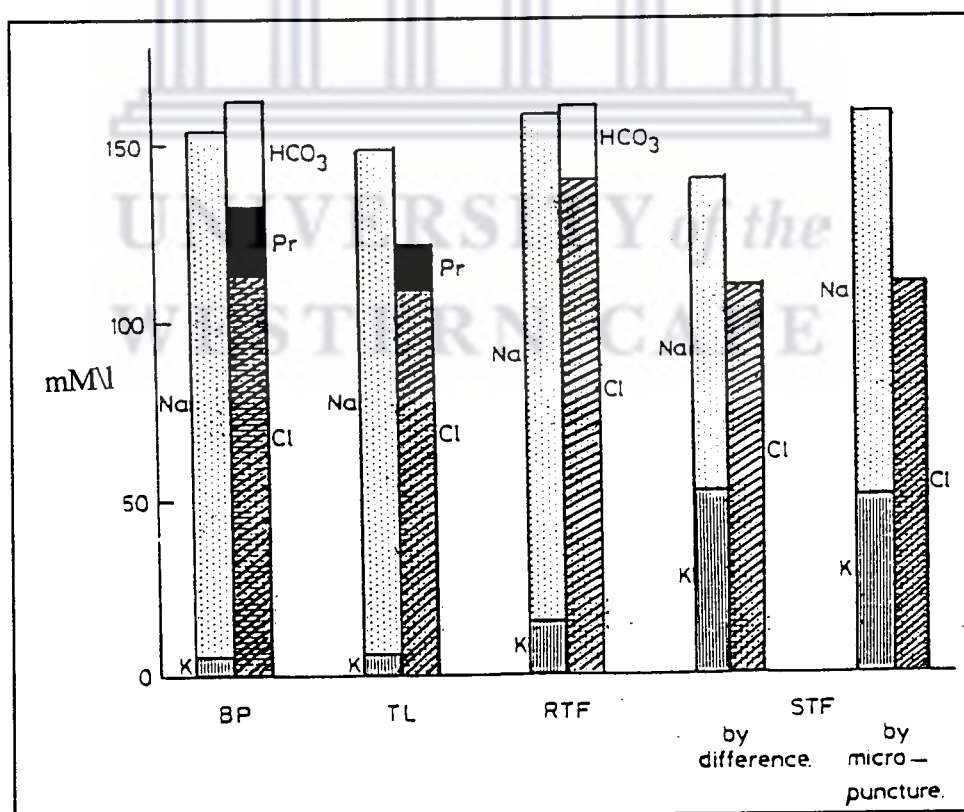


Figure 1.7: The concentrations of sodium, potassium, bicarbonate, chloride and protein (Pr) in blood plasma (BP), testicular lymph (TL), rete testis fluid (RTF) and seminiferous tubule fluid (STF) from rats (taken from Setchell, *et. al.*, 1978).

1978; Hinton and Howards, 1982). There is almost ten times as much potassium in the seminiferous tubular fluid (STF) as in the blood plasma (see figure 1.7) (Setchell, 1979). The chloride and calcium concentrations of the STF are similar to plasma, whereas magnesium and total phosphorus are higher in the STF (Setchell and Brooks, 1988). Transferrin is approximately 25 times lower in the STF than in the blood plasma or the interstitial fluid of the testis (Slyvester and Griswold, 1984). Furthermore, glucose cannot be detected in the STF, while inositol is 100 times more in the STF than in blood plasma (Hinton, *et. al.*, 1980).

1.7.5 Osmolality and pH of the Seminiferous Tubular fluid

Fluid, obtained by micropuncture (see appendix A) of seminiferous tubules of rats, has an osmolality of 337 ± 12 mOsm/Kg H₂O (Tuck, *et. al.*, 1970; Levine and Marsh, 1971). Fluid secreted by the seminiferous tubule appears to be isotonic, or at most, slightly hypertonic to plasma (osmolality: 328 mOsm/Kg H₂O (Tuck, *et. al.*, 1970).

Tuck, *et. al.* (1970) reported the pH of fluid from the lumen of the seminiferous tubules to be approximately 7.2. However, later studies, using pH sensitive microelectrodes, consistently showed the luminal environment of the seminiferous tubules to be much more acidic at 6.95 and 6.97 (Cafilisch and DuBose, 1990a, 1990b). Although it is not known why luminal *milieu* is acidic, it has been suggested that this may play an important role in the sperm maturation process.

1.7.6 Androgen Transport into Seminiferous Tubules

Testosterone is the major androgen in rat testicular interstitial fluids and tissues, but the content of testosterone in the tubular lumen depends on the stage in the spermatogenic cycle of the seminiferous epithelium (Turner, *et. al.*, 1984). 5α -Dihydrotestosterone (DHT) is present in the seminiferous tubule tissue, but does not appear to be the active androgen there, since testosterone is the predominant androgen form bound by the rat seminiferous tubule nuclei (Turner, *et. al.*, 1984).

Rat androgen-binding protein (ABP) is an approximately 90 000 mol. wt. compound and is secreted by the Sertoli cells under the influence of FSH. ABP has a higher affinity for DHT than testosterone (Turner, *et. al.*, 1984) and its secretion is stage dependent (Ritzen, *et. al.*, 1982). Rat Sertoli cells have been shown to secrete 80% of their ABP into the seminiferous tubule and 20% across their basal membranes into the interstitial compartment (Gunsalus, *et. al.*, 1980; Turner, *et. al.*, 1984).

Androgens have a low access into seminiferous tubules and has been demonstrated by many studies (Parvinen, *et. al.*, 1970; Setchell and Main, 1975; Turner, 1988; Yamamoto, *et. al.*, 1991). These studies have shown that intraluminal concentrations of androgen are between 15 to 20% of the concentration in the extracellular compartments, whether the androgens originated from the vascular or the interstitial compartments. Also, intraluminal concentrations of androgens exist in an excess of ABP and therefore it is not necessary to call upon ABP as a retainer of testosterone in the lumen of the

Chapter 1: Review: The Seminiferous Tubule

seminiferous tubule (Turner, *et. al.*, 1984). When testosterone concentration was increased in the blood using a parenteral injection of the steroid in oil, the concentration of testosterone in the tubular fluid did increase, but not to the same extent as the testosterone concentration in the blood; this was taken as evidence that testosterone was entering the tubules by a process involving facilitated diffusion (Setchell and Brooks, 1988).

1.7.7 The Amino Acids of the Seminiferous Tubular Fluid

Hinton (1990) measured the concentrations of amino acids in the arterial and testicular venous blood and in the fluids, obtained through micropuncture methods, of the seminiferous tubule of the rat. There were no significant differences in the concentrations of amino acids between the arterial blood and the testicular venous blood, but between the seminiferous tubular fluid and the interstitial fluids of the testis significant differences were found (see table 1.1). Glutamate, glutamine, glycine and alanine are the dominant amino acids found in the tubular fluid. Setchell *et. al.* (1967) suggested that during shortage of glucose, it was synthesized from these high concentrations of amino acids, and in this way the testis was similar to the mammary gland and the brain.

1.7.8 Endocrine Effects on Fluid Secretion

Hypophysectomy had no immediate effect on fluid secretion, although there maybe a small decrease before the testis begins to shrink (Setchell, 1970; Jegou, *et. al.*, 1983).

Amino Acid	Testicular Interstitial Fluid	Seminiferous Tubular Fluid
Tau	203±24	200±87
Asp	13±4	205±48*
Thr	338±16	299±98
Ser	232±11	285±60
Asn	117±11	n.d.*
Glu	78±13	917±48*
Gln	866±87	794±180
Gly	324±4	2447±246*
Ala	585±18	1038±165*
Val	193±9	273±24*
½Cys	38±3	101±64*
Met	67±3	53±8
Iso	70±2	36±13
Leu	144±7	146±21
Tyr	104±14	92±47
Phe	80±3	92±46
Trp	26±1	119±74
Lys	461±59	433±49
His	87±5	276±35*

Table 1.1: The above concentrations of amino acids ($\mu\text{mol/L}$) are presented as means \pm seminiferous tubules. These values were obtained from Hinton (1990). n.d - not detected.* indicates significant differences between the interstitial and luminal fluids.

Treatment of rats with FSH produced a small increase in fluid secretion, but LH, growth hormone or testosterone were without effect (Setchell, *et. al.*, 1973; Jegou, *et. al.*, 1982).

1.7.9 Temperature and Fluid Secretion

Local heating of the rat testis produced aspermatogenic testes, but did not effect fluid secretion (Setchell and Waites, 1972). Furthermore, Setchell (1970) showed that returning the rat testis to their abdominal cavities had no immediate effect on fluid

secretion.

Preliminary observations showed that the effects of cold decreased fluid secretion in isolated seminiferous tubules (Cheung, *et. al.*, 1976).

1.8 The Effects of Temperature on the Testis

1.8.1 Introduction

The scrotal testis is exceptional because it is an abdominal organ which is maintained at a temperature between 2 and 7°C lower than core temperature (Waites, 1970, 1976). In most mammals the testes migrate from the abdominal cavity and, in many, pass into an invagination of the peritoneum to form a scrotum (Setchell and Brooks, 1988). It is usually thought that the scrotum evolved to reduce the temperature of the testis below that of the core temperature of the body (Cowles, 1965). Presumably, the migration confers some evolutionary advantage on the species, possibly in order to reduce the spontaneous mutation-rate (Erenberg, *et. al.*, 1957).

1.8.2 The Effect of Temperature on Some Substances Entering the Tubule

The entry of I-iodoantipyrine into the rat testis during the first minute after intravenous injection increased sharply as the temperature of the testis was raised to 43°C or 45°C, suggesting that blood flow was substantially increased. However, the permeability of

rubidium was less at the higher temperature. In addition, the permeability of isolated tubules to rubidium was greater at 33°C and decreased at higher temperatures. (Setchell and Waites, 1975).

1.8.3 Cryptorchidism

It is well known that cryptorchid testes (i.e. testes that failed to descend from their abdominal cavity) are invariably aspermatogenic. As early as 1891, Piana and Savarese showed that when the scrotal testes of rats atrophied when they were pushed into the abdomen and retained there surgically. Histological changes appear within 2 days; after 2 weeks only Sertoli cells and a few spermatogonia remain. The testis became normal again if returned to the scrotum, provided that the period spent in the abdomen was not too long (Hagen, 1971).

It has also been found that temperatures above 37°C are effective in most animals, and that the higher the temperature, the shorter the exposure needed (Setchell and Waites, 1972). Furthermore, repeated applications of heat progressively produced more damage (Bowler, 1972).

1.8.4 Cell types Damaged by Heat

Not all the cells in the testes are damaged by increased temperature to the same extent. The most sensitive cells seem to be the primary spermatocytes during pachytene and the

young spermatids. The later spermatids and spermatogonia in the rat appear to be resistant to heat (Chowdhury and Steinberger, 1964).

Recovery from even moderate heating is not usually complete in rats for at least 60 days. This suggests that the spermatogonia which were undergoing mitosis at the time of heating were killed but those which were not dividing were more resistant (Bowler, 1972).

1.8.5 Effect of Heat on Androgen Production

Leydig cells, during and after exposure to heat, still respond to exogenous gonadotrophins (Setchell, 1978). Direct measurements of circulating testosterone levels confirm that a moderate decrease in testosterone does occur in response to heat treatment (Liptrap and Raeside, 1970).

1.8.6 Temperature Conclusion

From the above discussion it is clear that the regulation of temperature is absolutely necessary for the completion of spermatogenesis. The endocrine function of the testis, however, is decreased but not terminally affected by increases in temperature.

In the next section the electrophysiology of the seminiferous tubule is reviewed.

1.9 Electrophysiology of the Seminiferous Tubule

1.9.1 Introduction

Much of the accumulated evidence suggest that Sertoli cells play a central role in the regulation of spermatogenesis (Jégou, 1992). These columnar, highly polarized cells extend across the seminiferous epithelium, remaining in close contact with the developing germ cells. During early sexual development (puberty) in mammals, the Sertoli cells develop unique tight (occluding) junctions in the basolateral aspect of their membranes, which form the basis of the blood-testis barrier and divide the tubular epithelium into the adluminal and basal compartments (Dym and Fawcett, 1970).

The chemical *milieu* of the adluminal is strikingly different to that of the interstitial fluid and this difference is of critical importance for the spermatocyte to complete meiosis and proceed through the stages of spermiogenesis (Fawcett, 1975). Among the most striking differences between the tubular fluid and that of other body fluids is the high concentration of potassium (e.g. 40 mM in the rat) (Tuck, *et. al.*, 1970). It is generally believed that the differences between the basal and tubular fluid are maintained and regulated by 1) Sertoli cell selective transport and polarized secretions and 2) the relative impermeability of the occluding junctions to macromolecules and some ions (Setchell and Waites, 1975).

Chapter 1: Review: The Seminiferous Tubule

Researches have used electrophysiological techniques in an attempt to gain more information about the physiological mechanisms and the effects of chemicals (e.g. hormones) involved in the regulation of ion transport and the permeability of the blood-testis barrier.

1.9.2 General Background

In 1970 Tuck and colleagues used microelectrodes to measure the potential difference across seminiferous tubules for the first time. Potential difference in these tubules were measured during two micropuncture procedures used to collect the tubular fluid: 1) free-flow fluid, i.e. the fluid which normally lies in the lumen of an undisturbed seminiferous tubule, and 2) primary fluid, i.e. fluid which is secreted into oil placed into the seminiferous tubular lumen (for an extensive review on micropuncture techniques see Hinton and Howards, 1982). Recordings showed that the lumen was negative with respect to the interstitium. The average potential difference for tubules that were filled with free-flow fluid was -7.4 ± 0.5 mV, while the tubules which had been injected with oil and had primary fluid secreted into oil, had an average potential difference of -1.2 ± 0.3 mV. Subsequent studies (Levine and Marsh, 1971; Cuthbert and Wong, 1975) confirmed that the lumen of the seminiferous tubule was negative with respect to the outside and that the transtubular potential was approximately -4.8 mV (Levine and Marsh, 1971).

The above results were endorsed by Cuthbert and Wong (1975), who, also with the use of microelectrodes, recorded the intracellular potentials of cells in the isolated

Chapter 1: Review: The Seminiferous Tubule

seminiferous tubules. Their recorded intracellular potentials ranged from -8 to -50 mV, with a mean value of -28.2 mV. The main criticism of this study was that the authors were not sure if impalements had been in Sertoli cells or germ cells. Eusebi and colleagues (1983) also endorsed the above intracellular results, but repeated the study using seminiferous tubules which were obtained from 20 day old rats, irradiated *in utero* on the 19th day of gestation, and in which selective depletion of germ cells is practically complete. They found a higher intracellular resting potential of -37.8 mV, a finding which probably reflects the presence of single cellular population.

More recently the trend has been to study electrophysiological properties of cultured Sertoli cells grown on plastic surfaces. However, such cultured cells do not show the elaborate columnar form of the Sertoli cells seen *in vivo*. Numerous investigators have attempted to improve the state of differentiation of cultured Sertoli cells, usually by providing a suitable matrix on which to grow the cells (Hadley, *et. al.*, 1985; Djakiew, *et. al.*, 1986).

On these cells, or confluent layers of cells electrophysiologists have used microelectrode techniques as well as patch clamping techniques to investigate regulatory physiological mechanism at membrane and intermembrane (effectiveness of junctions) level.

1.9.3 Electrophysiological Effects of FSH

The regulation of Sertoli cell function by FSH has been studied extensively. FSH does

Chapter 1: Review: The Seminiferous Tubule

not penetrate readily into the luminal fluid (Setchell, *et. al.*, 1976) although its major site of action in the testis is on the Sertoli cells (Fritz, 1978). Orth and Christensen (1977) showed that receptors for FSH *in vivo* appeared to be localized at the basal surface of the Sertoli cell.

In control studies of confluent monolayers of Sertoli cells, repetitive measurements of transepithelial electrical resistance (TER) showed that these cultures developed stable TER of 100-145 Ωcm^2 . The addition of FSH resulted in an decrease of TER to 35-40 Ωcm^2 (Janeki, *et. al.*, 1991). These authors also showed that in the concomitant presence of testosterone TER developed the highest values: 580-1200 Ωcm^2 , suggesting a synergistic effect of the two hormones on TER development.

FSH and cAMP has been shown to stimulate potassium transport in Sertoli cells (Muffly and Hall, 1988). FSH brings about this effect by increasing intracellular cAMP. This vectorial transport of K^+ is inhibited by vanadate which indicates that this activity involves phosphorylation. Such a conclusion is consistent with the involvement of a basolateral ATPase (Muffly and Hall, 1988).

Early studies on seminiferous tubules reported that FSH had no effect on the intracellular potential of the cells of seminiferous tubules (Cuthbert and Wong, 1975). However, later studies showed that in tubules that were depleted of germ cells (rats irradiated *in utero*) FSH produced a biphasic intracellular potential response: a rapid (<3 seconds) hyperpolarization followed by a prolonged depolarization. Verapamil, a Ca^{++} channel

blocker, nullified this FSH effect (Wassermann, *et. al.*, 1992).

Roche and Joffre (1989) also showed that by decreasing external Ca^{++} or by adding EGTA to the medium bathing Sertoli cells showed that the FSH induced hyperpolarization was prevented. Grasso and Reichert (1989) showed that FSH stimulated Ca^{++} influx in Sertoli cells. These studies clearly showed that intracellular Ca^{++} played a vital role in the FSH mechanism of action.

Direct evaluation of electrical coupling between Sertoli cells in culture was made by means of two electrodes. It showed that unstimulated cells were effectively coupled. Roche and Joffre (1989) reported that any treatment that increased the intracellular Ca^{++} concentration decreased the electrical coupling between cells. They associated this uncoupling between Sertoli cells with cellular depolarization. Their study further suggested that via FSH control of intracellular calcium the junctional complexes between the Sertoli cells could be controlled. Eusebi, *et. al.* (1983) suggest that the morphological distinct junctions in the germinal epithelium of the rat might provide a low-resistance pathway that mediates cell-to-cell communication between nearby cells. This is endorsed by the decreases in the space constant for intracellular current spread and junctional conductance which occurs concomitantly at puberty, at which time there is also a decrease in the number of gap junctions (Gilula, *et. al.*, 1976; Meyer, *et. al.*, 1977).

1.9.4 Ouabain

Several studies have reported that the glycoside ouabain, a potent inhibitor of the Na^+K^+ ATPase, has no effect on the basolateral potassium pump of Sertoli cells (Muffly, *et. al.*, 1985; Roche and Joffre, 1989; Kew, *et. al.*, 1986; Reisin and Cerejido, 1969). This is unusual for ion pumps that employ sodium and potassium as substrates, but it is not unique because such ouabain-resistant pumps are seen in dog erythrocytes (Parker, 1973) and hog stomach cells (Faller, *et. al.*, 1985). In contrast to these studies Cuthbert and Wong (1975) showed a small but significant decrease in the intracellular potential in response to treatment with ouabain. However, it must once again be pointed out that these authors could not be certain which cells in the germinal epithelium of the rat seminiferous tubule were impaled by the recording microelectrodes.

1.9.5 Dinitrophenol and Glucose Deprivation

Treatment with the metabolic inhibitor, 2'-4' dinitrophenol, interrupted secretion in isolated rat seminiferous tubules (Cheung, *et. al.*, 1976). Cuthbert and Wong (1975) showed that the intracellular potential decreased by 50% in 30 minutes.

Also, glucose deprivation in isolated rat seminiferous tubules caused a significant decrease in the intracellular potential from -31.6 to -22.6 mV (Cuthbert and Wong,

1975). This suggests that an active transport mechanism is essential to drive fluid secretion.

1.9.6 High Potassium Concentration

Muffly and Hall (1988) proposed a mechanism for the transport of K^+ vectorially across Sertoli cells. Briefly, it was proposed that the basolateral membrane contained a potassium pump that delivers this ion at a rapid rate to the interior of the Sertoli cell. The constant concentration of intracellular potassium is maintained by the loss of this ion by way of the apical membrane. This loss of potassium via the apical membrane occurs at the same rate as the influx via the basolateral pump. Although nothing is known about the potassium apical efflux, it presumably takes place through some type of potassium channel. The rate of efflux via the apical membrane is unaffected by either the presence or absence of potassium in the bathing medium (Muffly and Hall, 1988). These authors also showed in their study that the pump is activated by K^+ . This theory is supported by the data of Cuthbert and Wong (1975) which showed that a tenfold increase in the potassium concentration bathing the outside of the isolated rat seminiferous tubule, caused 16 mV depolarization in the intracellular potential.

1.10 Conclusion

Although a large body of literature covers the subject of the testis, relatively little is known of the physiological transport mechanisms that govern the transport of substances across the blood-testis barrier. Although there is a small body of literature that covers the electrophysiology of seminiferous tubules (mostly accomplished through microelectrode studies), little or nothing is known about the electrophysiological properties of the three dimensional rat seminiferous tubule. Valuable information from type of study concerning the transport mechanisms and permeability parameters of the seminiferous tubule could improve the understanding of the germinal epithelium.

In view of the relatively large quantities of cell culture research compared with *in vivo* research, the view expressed in the review by Russell and Steinberger (1989) should be emphasized: That extreme caution is urged in “interpreting *in vitro* results to the intact animal without their validation *in vivo*” and that “every attempt should be made to verify an *in vitro* finding in an *in vivo* system”. However, let the former statement not in any way detract from the value of cell culture research when used as a tool with which to investigate physiological and biochemical mechanisms.

Furthermore, if the importance of the blood-testis barrier can be defined, it may be possible to selectively interfere with its function in spermatogenesis, or to be able to

restore it if defective. In the light of this, continued study of the germinal epithelium is more than justified.

1.11 The aims of the study

- i. The first aim of the current study was to determine the feasibility of perfusing isolated segments of seminiferous tubule while concurrently using alternative techniques to measuring transepithelial potentials. Morphological monitoring of the seminiferous tubules was important in this context.
- ii. The second aim of this study was to test the validity of applying cable analysis to the isolated perfused seminiferous tubule of the rat and subsequently obtain standard cable parameters. Cable parameters would provide valuable insights into the ionic transport mechanisms across the seminiferous tubule.
- iii. The third aim of this study was to observe the effects of changing the external ionic concentrations, administering inhibitors of ion transport and blockers of ion channels on the transepithelial potential and cable parameters (e.g. transepithelial resistance).
- iv. The fourth aim of this study was to attempt to use the electrical data obtained

Chapter 1: Review: The Seminiferous Tubule

during cable analysis to model the ionic pathways across the seminiferous tubule, using a simple equivalent electrical circuit.

The next chapter reports in detail on the various methods and techniques that were used to obtain the data experimentally.



Chapter 2

METHODS AND MATERIALS

2.1 Animal Treatment

Adult male Wistar rats, aged between 90 and 120 days, bred at the Medical Research Council, were used for these studies and were maintained in a controlled environment with free access to food and water. Room temperature was kept at 22°C and a day-night cycle of 12 hours was maintained. Rats were allocated randomly at between four and six per cage.

2.2 Dissection and Transfer of Tubules

Animals were anesthetized with an intraperitoneal injection of sodium pentobarbital (Sagatal; Rhône-Poulenc Animal Health SA (Pty) Ltd.) using a dose of 60 mg/kg body weight. A midline incision was then made through the scrotum, abdominal skin and rectus muscle superior to the pelvis. A single testis was then excised and transferred to a dissection petri dish filled with Ringers which was continuously bubbled with oxygen (bath-B Ringers: see table 2.1). The temperature, throughout the dissection of tubules, was maintained at 35°C using a thermostatically regulated warm stage (Linkam Scientific

Instruments Ltd.; model CO102). The *tunica albuginea* was subsequently removed and the central portion of the testis was teased apart gently using watchmakers forceps, and seminiferous tubules segments (3 mm to 10 mm in length) were isolated. The procedure for the transfer of tubules involved the aspiration of the tubule into a capillary tube, by means of a custom made mechanical micro aspirator. The initial use of fibres to hook out the tubules proved too harsh a method. In the latter case the surface tension of the dissection medium resulted in tearing between the germinal epithelium and the myoid layer. Great care was taken to exclude segments that were damaged or stretched.

2.3 Aeration and Temperature Regulation During Perfusion

The bath Ringers was constantly aerated with a 95%O₂/5%CO₂ air mixture in a chamber above the perfusion bath. The bath Ringers flowed into the perfusion bath by gravity via a set of coiled tubes (Narishiga biowarmer: model MT-2). The set of coiled tubes laid on top of the heater glass of the biowarmer stage and therefore enabled the entering Ringers solution to have the same temperature as the Ringers in the perfusion bath. This prevented any temperature transients in the bath. The bath was prevented from overflowing by pumping out the excess Ringers at the other end. Thus, the bath Ringers was constantly replaced preventing any transient ionic concentrations. Furthermore, bath Ringers was aerated at a distal site (i.e. in the perfusate chamber; see figure 2.1) which averted damaging the fragile tubules by bubbling air into the perfusion bath.

2.4 The Perfusate Reservoir

A 10ml reservoir which contained the perfusate was connected via a tube to the perfusion pipette. The reservoir could be vertically adjusted to regulate the hydrostatic pressure which in turn controlled the rate of perfusion. The hydrostatic pressure is directly proportional to the rate of perfusion.

2.5 Perfusion Apparatus

Micropipettes used for perfusing the seminiferous tubules were fabricated from R6 glass (Drummond Scientific Company, Broomall, PA) with a custom made microforge as previously described for pipettes used in the perfusion of renal tubules (Burg, *et. al.*, 1966). Figure 2.1 shows a set of 3 concentric micropipettes which were secured by a series of custom made perspex holders. The holders in turn were positioned on an aluminium base which was designed so that the position of the pipettes could be axially changed with respect to one another. The latter arrangement allowed the perfusion pipette to be moved into the lumen of the tubule after it was attached to the outer holding perfusion pipette by aspiration. The aluminium base which held the set of pipettes in position was attached to a three dimensional microminipulator (Leitz) which was fixed to an aluminium base plate. The collection pipette was similar in design to the perfusion holding pipette and was attached to a three dimensional microminipulator. The collection pipette was used for the aspiration of the distal end of the tubule.

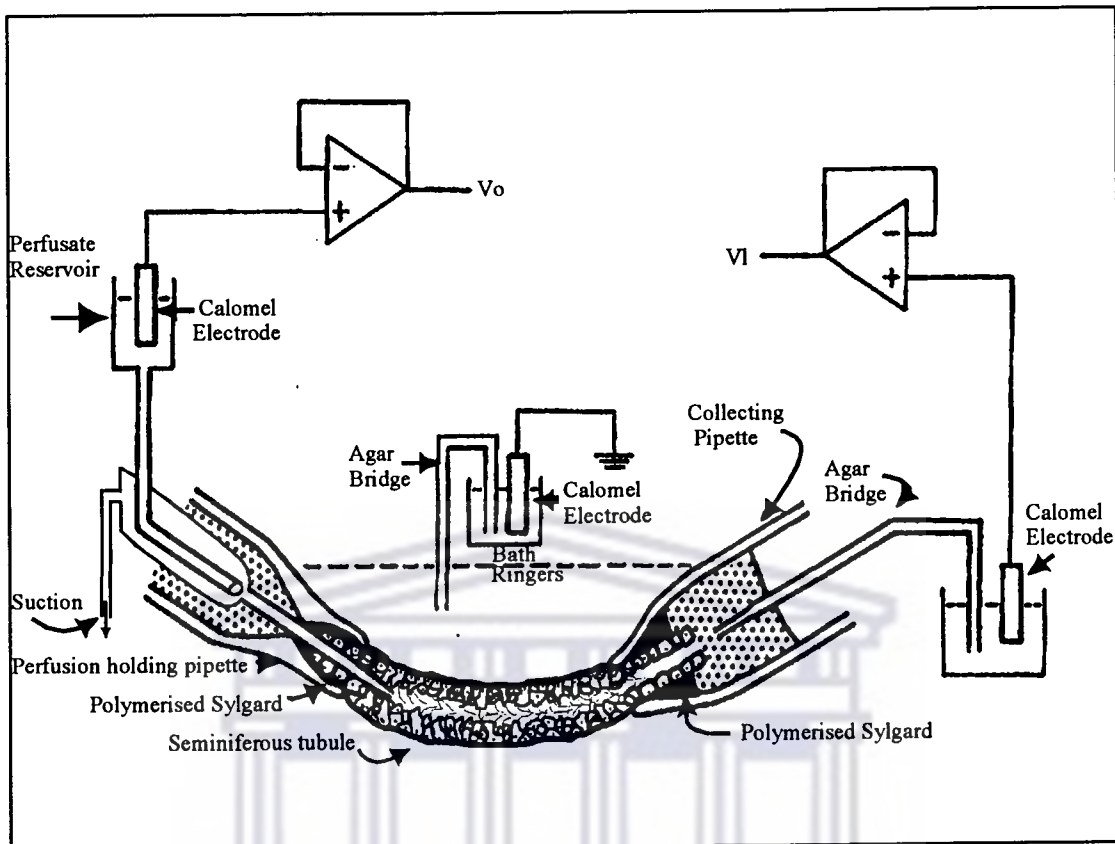


Figure 2.1: The above diagram represents the perfusion apparatus with a simplified electrical circuit. The dots inside the perfusion and collecting holding pipettes refer to the Ringers aspirated into the pipette during the suction of the tubule into the pipette orifice. The arrow denoted as 'suction' refers to the action required to change the perfusate rapidly and/or to remove bubbles trapped in the perfusion pipette.

The perfusion of seminiferous tubules is technically similar to that of rabbit proximal tubules (Burg, *et. al.*, 1966), with one minor difference: the perfusion pipette tip's diameter was decreased to 15-30 μm to further decrease the effects of perfusion changes on the fragile germinal epithelium of the rat seminiferous tubules (see chapter 3 for further explanation).

2.6 The Agar Probe

In an attempt to record the transtubular potential across the seminiferous tubule without

changing the internal *milieu* of the lumen or damaging the germinal epithelium, an agar probe was designed to be used in conjunction with the perfusion apparatus. Essentially, the perfusion pipette was replaced with a pipette similar in shape, but with a tip diameter that was 50-65 μm . A tube was attached to the pipette and then both filled with agar (3g of agar per 100 ml of perfusate Ringers).

This arrangement in conjunction with the perfusion apparatus allowed the positioning of the agar probe within the lumen of the seminiferous tubules. This allowed both for the recording of the transtubular potential under controlled conditions and for changing the bathing media, while not interfering with the luminal environment.

Twenty-two rats were used in this series of experiments which resulted in 20 seminiferous tubules used.

2.7 The Oil-gap Technique

The oil-gap technique was developed by an insect physiologist in 1954 (Ramsay, 1954) and subsequently modified to measure transtubular potentials in Malpighian tubules and salivary glands (O'Donnell and Maddrell, 1984; Berridge and Prince, 1972). In this study, a custom made oil-gap bath (perspex) consisted of three compartments, the central one filled with non conducting liquid, *viz.* oil or liquid paraffin, while the two lateral compartments were filled with Ringers. A thin cover-slip formed the base of the bath. A length of tubule (6-10mm), with one end tied, was carefully dissected from the testis and

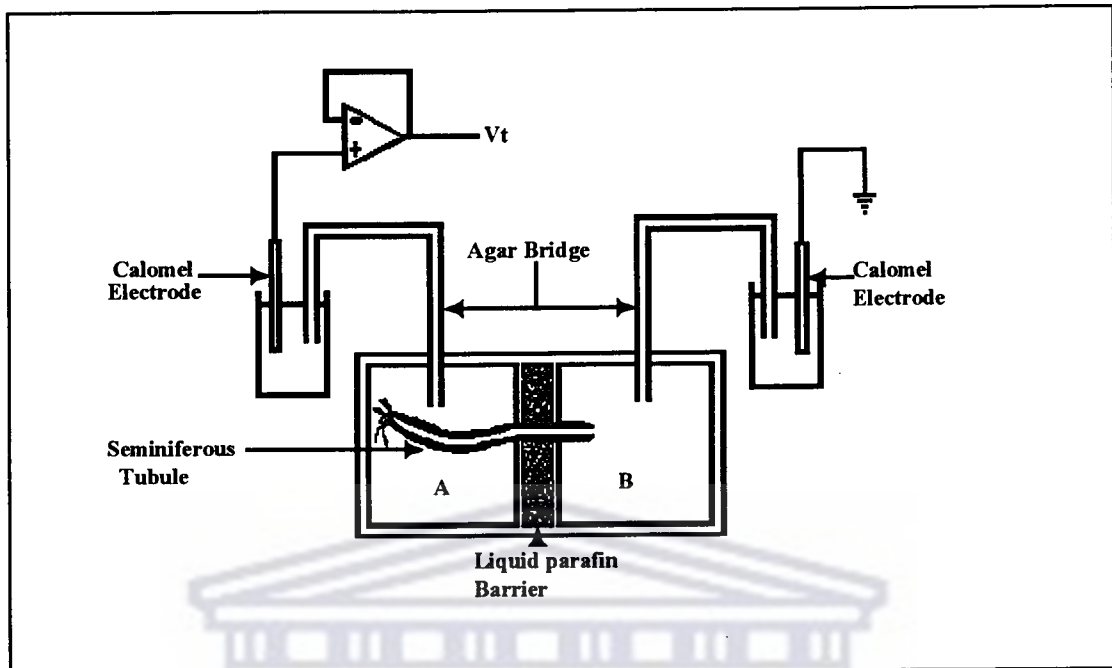


Figure 2.2: The above diagram shows a top view of the oil-gap technique. Also shown is the essential components of the electrical circuits used for recording the transtubular potential.

transferred to the oil-gap bath. In order to measure transtubular potential (V_t) the tubule was positioned across the three compartments with the two ends bathed in Ringers, each electrically insulated from the other by the central compartment filled with liquid paraffin. The tubule was positioned across these compartments in such a manner that the tied-off end of the tubule was the longer segment, while the open end formed the shorter segment (see figure 2.2). The bath was placed on a hot plate (Linkam: Scientific Instruments, Ltd., England: model CO102) and regulated to 35°C . The Ringers solution on the tied segment of the tubule was aerated with $5\%\text{CO}_2/95\%\text{O}_2$. Two agar bridges connected the lateral compartments to calomel half cells which in turn were connected to the head stage of the Axon amplifier (Axoclamp-2A: Axon Instruments) which recorded the transtubular potential. The bath was positioned under a stereo dissection microscope (Vickers Stereo microscope: Vickers Instruments, Japan). The entire setup,

excluding the amplifier, was placed within an earthed Faraday cage in order to exclude as much electrical noise as possible.

Eighteen seminiferous tubules were dissected from 18 rats for the oil gap series of experiments.

2.8 The Electrical Measurements During Perfusion

The main features of the electrical circuit and pipette system are shown in figure 2.1. The perfusion pipette was used to both measure the transepithelial potential (V_o) as well as to allow for concurrent pulses of constant current (I_o) could be injected into the lumen of the seminiferous tubule. The potential at the distal end of the tubule (V_l) was measured via an agar bridge connected to a second headstage of the Axon amplifier. This voltage (V_l) was monitored on a second digital panel meter of the amplifier. A bridge circuit, which formed an integral part of the Axoclamp-2A amplifier (Axon Instruments, Inc), served to null the resistance of the perfusate tubing, pipettes and perfusion tip so that during injection of current the changes of V_o could be used to estimate the input resistance, R_i (see equation 3). The bridge was routinely checked after each experiment, and if found to be unbalanced, the cable data was rejected. All electrical potentials, changes in V_o and V_l and injection of current pulses (200 ms^{-1}) were amplified and

1

Although current pulses of 200 ms duration were used, voltage changes were only sampled in the latter 100 ms, i.e., during the voltage waveform that was not affected by initial capacitance effects.

displayed on the digital panel meters of an Axoclamp-2A amplifier (Axon Instruments, Inc.). Simultaneously, a program (version 6: Pclamp by Axon Instruments, Inc.) run on a 120 Mhz Pentium computer which used a TL-1 Lab Master interface (Axon Instruments, Inc.) to capture the data digitally, displayed graphically the current pulse waveform and all resultant changes in the measured potentials (i.e. ΔV_o and ΔV_l) that occurred during a current injection episode which lasted 200 ms. Pclamp also directly controlled the waveform (i.e. the length and amplitude) of the current pulse that was injected into the lumen of the tubule. The program saves the data and allows subsequent retrieval for data analysis.

All headstages used to measure V_o and V_l , had an input impedance of greater than 10^{10} Ω . The bath was grounded to earth via an agar bridge and calomel electrode using VG-2A-x100 headstage (Axon Instruments, Inc.). This headstage allows the bath to be clamped at zero, thereby eliminating the voltage error due to current flow across the bath-grounding electrode. Furthermore, this headstage also compensates for shifts in bath potential due to changing solutions or temperature. Both V_t and V_{bl} were referenced to the bath solution and recorded on a three pen trace recorder (Rikadenki Kogyo, Co., Ltd). The entire setup, excluding the amplifier, was placed within an earthed Faraday cage in order to exclude as much electrical noise as possible. Earth loops were avoided by attaching all earths to one point on the oscilloscope (Leader Electronics Corp., Japan).

2.9 Cable Analysis

The transtubular resistance, R_t (Ohm.cm), was calculated using cable analysis (Burg, *et. al.*, 1968; Lutz, *et. al.*, 1973; Lapointe, *et. al.*, 1984). To measure the transtubular resistance (R_t) the changes in voltage at both the proximal (ΔV_o) and distal (ΔV_l) ends of the tubule were recorded, as well as the length of the tubule (L). ΔV_l was recorded via an agar bridge that made contact with the fluid in the collection pipette while the other end via calomel electrode to the headstage (input impedance $> 100 \text{ M}\Omega$) (see figure 2.1). These voltage changes in response to the injection of current pulses are used to calculate the length constant, λ (Eq.1):

$$\frac{L}{\lambda} = \cosh^{-1}\left(\frac{\Delta V_o}{\Delta V_l}\right) \dots\dots\dots \text{Eq.1}$$

Once λ has been computed R_t can be readily calculated using Eq.2:

$$R_t = \frac{\Delta V_o \lambda}{I_o} \tanh\left(\frac{L}{\lambda}\right) \dots\dots\dots \text{Eq.2}$$

Equation 3 allows for the calculation of the luminal resistivity to current flow, and is also called the core resistance, R_c .

$$R_i = \frac{\Delta V_o}{I_o} = \sqrt{\frac{R_c}{R_t}} \cdot \coth\left(\frac{L}{\lambda}\right) \dots\dots\dots \text{Eq.3}$$

Cable analysis uses the core resistance and the perfusate resistivity, ρ , to evaluate the electric lumen diameter, D_e (see equation 4).

$$D_e = \sqrt{4\rho / \pi R_c} \dots\dots\dots \text{Eq.4}$$

The electric luminal diameter can be compared to the optically measured luminal diameter to provide an important test of the validity of cable analysis in estimating R_t (Lapointe, *et. al.*, 1984).

The short-circuit current, a measure a combination of active transport pump activity and ionic channel activity, may be calculated either corrected for surface area (SCC; $\mu\text{Amp}/\text{cm}^2$; see equation 5 where D = lumen diameter) or as the ‘virtual’ short circuit current (SCC_v; $\mu\text{Amp}/\text{cm}$; see equation 6).

$$SCC = \frac{V_o}{R_t * \pi * D} \dots\dots\dots \text{Eq.5}$$

$$SCC_v = \frac{V_o}{R_t} \dots\dots\dots \text{Eq.6}$$

Although 25 rats were used during this series of experiments only 14 cable experiments were successfully accomplished.

2.10 Composition of Solutions

The solutions were designed to approximate the fluid in the seminiferous tubule lumen and those bathing the outsides of the tubule (Levine and Marsh, 1971). The compositions of the solutions are summarized in Table 2.1. Ringers were adjusted with mannose (BDH Chemicals, Ltd.) to an average osmolality of 325 mOsm/L and 310 mOsm/L (Tuck, *et al.*, 1970; Levine and Marsh, 1971) for the perfusate and bath solutions using a calibrated vapour pressure osmometer (model 5100C, Wescor, Inc.). Solutions were adjusted to pH 7.4 with 0.1N NaOH or 0.1N HCl, prior to use. All solutions were equilibrated with air (5%CO₂/95%O₂) to maintain the pH at 7.4 (Levine and Marsh, 1971). Bumetanide (4x10⁻⁶M; Sigma), 1 mM/L 2',4'-dinitrophenol (Sigma), 2mM BaCl₂ (Sigma) and Furosemide (10⁻⁴M; Sigma) were added at various times to the bathing medium once a stable potential was reached.

The vital stain trypan blue (0.4g/100ml; Sigma) was passed through a 0.7 µm type-HA filter (Millipore, Bedford, MA) before use. When added to the perfusate it was used to measure the time lag between changing perfusate solution and entering the perfusion bath. Furthermore, it was used as an indicator of the viability of cells in perfused tubules (Weisbren, *et al.*, 1994). Tubules with cells which were stained with trypan blue were regarded as damaged.

2.11 Statistical Analysis

All data are presented as means \pm standard deviation unless otherwise denoted. Data were compared by paired or unpaired Student's *t* test, unless stated otherwise. One way Anova was carried out to evaluate differences between groups. Significance was accepted at $P < 0.05$.



	Perfusate	Bath B	Bath C (-Cl)	Bath D (Low Cl)	Bath E (High-K)
NaCl	57	103	-	-	57
NaHCO ₃	-	25	25	25	25
Na gluconate	42	19			42
Na ₂ SO ₄	-	-	61	61	-
Na acetate	-	1	1	1	1
NaH ₂ PO ₄	1.2	1.2	1.2	1.2	1.2
K ₂ SO ₄	-	-	2.5	2.5	-
KCl	40	5	-	-	50
Choline Cl	10	-	-	-	-
CaSO ₄			1	-	
CaCl ₂	1	1	-	1	1
MgSO ₄			1	-	
MgCL ₂	1	1	-	1	1
PIPES	-	-	-	-	-
Glucose	5.5	5.5	5.5	5.5	5.5
Aspartic acid	0.2	0.017	0.017	0.017	0.017
Glutamine	0.9	0.582	0.582	0.582	0.582
Proline	1.264	0.152	0.152	0.152	0.152
Glycine	2.447	0.339	0.339	0.339	0.339
Alanine	1.038	0.569	0.569	0.569	0.569
Lysine	0.433	0.341	0.341	0.341	0.341
Myo-inositol	3.5				
pH	7.4	7.4	7.4	7.4	7.4
Total Na ⁺ (mM)	100.2	149.2	149.2	149.2	138.2
Total K ⁺ (mM)	40	5	5	5	50
Total Cl ⁻ (mM)	111	111	-	2	111

Table 2.1: All concentrations are given in mM. Amino acid concentrations were taken from Hinton (1990).

CHAPTER 3

Effects of Experimental Techniques on the Morphology of Rat Seminiferous Tubules

3.1 Introduction

Studies on the proximal convoluted tubules of the rabbit (Lapointe, *et. al.*, 1984) and on the Malpighian tubules of a desert beetle, called *Omnymacris plana* (Isaacson, *et. al.*, 1989) indicated that the morphology of these tubules were not significantly affected by



Figure 3.1: The above tubule was perfused from a height of 10 cm above the bath. The contents spued out of the far end of the tubule are clearly visible. The surrounding medium is littered with cellular debris; groups of spermatids are still attached to each other and to cellular debris. Also clearly seen is the area of myoid cell contraction. The intensity of the contraction varied from time to time. A microelectrode can be seen impaling cells at the distal portion of the contraction. (x44).

the rate that perfusate passed through their lumen or the perfusate pressure. However, this was clearly not the case in the rat seminiferous tubules.

During the first trials of this project, perfused, isolated rat seminiferous tubules were observed to extrude immature spermatozoa as well as cellular debris from its distal end (figure 3.1). It was therefore crucial to investigate the morphological state of the seminiferous tubules during and after a perfusion episode.

The perfusate passing through the lumen of the tubule appeared to apply a shear stress which loosened the cells from each other in the adluminal compartment and which



Figure 3.2: After some 70 minutes of perfusion most of the cellular contents had been washed out. The tubule is now completely translucent. The constriction is still present due to the contraction of the myoid layer. At this stage the cellular organization of the myoid layer clearly visible. (x44).

eventually washed out of the open end of the tubule. Longer perfusion periods sometimes resulted in a tubule which became translucent. These translucent tubules produced a low transepithelial voltage ($<1\text{mV}$) and through the inverted microscope the cell structure making up the translucent tubule was clearly observed (see figure 3.2). It was clear at this stage that perfusate caused some disruption of the morphology of the tubule. However, the extent of morphological change and damage on the germinal epithelium of the seminiferous tubules caused by perfusion was not known. The possibility existed that the perfusion technique was not suitable to investigate the electrophysiological properties of the seminiferous tubule. It was therefore important to investigate the possible problems associated with perfusion as well as the application and development of alternative electrophysiological techniques.

The purpose of this study was therefore to investigate the effects of perfusion (perfusion rate) and non perfusion (alternative) electrophysiological techniques on the morphology of seminiferous tubules.

3.2 Materials And Methods

3.2.1 The Experimental Design

Tubules were generally exposed to two types of experimental techniques prior to being processed for their gross morphology. Figure 3.4 shows a flow diagram indicating the different sets of experiments and controls used in the experimental design of this study.

1. **Perfused tubules:** A set of experiments was designed to test the effects of different perfusion pressures on the morphology of the germinal epithelium of rat seminiferous tubules. Tubules were dissected out and perfused as described in

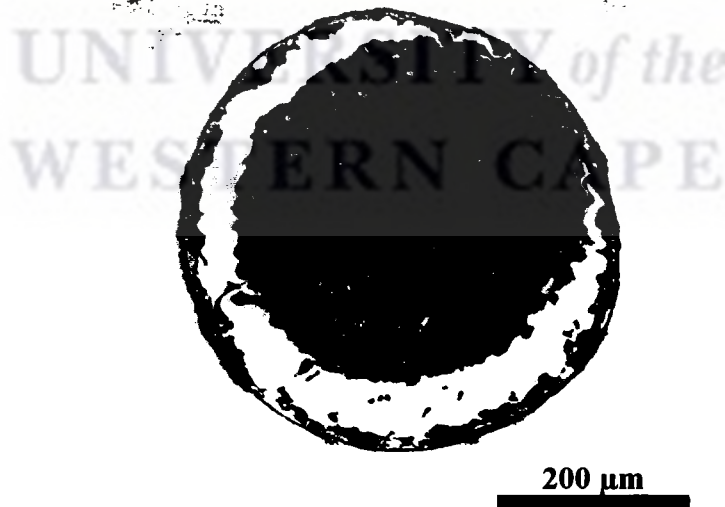


Figure 3.3: The photograph depicts a cross section of a tubule in which typical tearing had occurred between the myoid layer and the germinal layer. This case occurred because the precautions explained in the text, were not followed during the early part of the project.

chapter 2. During these experiments, tubules were perfused under control conditions and no experimental permutations were carried out on the tubules. In some experiments the perfusion pipette tip was modified by narrowing the tip down to 15 to 30 μm in diameter. The morphology of these tubules was also studied. All tubules were perfused for 30 - 40 minutes and then exposed to a tissue fixing protocol explained in section 3.2.3.

2. **‘Non perfused’ tubules:** Two types of ‘non perfused’ experiments were carried out: (i) oil-gap experiments and (ii) the luminal agar electrode experiments. (See chapter 2 for details of the experimental techniques mentioned above; also see figure 3.4). Tubules were taken directly from their experimental set-up and subjected to the tissue fixing protocol described below (section 3.2.3).

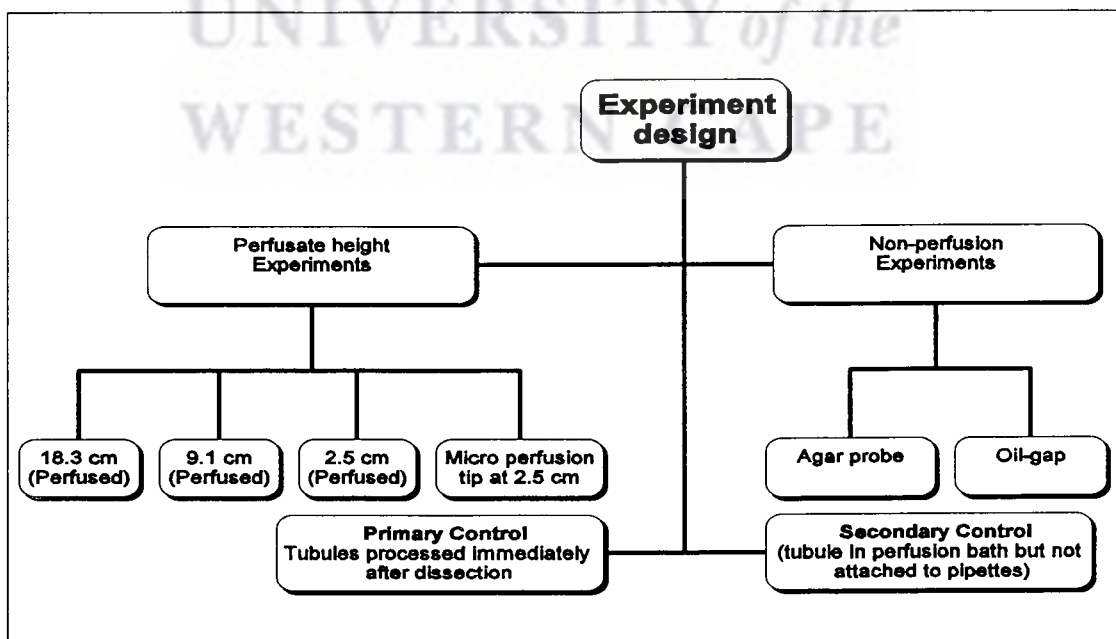


Figure 3.4: The above flow diagram represents the experimental design of the morphology study.

3.2.2 Transfer Procedures

The rat seminiferous tubule is extremely fragile. During the early part of this morphology study tearing between the myoid and germinal layers had occurred during the transfer of the tubules from the perfusion bath to the fixation vials. A fine fibre was used to lift the tubule out of the perfusion bath and into the vial containing the buffered 2.5% glutaraldehyde. However, the surface tension of the perfusion bath was sufficient to mechanically distort the tubule to the point where tearing occurred (see figure 3.3). This was prevented subsequently by introducing the 2.5% glutaraldehyde into the perfusion bath after an experimental procedure had been concluded. This resulted in a tubule which was mechanically harder and easier to move by the suction method described in chapter 2 (methods). However, this procedure was not always successful in the oil-gap method, as the viscosity and surface tension of the oil was considerably greater than the Ringers in the perfusion bath. In an attempt to prevent tearing during the transfer from the oil gap bath the oil in the gap was gently washed off with Ringers followed by liberally dousing the tubule with 2.5% glutaraldehyde. This appeared to largely solve the problem.

3.2.3 Processing Protocol for Perfused Seminiferous Tubules

Four electrophysiological procedures were carried out prior to the tissue processing procedure, which was kept constant throughout. Briefly, the three electrophysiological procedures consisted of (1) perfusing tubules at different perfusion pressures, viz. at 18.3 cm, 9.1 cm and 2.5 cm, (2) tubules used in the oil-gap experiments, (3) tubules in which

the transepithelial potential was measured using an agar luminal electrode in conjunction with the perfusion holding pipette setup and (4) tubules which were 'perfused' using a perfusing pipette which had a tip diameter of less than 25 μm (see chapter 2 for a detailed discussion on the various electrophysiological methods).

A primary and a secondary control were used during this study. In the primary control (in 3 rats both testes were used) a male rat was anaesthetised and its testis removed and placed immediately into 2.5% glutaraldehyde in 0.1 molar PO_4 buffer for dissection. A few segments of seminiferous tubules (3-5mm long) were quickly dissected out using a dissecting microscope and left in this medium on ice for 2 hours for initial fixation (the total number of seminiferous tubules used for the primary control study was 12). The secondary control involved the removal of the seminiferous tubules from the testis which were then placed for about 30 minutes in the perfusion bath alongside the perfused tubule (12 seminiferous tubules from 6 rats). All other tubules were firstly subjected to an experimental electrophysiological procedure (mentioned above) before being pre-fixed (Dym and Fawcett, 1970) for two hours in 2.5% glutaraldehyde in a 0.1 molar phosphate buffer (20ml 0.2M NaH_2PO_4 , 80ml 0.2M Na_2HPO_4). All seminiferous tubules were then rinsed twice in a 0.1 molar phosphate buffer for a period of 15 minutes at room temperature. The tubule specimens were then post-fixed in 1% osmium tetroxide in a 0.1 molar buffer for 60 minutes at room temperature. Tubules were then rinsed twice in distilled phosphate water for a period of 20 minutes. Tubules were then stained *en bloc* with 2% uranyl acetate in 70% ethanol; this process required 2 rinses for a period of 15 minutes. Tubules were then dehydrated in ascending concentrations of ethanol: starting

Chapter 3: Effects on tubular morphology

with two washes in 80% ethanol for 10 minutes, then two washes in 95% ethanol for 10 minutes, three washes in 100% ethanol for 30 minutes and finally two washes in acetone for 30 minutes. The tubules were then impregnated in a 1:1 ratio of acetone to Spurr resin (Taab Laboratories Equipment, Ltd., England) overnight (approximately 12 hours) at room temperature. Tubules were then impregnated with fresh Spurr resin for one hour at room temperature. This was followed by tubules impregnated with fresh resin for 5 hours under a vacuum. Tubules were then embedded in oven dried moulds with fresh resin which was left to polymerise for 16 hours at 60°C.

Semithin sections (1 µm thick) were cut by means of an ultra-microtome (Reichert ultratome - OMU3) and prepared for microscopy via the following procedure: Cut sections were placed on slides (which were dried for 5-10 minutes on a hot plate (80°C)). This was followed by 3 ml sodium methoxide (2.5g metallic sodium dissolved in 25 ml methyl alcohol and added to 25 ml of benzene) pipetted on to the slide sections for a few seconds in order to dissolve the resin and to leave only the fixed cellular component on the slide. The slide was then dipped successively into two changes of 100% ethanol, and then washed off with tap water. This was followed by dropping 1% methylene blue on the sections for a few seconds, and then rinsing the slide with tap water. The superfluous water was removed by shaking and the slide finally dried on a hot plate before being viewed under the microscope.

3.3 Results

3.3.1 Effects of Perfusate Height on Perfusion Rates

Perfusion rates were determined by measuring the volume of perfusate that left the perfusate chamber by gravity per minute for a set perfusion chamber height. Three arbitrary perfusate heights were used to gauge the effects of the perfusion: 2.5, 9.1 and 18.3 cm. The 18.3 cm height represented the upper limit of perfusate height and 2.5 cm the minimum distance the perfusate chamber could descend in the Faraday cage, while the 9.1 cm height was approximately mid way between the two. The perfusion height was the vertical distance between the top of the fluid in the perfusate chamber and the tip of the perfusing pipette in the bath.

Perfusate Volume versus Time						
Height	18.3 cm		9.1 cm		2.5 cm	
Microliters	\bar{x} (mins)	\pm S.D.	\bar{x} (mins)	\pm S.D.	\bar{x} (mins)	\pm S.D.
0	0.00	0.00	0.00	0.00	0.00	0.00
10	8.62	0.20	5.46	0.14	70.68	0.59
20	20.12	0.03	25.43	0.06	139.95	0.06
30	34.18	0.16	54.86	0.07		
40	49.40	0.32	78.70	0.03		
50	64.24	0.06	102.60	0.02		
60	78.42	0.10	135.84	0.04		
70	95.03	0.09				
80	110.60	0.22				

Table 3.1: For all means (\bar{x}) above, n=3. For each height the same set of pipettes were used. The three heights refer to the vertical distance between the *in vitro* bath and the meniscus of the perfusate above. For the perfusate height of 2.5 cm only 3 points over an average time of 139 minutes was necessary to draw the curve (see figure 3.5).

The perfusate rate was measured for three periods and remained remarkably linear for more than two hours. The small standard deviation in the time domain for a given volume of perfusate at a given height also indicated the repeatability of flow rates (see table 3.1).

Because of the constancy of the flow rate, the relationship between time (minutes) and perfusate flow (μl) was linear and therefore flow rate was simply calculated using the slope for the different perfusate heights (see figure 3.5). Flow rates for perfusate heights of 2.5 cm, 9.1 cm and 18.3 cm were respectively 0.14 $\mu\text{l}/\text{min}$, 0.42 $\mu\text{l}/\text{min}$ and 0.68 $\mu\text{l}/\text{min}$.

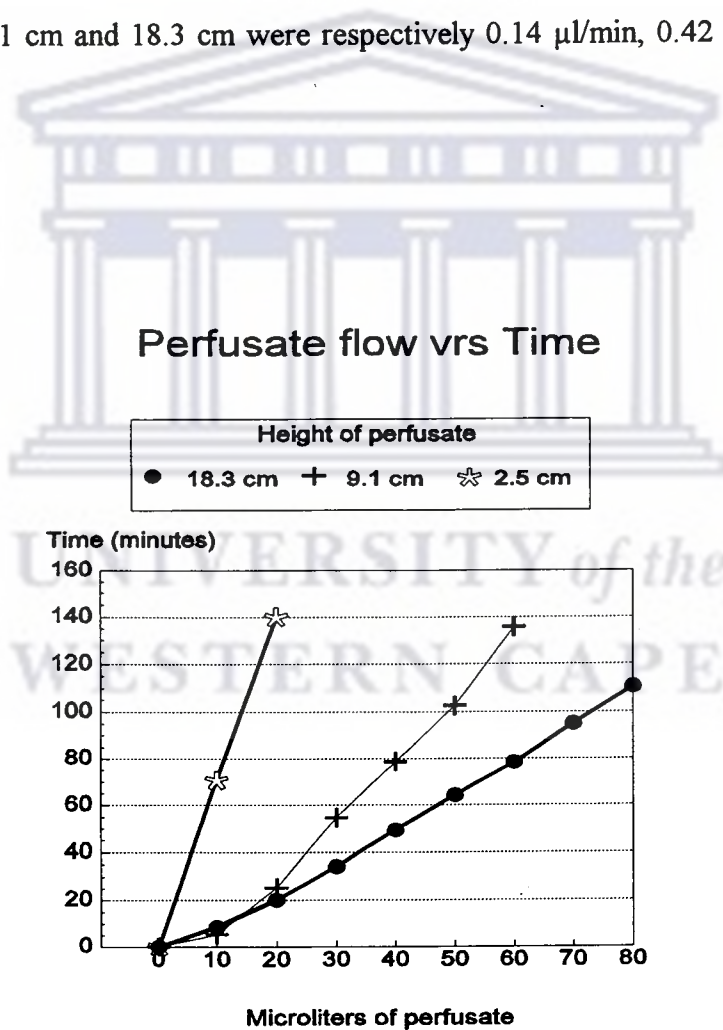


Figure 3.5: The slope of the linear sections of the above graphs was used to calculate the change in the perfusion rate versus the height of perfusate above the bath.

3.3.2. Effects Perfusate Flow on the Morphology of the Germinal Epithelium

3.3.2.1 Controls

Secondary control tubules (see figure 3.4) were not perfused but were simply dissected out and placed into the perfusion bath for 45 minutes and were then processed as normal (see fig 3.6a). These tubules were in turn compared to the primary control (see figure 3.4), i.e. the testis was placed in buffered 2.5% glutaraldehyde and thereafter tubules that were dissected out and immediately processed as described in the methods section (see figure 3.6b). There were no differences between the central parts of these tubules. However, the tubules that were exposed to the perfusion bath exhibited differences at their dissected ends where contraction of the myoid layer had resulted in the expulsion of luminal contents. It must be stressed here though that these morphological changes were limited to the extreme ends of the tubule and did not extend to what would make

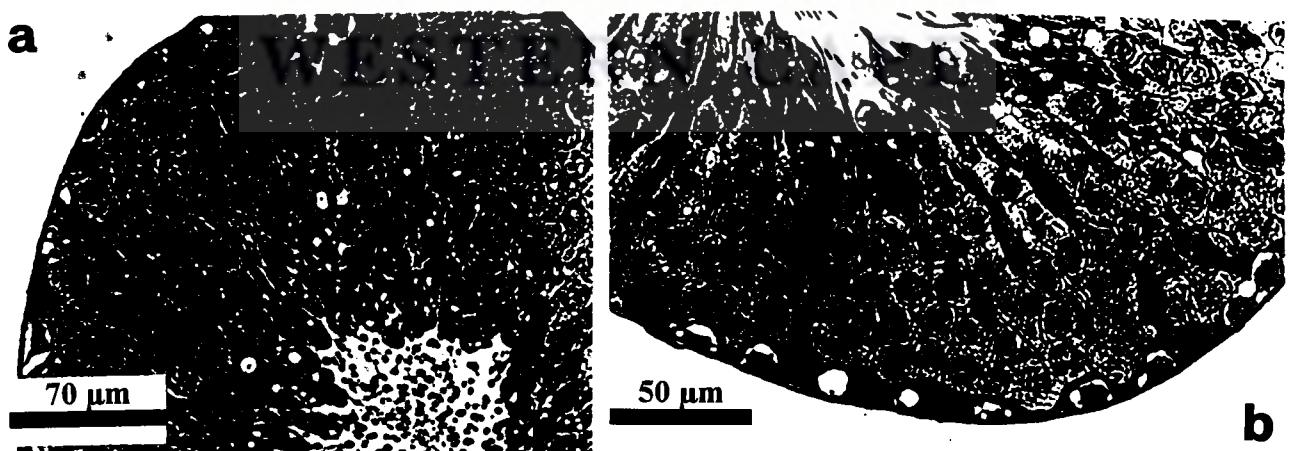


Figure 3.6: The above micrographs represents the control tubule for this study. (a) This tubule was perfused with 2.5% glutaraldehyde immediately after dissection and then subjected to the processing procedure outlined in the text. In (b) the tubule was placed in the perfusion bath for 45 minutes before it was processed.

up the central areas of the tubule.

3.3.2.2 Effects of High Perfusate Flow Rates on Tubular Morphology

In the high perfusate flow rate category the morphology of both 0.68 $\mu\text{l}/\text{min}$ (18.3 cm) and 0.42 $\mu\text{l}/\text{min}$ (9.1 cm) exposed tubules will be described collectively, as there was very little difference between the two categories in terms of effects on the morphology of the tubules.

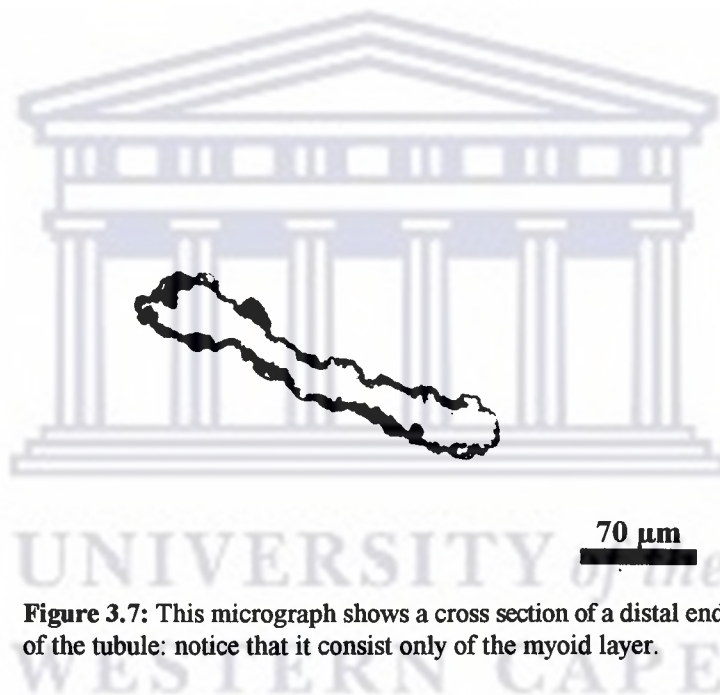


Figure 3.7: This micrograph shows a cross section of a distal end of the tubule: notice that it consist only of the myoid layer.

These tubules exhibited a wide range of morphological damage, which ranged from large vacuoles forming within the germinal epithelium to the stripping off of the entire germinal epithelium (see figure 3.8a-d), the latter case representing the most severe morphological damage. In the latter case (i.e. stripping of the germinal epithelium), spermatids and other cellular debris constantly washed out at the distal open end of the perfused tubule, the proximal end being attached to the holding and perfusing pipettes. After some 20-30 minutes of the extrusion of cellular contents, the tubular structure that was left and being

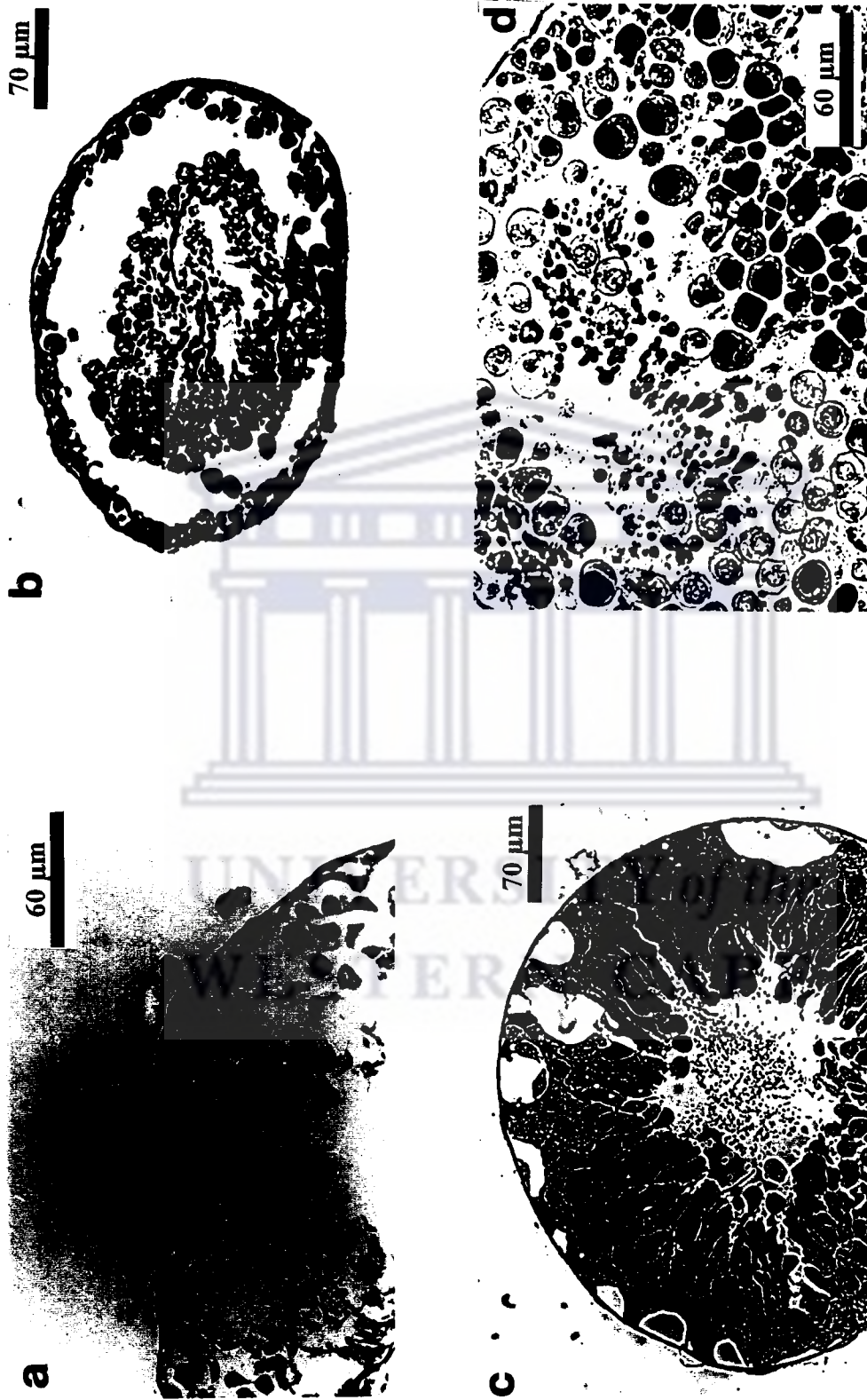


Figure 3.8: (a) This micrograph represents the shearing effects of high perfusion rates ($0.68\mu\text{l}/\text{min}$) on the morphology of germinal epithelium. (b) The micrograph depicts how the entire germinal epithelium is dislodged from the myoid layer (also see figure 3.2). (c) At the lower perfusion rate ($0.42\mu\text{l}/\text{min}$) large vacuoles developed in the germinal epithelium. (d) The micrograph shows how the germinal epithelium has broken down into various cells, totally unattached from each other: these cells would eventually all be washed out of the tubule.

perfused was the outer myoid layer. This outer myoid layer was able to withstand high perfusion pressures and also exhibited a small voltage (less than 1 mV). These polygonally shaped cells in this layer could be clearly seen through the inverted microscope at low magnification (x44) (see fig 3.2) and furthermore, they certainly appeared viable because when perfused with trypan blue in the Ringers, these cells excluded the trypan blue. Occasionally, the shearing force of the perfusate appeared to tear the epithelium away from the basement membrane.

These morphological changes also appeared in tubules that were perfused from a height of 4.5 cm although less germinal epithelium breakup occurred here, as the perfusate flow rate was only 0.2 $\mu\text{l}/\text{min}$.

3.3.2.3 Effects of Low Perfusate Flow Rates on Tubular Morphology

In the 0.14 $\mu\text{l}/\text{min}$ perfusate flow rates the morphology of the germinal epithelium compared favourably with the control tubule morphology (see figure 3.9). Mechanical damage occurring at the ends of the tubules because of dissection was not of concern because the proximal end of the tubule was always found within the lumen of the perfusion holding pipette, which in turn was filled with electrically insulating Sylgard. This is important to prevent either perfusion shunts via the damaged end or electrical short-circuiting of the tubule. Furthermore, some of the damage to the germinal epithelium at the tubular ends occurred because of the contraction of the myoid layer which resulted in the squeezing out of some of the most proximal and distal cells.



Figure 3.9: A cross section of tubule perfused at 0.14 $\mu\text{l}/\text{min}$.

A draw back of this method occurs when rapid changes are made to the perfusate resulting in an inward suction from the lumen through the perfusion pipette that is severe enough to break up patches of the epithelium. This can be avoided if the perfusion pipette tip is narrowed (see section 3.3.2.6).

3.3.2.4 Effects of Oil-gap Technique on Tubular Morphology

The design of the oil-gap technique allowed even less interference with the physiological status quo of the tubule than any of the other *in vitro* electrophysiological techniques. The areas in which differences could be noticed were once again the ends of the tubule (for reasons given in section 3.3.2.3), otherwise the tubule's central areas did not differ from the control tubules (see figure 3.10a).

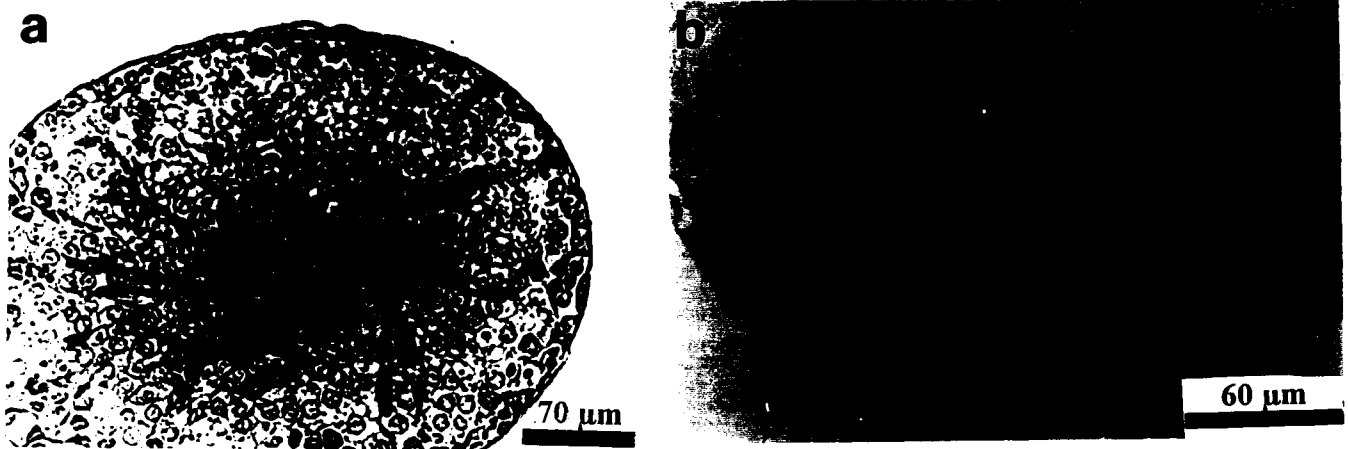


Figure 3.10: A cross section of tubule used in oil-gap experiment (a); the compact lumen might have been caused by the myoid layer contraction, but may also be indicative of a reduced fluid secretion. (b) A cross section of tubule in which the agar probe was used to monitor V_t .

3.3.2.5 Effects of the Agar Probe on Tubular Morphology

The use of the agar probe to investigate the transepithelial potential did not cause any morphological changes to the tubules (see figure 3.10b), as this technique did not in any way influence the luminal internal milieu. However, the disadvantage of this method was that the effects of ionic changes to the lumen could not be tested. Other difficulties encountered with this technique are described in chapter 2.

3.3.2.6 Effects of Micro Perfusion Pipette on Tubular Morphology

The very small perfusion pipette tip (15-30 μ m) prevented flushing of the lumen caused by retro suction during perfusate changes and also further reduced the flow rate (see discussion). Thus, the decreased perfusate flow rate and the avoidance of epithelium damage during perfusate changes reduced the risk of germinal epithelium damage. The

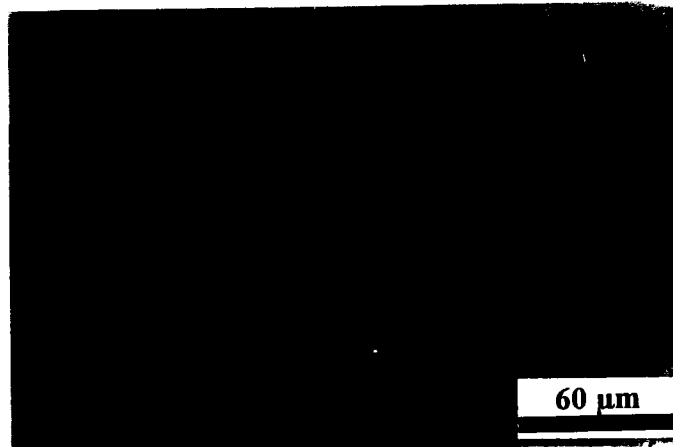


Figure 3.11: A cross section of tubule perfused with a micro perfusion pipette.

morphology of these tubules was similar to that of the control tubules (see figure 3.11).

3.4 Discussion

It was not the aim of this study to describe the microscopic detail of the rat seminiferous tubules (as this was already exhaustively described by de Kretser and Kerr (1988) and Pelletier and Byers (1992) among others), but simply to describe the gross morphological effects of the experimental procedures. It became abundantly clear in this study that the rat seminiferous tubule is very fragile and especially susceptible to mechanical damage.

Researchers (Sharpe, *et. al.*, 1992) involved in the isolation of tubules for tissue culture have alluded to the fragility of rat seminiferous tubules and were careful to exclude stretched or damaged tubules from their procedure. In this study, great care was taken right from the dissection stage of the procedure to prevent tubular damage. It is not the outer myoid layer that cannot endure mechanical distortion, but the germinal layer which

is attached to the myoid layer. This was evident in the first set of perfusion experiments in which a more robust technique was utilized to transfer the tubules to the perfusion bath. During these occasions large strips of the germinal epithelium became detached from the myoid layer. Indeed, low perfusion pressures (i.e. perfusate from 4.5 cm above perfusion bath) resulted in cells of the germinal epithelium being washed out of the distal end of the tubule. Moreover, the contractions of the myoid layer (visible under low magnification) apparently contributed to the ejection of a detached or broken down germinal epithelium. This observation was supported when dissected tubules were left in the perfusion bath without being attached to the perfusion pipettes: in this case the phenomenon of germinal cell ejection was limited to either of its ends. The ejection of luminal contents always occurred and did not depend on the method of transfer or the meticulous dissection of the tubules. It is important to stress here that the ejection of luminal contents by the myoid layer contracting were limited to the ends of the tubule only and did not affect the morphology of the middle sections. The tissue damage at the ends of the tubule which resulted in this limited ejection of cells, probably occurred because of the mechanical damage caused during the cutting of the ends of the tubule.

Isolated seminiferous tubules in saline have been observed to show peristaltic movements as early as 1951 (Roosen-Runge) and Tuck *et. al.* (1970) showed that droplets of oil can be carried rapidly from one segment of a tubule to another. In this study, contractions by the myoid layer along the entire length of the tubule occurred periodically; this normally was not associated with detachment of the germinal epithelium, but probably with the normal functioning of the seminiferous tubules in propelling its luminal contents towards

its ends (see figure 3.1).

3.4.1 Perfusing Technique and Morphology

Most of the studies (Levine and Marsh, 1970; Mattmueller and Hinton, 1991; Henning and Young, 1971; Hinton, 1990; Tuck, *et. al.*, 1970; Turner, 1988; Yamamoto, *et. al.*, 1991) investigating the internal *milieu* of the seminiferous tubules have used the micropuncture technique or variations thereof. However, microperfusion of seminiferous tubules using the techniques pioneered by Burg, *et. al.* (1966,1968) has not been attempted.

3.4.1.1 The Relationship Between the Perfusate Height and Perfusate Rate

The data presented in the results clearly shows the relationship between the amount of perfusate flowing through the perfusion pipette's tip as a function of time. Using the slope of these linear graphs it was simple to calculate the average perfusion rate. It was therefore interesting to plot perfusate height as function of the resultant slopes (or perfusion rates) for this one set of perfusion pipettes. The relationship between perfusate height and flow rate appears virtually linear (figure 3.12). This supports the assumption that flow rate is a linear function of changing the height of the perfusate. One could safely predict, therefore, using regression analysis (see caption of figure 3.12), the flow rate for any random height (eg. perfusate height = 4.5 cm: 0.23 μ l/min). This is expected for any one set of perfusion pipettes. It is important to note that no two sets of perfusion pipettes

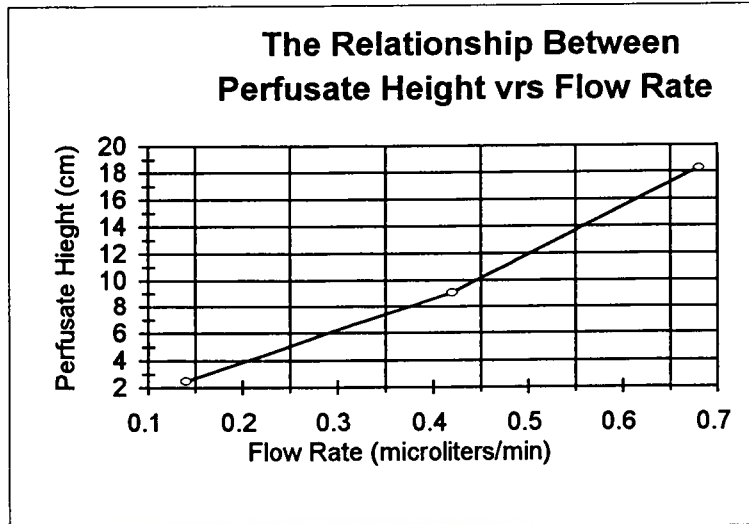


Figure 3.12: The above graph depicts the relationship between perfusate height and flow rate. Regression analysis: $y = -2.1 + 29.2x$ ($r = 0.98$) (Software: Medcalc).

could be absolutely identical, as a difference of just a few nanometres to the perfusion tip could result in a dramatic change in flow rate (i.e. flow in any tube is proportional to $[\text{radius}]^4$). This argument holds for the length of the shank and tip as well. It was therefore important that one set of custom made glass pipettes was used throughout this series of experiments to ensure repeatability.

3.4.1.2 Effects of Perfusate Rates

The definition of “high perfusate rates” does not pertain to the perfusate rate *per se*, but actually to the effects of the perfusate rate on the germinal epithelium. For the purposes of this discussion all perfusate rates above $0.14 \mu\text{l}/\text{min}$ will be defined as high, as these perfusate rates all gave rise to morphological damage. The shear stress of a high pressure, fast flowing perfusate through the lumen of the seminiferous tubules appeared to tear off the cellular extensions of the Sertoli cells which project into the lumen. These fragile

Sertoli cellular extensions apically surround the developing spermatids. As the shearing action of the passing perfusate tears off these cellular luminal extensions, the Sertoli cell is compromised, leading to the breakup of the cell. It is possible, once one Sertoli cell is broken down, that the adjacent Sertoli cells start to breakup or tear away from the basement layer resulting in a 'zipper' effect which eventually strips the entire germinal epithelium distal to the first point of break down. It was clear from the results that any perfusate rate higher than 0.14 $\mu\text{l}/\text{min}$ would result in varying degrees of morphological damage to the germinal epithelium, the worst being the stripping of the entire germinal epithelium. In the latter case the tubule's myoid layer was left intact, clearly showing its polygonally shaped cells forming the outer myoid layer of the seminiferous tubule. The intracellular compartment of the myoid cells also excluded trypan blue in the perfusate, further endorsing these cells' viability. This showed that the germinal and myoid layers which make up the seminiferous tubule are entirely separate layers from a morphological point of view. However, from a physiological perspective there is strong evidence in the literature which supports the view that these two layers are paracrinally interconnected with each other (Lian and Enders, 1994; Tung and Fritz, 1991; Zwain, *et. al.*, 1993). Vogl and Soucy (1985) also demonstrated that these two layers could easily be separated in the ground squirrel when exposed to EDTA in a phosphate buffered saline. Russell *et. al.* (1989) used this technique in rats to isolate sheets of germinal epithelium and myoid sleeves. They also showed that the myoid sleeves could be made to contract when exposed to Ca^{2+} and ATP.

Studies have shown that the myoid layer forms the first part of the blood-testis barrier,

while the Sertoli cell layer forms the second part of this barrier (Dym and Fawcett, 1970) (also see chapter 1). Therefore, if the germinal layer could be stripped from a perfused seminiferous tubule using high pressure perfusion, an excellent opportunity is presented to study the myoid layer on its own in its three dimensional tubular shape.

3.4.2 Alternative Methods

In addition to studying the effects of various perfusate flow rates on the morphology of the seminiferous tubules, various alternative techniques were either developed or modified and then investigated in an endeavour to find the best method to measure potentials across the seminiferous tubular epithelium.

3.4.2.1 The Agar Probe

Essentially the difference between this technique and the normal method of perfusion (Burg, *et. al.*, 1966) is that the perfusion pipette is substituted for a pipette with similar dimensions, but filled with agar. The agar in the perfusion pipette creates an electrical continuum which connects the luminal environment with the headstage measuring V_t . Thus, this method succeeds at positioning an electrical probe within the lumen of the seminiferous tubule. The main physiological disadvantage using the agar probe technique was simply that the lumen was not perfused and therefore the chemical make up of the luminal environment had to be assumed. However, the ionic concentrations of the bath with Ringers could be changed *ad libitum* and the resulting changes to V_t could be

investigated without disturbing the internal *milieu* of the lumen.

3.4.2.2 The Micro Perfusion Pipette

During the normal running of an experiment it is customary to change the perfusate or merely just to remove a piece of debris (or an air bubble) blocking the perfusion tip by retro suction of the perfusion pipette. This is accomplished by applying a large retro suction pressure via a syringe connected to the perfusion pipette. This produces a suction affect at the perfusion tip which by virtue of its function is positioned within the tubular lumen. If the tip diameter is too large (approximately 30-50 μm) some of the luminal contents could be sucked back through the perfusion pipette damaging the germinal layer, resulting in an immediate irrecoverable drop in V_t . Tip diameters of micropipettes used in micropuncture studies were typically between 25 and 50 μm (Levine and Marsh, 1971; Mattmueller and Hinton, 1991).

This scenario, however, can be avoided if the perfusion tip is made very small (approximately 15-25 μm). The advantage of this modification to the perfusion tip is that retro suction can no longer affect the lumen adversely because the small tip size now prevents large suction forces at the luminal side of the perfusion tip, thus preventing damage to the germinal layer. Furthermore, because the flow rate is even further reduced by the small tip size, the effects of perfusate flow through the lumen is a far less damaging factor.

3.4.2.3 The Oil-gap Method

The oil-gap method is an elegant technique (Ramsay, 1954) which provides interesting insights to some general electrophysiological functions of any tubule. However, the shortcomings of the 'oil-gap' technique discussed in chapter 5, prevents it from being a first choice electrophysiological technique for seminiferous tubules.

In this study care had to be taken that the viscosity of the oil (liquid paraffin) that separated the two baths was low enough so that the tubule section which passed via the oil gap would not be compressed, so as to prevent the perfusion of the lumen. A limiting factor in this regard was that if the viscosity of the oil was too low the oil tended to wash out of the oil-gap which led to the effective short circuiting of the preparation (as the oil acts as the electrical insulation between the two baths - see chapter two).

Compression of the lumen always occurred to some degree but this did not appear to prevent electrical continuity of the lumen. Also, the compression did not disrupt the morphology of the germinal epithelium when compared to control tubules.

3.5 Summary and Conclusion: The best method?

Ideally, the best method would be one in which the *in vivo* anatomical and physiological properties are maintained throughout the experimental procedure. In an attempt to measure the electrical parameters across the seminiferous tubules the perfusion technique

had to be modified and fine tuned. Alternative techniques were also tested and compared. The best available method has to be one that interferes the least with the *in vivo* physiological state and also which enables the monitoring of the key variables.

The three techniques which have been evaluated here are: (i) the agar probe technique, (ii) the oil-gap technique and (iii) the perfusion technique, with its perfusion pipette tip modification (micro tip). The agar probe provides a good indication of the transepithelial potential (see chapter 4 and 5) without having interfered with the internal luminal milieu, but suffers the disadvantage of having to assume the ionic conditions of the lumen. Furthermore, V_t was not significantly different from the micro perfusion tip techniques. The oil-gap technique suffers from the liabilities that have been discussed above and in chapter 5, although it is an elegant alternative if the perfusion technique is not suitable. Furthermore, as in the case of the agar probe, luminal ionic conditions have to be assumed. In the case of the perfusion technique, the luminal ionic conditions are controlled and can be changed according to the requirements of the experimental protocol. Therefore, as long as the precautions, discussed above are observed and damage to the germinal epithelium is reduced to a minimum, the micro perfusion tip technique is probably the best method for investigating the transepithelial potential from a perfusion perspective.

In retrospect, the fragility of the rat seminiferous tubule presents so many areas of initial difficulty that the task of perfusion of seminiferous tubules remains a daunting task. Moreover, if the results of two dimensional cell culture studies correlate closely with this type of three dimensional perfusion study (assuming that the three dimensional study

most closely approximates the *in vivo* conditions), perhaps the best route to study physiological mechanisms across the seminiferous epithelium would be the former.



CHAPTER 4

Electrophysiological Results

4.1 Introduction

The electrophysiological data from three different techniques are reported in this chapter. In the oil-gap and agar probe techniques, only change in the transepithelial potential was measured, while the data collected using the modified perfusion technique includes preliminary cable data. All data reported in this chapter are means±standard deviation, unless otherwise stated.

4.2 Transepithelial potentials: A comparison of techniques in morphology study

The transepithelial potentials (V_t) recorded in seminiferous tubules using the oil-gap technique, the agar probe technique, the modified perfusion pipette technique and the perfusion technique (see chapter 2 for details) using three perfusion heights (viz. 2.5 cm, 9.1 cm and 18.3 cm) were compared using one way analysis of variance (Medcalc). The results are tabulated below (table 4.1) and are graphically presented using notched box-and-whisker plots (see figure 4.1). The V_t 's of oil-gap, the agar probe technique, the modified perfusion pipette technique and the perfusion technique (perfusate chamber height of 2.5 cm) were not significantly different from each other ($P < 0.05$) but were

significantly different from V_t 's recorded from the seminiferous tubules using a perfusate height of 9.1 cm and 18.3 cm (see table 4.1). The mean V_t s recorded from the 9.1 cm and 18.3 cm perfusate height experiments were either positive (18.3cm:) or closer to 0mV than the other techniques used. Using the statistical procedure of one way analysis of variance, the data from the oil-gap, agar probe, modified perfusion tip techniques and perfusion from a low perfusate height of 2.5 cm were combined and compared with V_t 's recorded using perfusate chamber height of 9.1 and 18.3 cm: the combined data (see table 4.2) resulted in a mean V_t of -5.141 mV which was significantly different from the 9.1 and 18.3 cm V_t groups ($P < 0.0001$).

Technique	n	mean (mV)±SD	Different from factor number ($P < 0.05$)
PH=2.5 cm (3)	8	-4.1250 ± 2.2	(2)(4)
PH=9.1 cm (4)	9	-0.6350 ± 1.5	(1)(3)(5)(6)
PH=18.3 cm (2)	7	0.8929 ± 3.4	(1)(3)(5)(6)
Oil-gap (6)	9	-5.0556 ± 2.4	(2)(4)
Agar Probe (1)	8	-5.6625 ± 1.5	(2)(4)
MPP (5)	17	-5.4176 ± 1.8	(2)(4)

Table 4.1: The means in the above table were derived using one way analysis of variance and were compared with each other using the statistical procedure 'Student-Newman-Keuls test for pairwise comparisons'. Perfusate height is denoted by PH, while modified perfusion pipette is denoted by MPP.

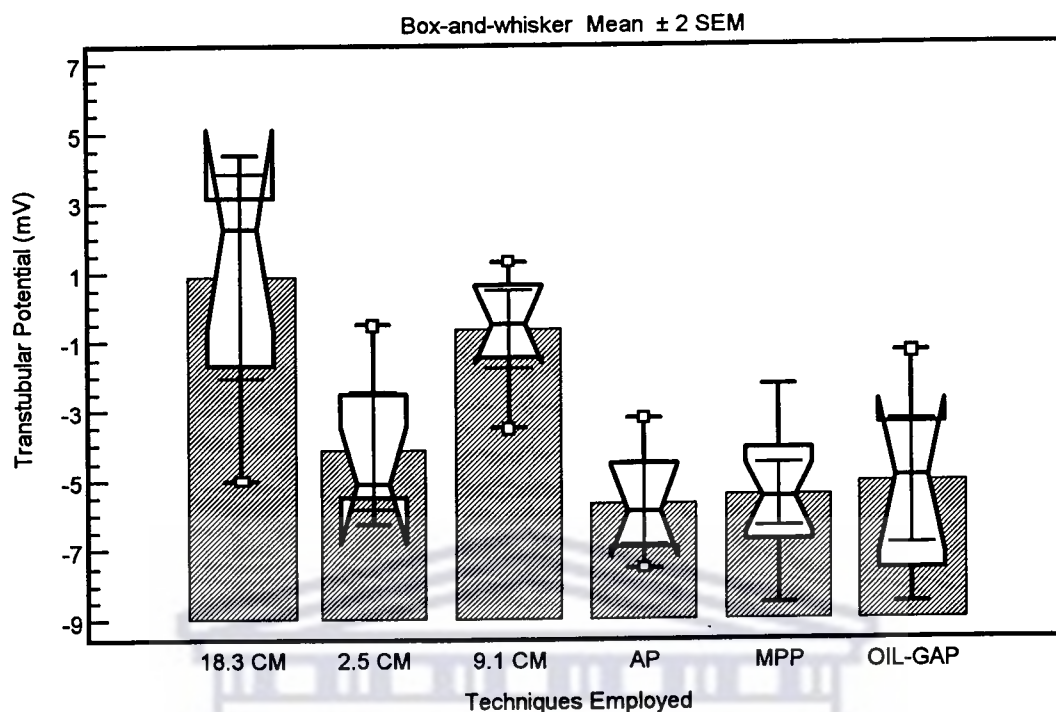


Figure 4.1: In the above diagram AP denotes agar probe while MPP denotes modified perfusion pipette. The values in centimeters (cm) on the X-axis indicate the height of the perfusate chamber above the perfusion bath (see chapter 2). See footnote¹ for interpretation of the Box-and-Whisker plots.

4.3 Equilibration Time

The transepithelial potential (V_t) recorded using the oil-gap, agar probe and modified pipette tip techniques generally settled down within a period of 5 to 10 minutes (see figures 4.2 to 4.4). All experimental permutations were only carried out once V_t had settled and was constant. Tubules with considerable drift were not included for statistical data collection. Reasons for drift of some of the tubules were unknown and could have

¹

The thick T-bar represents the data distribution from lowest to highest value. The notches indicate the standard deviation. The thin T-bar indicates the 95% confidence interval of the mean. These graphical presentations support the statistical analysis in table 4.1.

ONE-WAY ANALYSIS OF VARIANCE

DATA : Combined Vt data versus 9.1 and 18.3 cm experiment groups

Source of variation Sum of squares D.F. Mean square

Between groups
(influence factor) 319.3471 2 159.6736

Within groups
(other fluctuations) 252.6673 55 4.5940

Total 572.0144 57

F-ratio : 34.757

Significance level : $P = 0.023$

Student-Newman-Keuls test for all pairwise comparisons

Techniques	n	mean (mV)	Different from factor number ($P < 0.0001$)
(1) Combined data	42	-5.1405	(2)(3)
(2) PH=18.3 cm	7	0.8929	(1)
(3) PH=9.1 cm	9	-0.6350	(1)

Table 4.2: The table summarizes the Vt results of combined data (i.e. the different technique groups in which Vt data had not significantly differed from each other ($P < 0.05$)) versus the Vt data of the 9.1 and 18.3 cm perfusate height experiments using 'one way' anova test (Medcalc). PH=perfusate height above the perfusion bath; n=number of seminiferous tubules.

originated from a variety of causes. Usually, after a tubule developed substantial drift the entire recording system was checked and primed, which included anything from coating any silver wire electrodes with chloride to remaking the agar bridges. At times drift arose from the perfusion apparatus when a bubble developed in a perfusion tube or the perfusion pipettes. In the latter case drift could be eliminated simply through removing the bubble by sucking perfusate through the perfusion system.

4.4 Effects of bath temperature on V_t

The effect of different perfusion bath temperatures was tested on 5 perfused tubules which had developed a steady V_t . The mean V_t for these tubules was -5.1 ± 2.1 mV. The bath temperature (35°C) was initially decreased to room temperature (20°C) and then elevated to 38°C in steps of 2°C , while each change was held for a 10 minute period. There were no statistically significant changes in V_t between individual steps of temperature changes. However, across the entire decreased temperature range (35°C (control value) to 21°C), statistical analysis showed a small but significant change in V_t (-0.125 ± 0.05 mV; $P < 0.05$) while V_t increased slightly from control values when the temperature was increased to 38°C (0.204 ± 0.03 mV; $P < 0.05$).

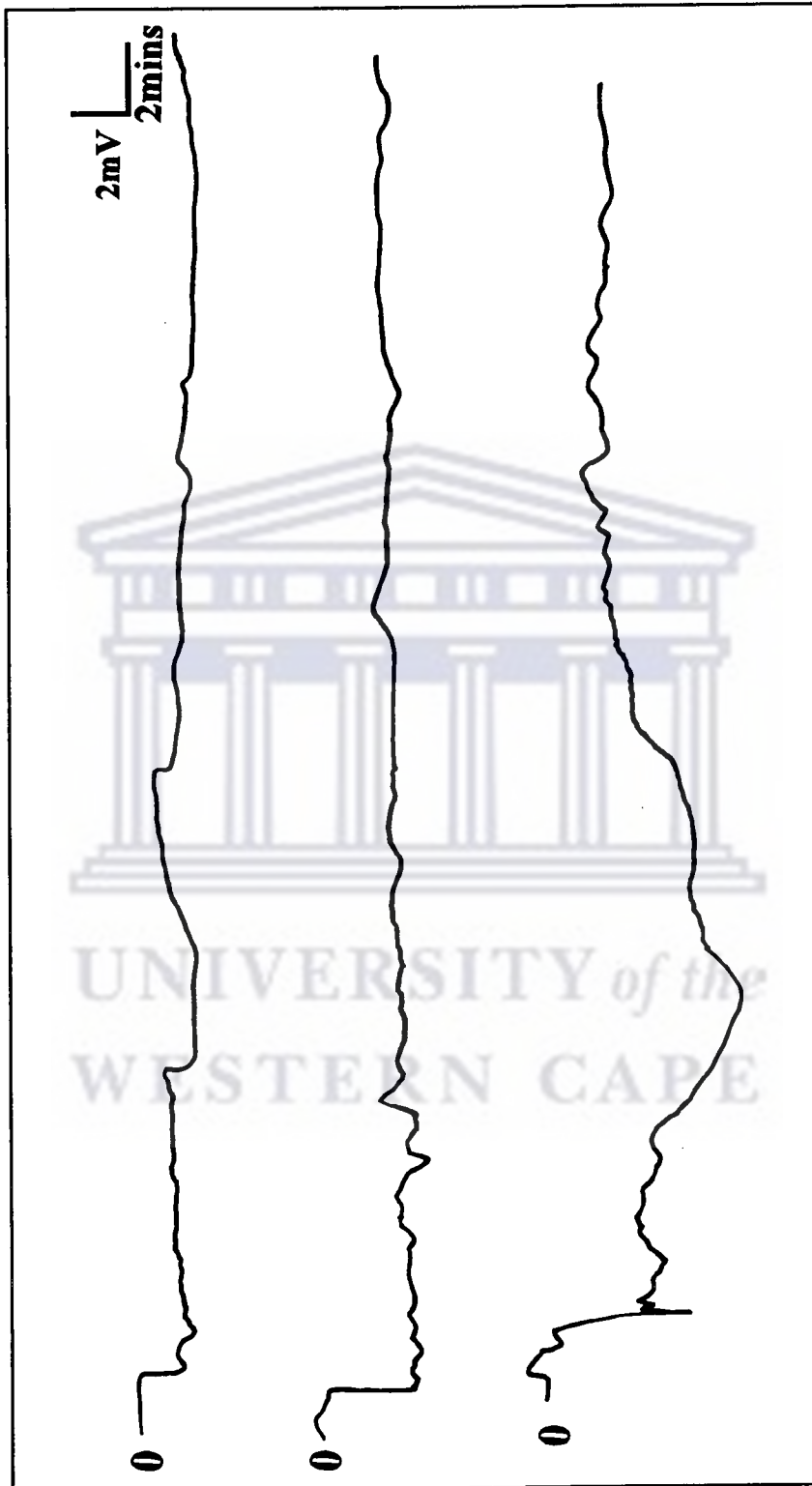


Figure 4.2: The above V_t traces were recorded using the agar probe technique. The zeros represent the 0mV baseline. The first part of the bottom trace represents a recorded V_t trace with excessive drift.

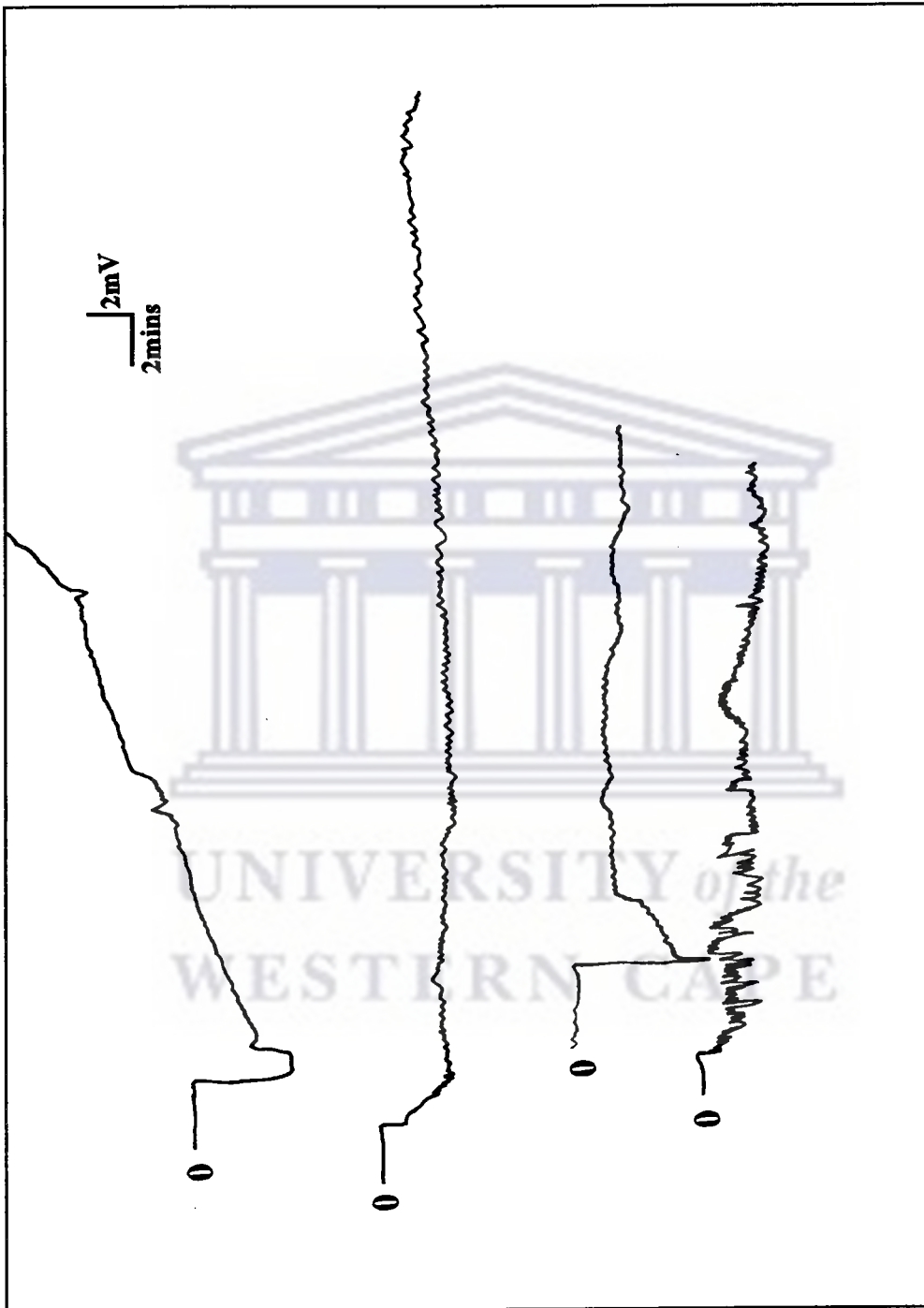


Figure 4.3: The above traces represent V_t recorded using the oil-gap technique. The zeros represent the 0mV baseline. The top trace shows the recorded V_t with excessive drift.

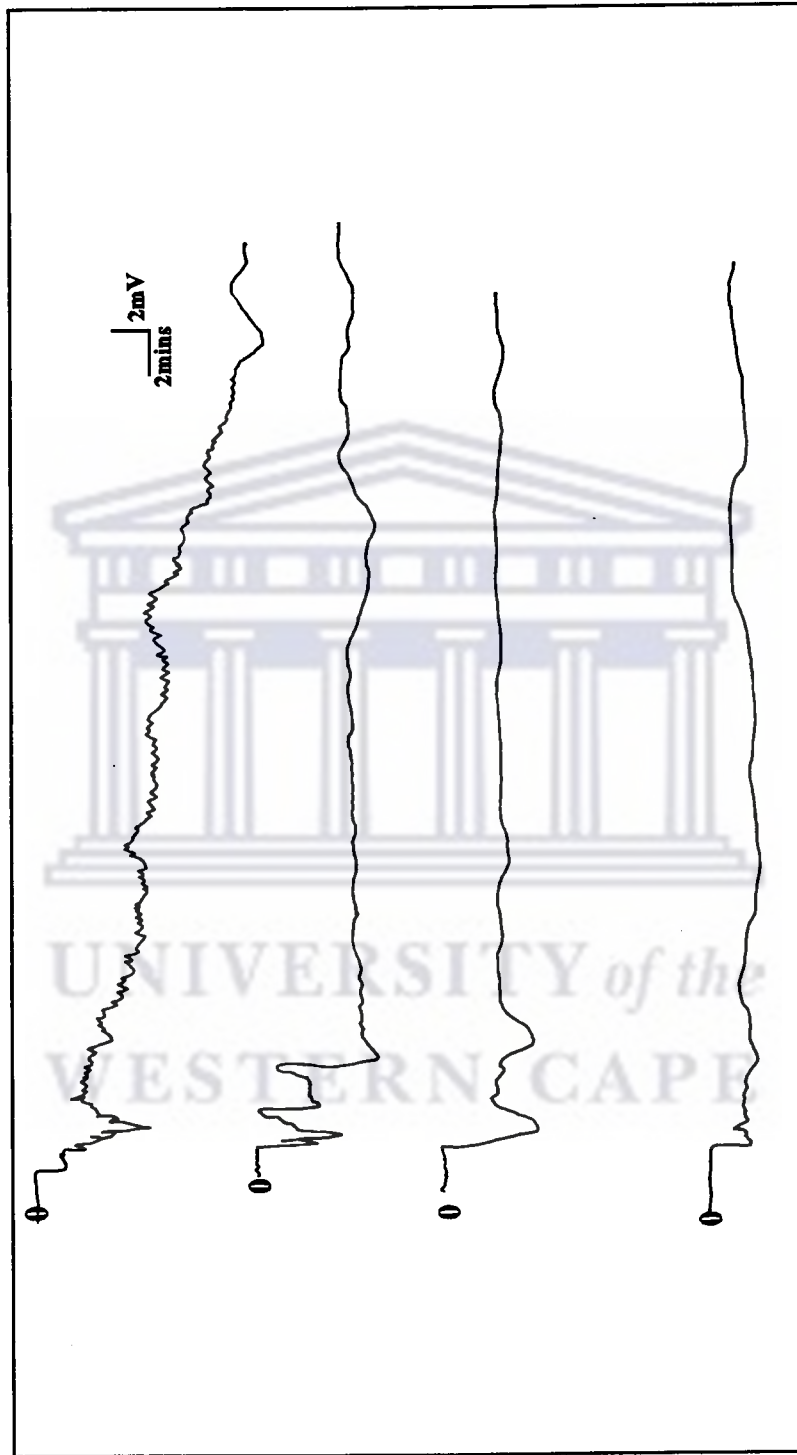


Figure 4.4: The above diagram represents Vt traces copied directly from the original hardcopies. The zeros represent the base line for 0mV. The top trace is an example of a trace with excessive drift.

4.5 Oil-gap experiments

Seminiferous tubules bathed in a control Ringer (for composition see bath B in table 2.1) had a mean V_t of -5.06 ± 2.45 mV ($n=9$), the lumen being negative with respect to the bath solution. Stable V_t 's often occurred within 2 to 5 minutes and would remain stable with relatively little drift for up to 180 minutes. Setting up the tubule in the oil-gap bath was carried out in such a way that the short, open end of the tubule (compartment B: figure 2.2) was always the same length. The length of tubule in compartment A varied from 12 mm to 20 mm in length. For the purpose of the current study it is important to note that V_t represents the transepithelial potential with reference to the bath (0 mV) and that a decrease or increase in V_t refers to a change in the magnitude of that value.

4.5.1 Effects of High potassium Ringers

It is well known that the concentration of K^+ is unusually high (46.2 ± 3.9 mM) in the lumen of the seminiferous tubules (Levine and Marsh, 1971). In order to investigate the

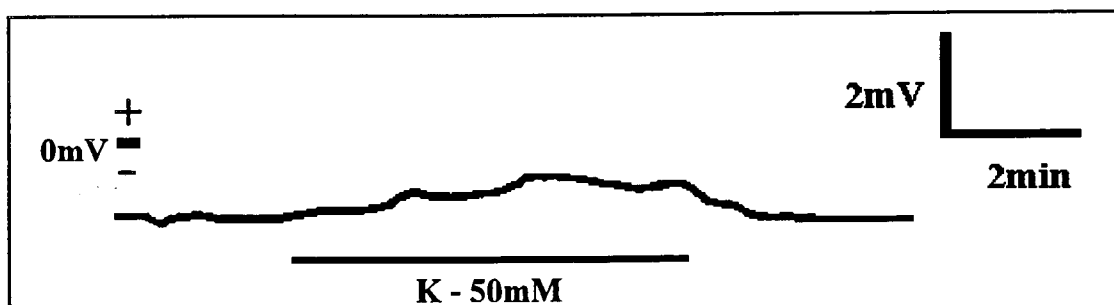


Figure 4.5: The above trace represents a typical V_t response to 50 mM potassium Ringers (bar) which was introduced into compartment A of the oil-gap bath.

effects of an elevated K^+ concentration the control Ringers (potassium concentration 5 mM) in both compartments was exchanged with Ringers (Bath E in table 2.1) having a total concentration of 50 mM potassium. The average V_t changed from -2.9 ± 1.5 mV to -1.96 ± 1.5 mV ($n=5$; $P < 0.0009$). Figure 4.5 represents a typical response. When control Ringers was reintroduced V_t recovered to a mean value of -2.7 ± 1.5 mV.

4.5.2 Effects of Low Chloride Ringers

The exchange of bath B Ringers (111 mM Cl^-) for low chloride Ringers (2 mM Cl^-) caused a transient deflection during which V_t became increasingly negative. This was followed rapidly by V_t falling to values close to zero (and in some cases the lumen developed positive V_t values) which subsequently stabilized (see figure 4.7). Table 4.3 shows mean values of V_t measured under control conditions and during periods of reduced Cl^-

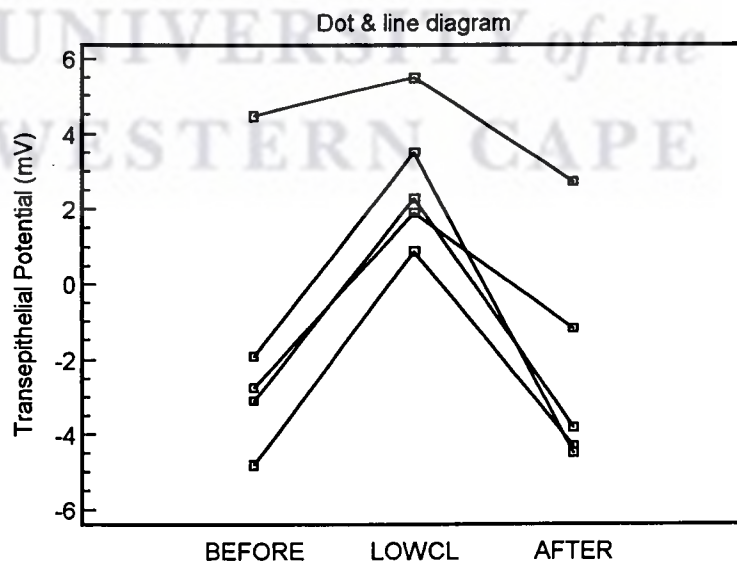


Figure 4.6: The above diagram shows the clear trend of an increased negative V_t in response to low chloride Ringers and the recovery of V_t in response to the reintroduction of control Ringers.

concentration. The table also shows that V_t tended to recover to baseline values after Cl^- was replaced ($P < 0.0065$).

	Control (mV)	Low Cl^- (mV)	Control (mV)
Mean	-1.6*	2.82**	-1.1 ⁺
\pm SD	3.6	1.7	3.57
Number of tubules	5	5	5

Table 4.3: Effects of reducing bath Cl^- from 111mM (control) to 2mM. Paired T-test showed control V_t significantly different from the low Cl^- group. V_t recovered after the control Ringers was reintroduced. $P < 0.0072^*$ and $P < 0.0065^+$.

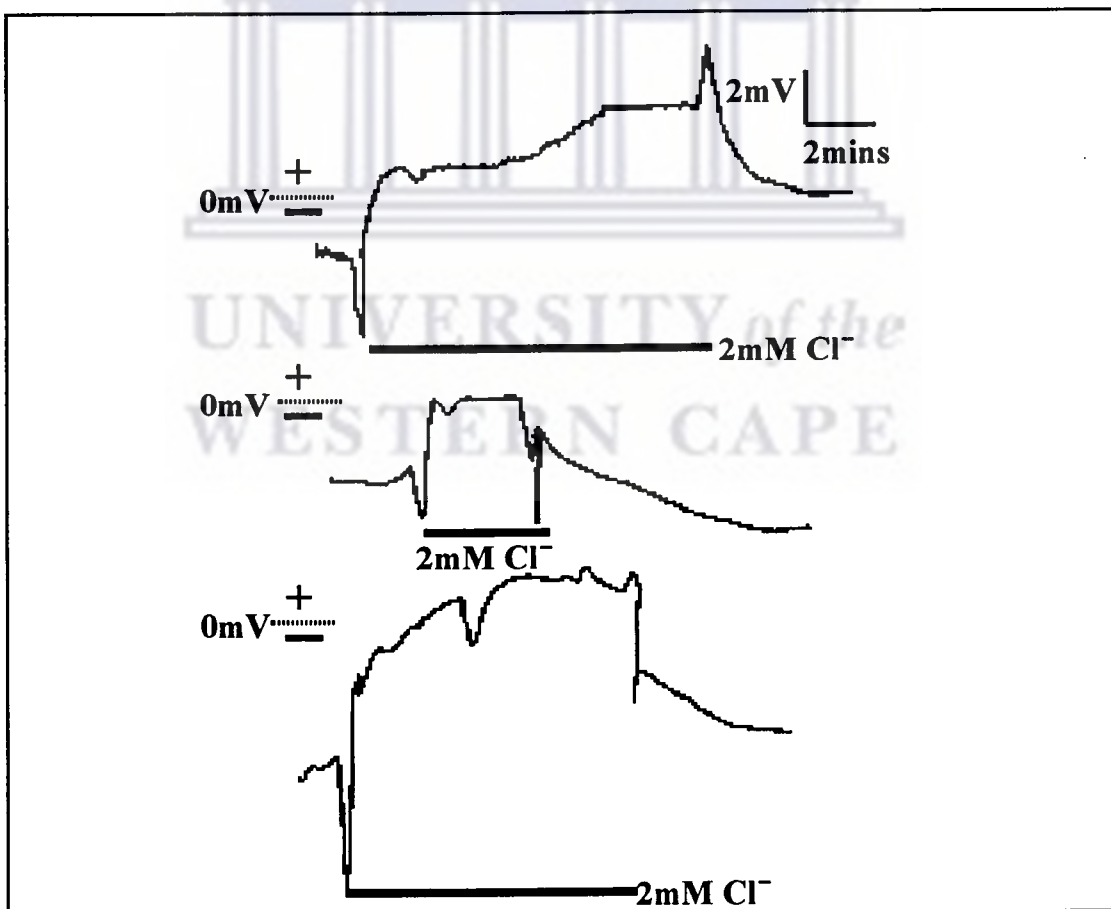


Figure 4.7: Effect of reducing the Cl^- concentration from 111 mM to 2 mM on tubule V_t . Bars denote periods during which Cl^- was reduced.

4.5.3 Effects of Furosemide and Bumetanide

Furosemide and bumetanide are drugs which are reported to inhibit sodium chloride co-transport processes in various tissues (Palfrey, *et al.*, 1983). At the introduction of furosemide V_t rapidly changed from a mean of -2.67 ± 3.7 mV to 2.08 ± 4.05 mV ($n=7$). At the reintroduction of the control bath Ringers (Bath B) this change was reversed to -4.76 ± 1.29 mV (see figure 4.9).

The introduction of bumetanide (10^{-4} M) into the bathing medium resulted in a similar response in V_t to that seen after furosemide (see table 4.4 for summary of results and figure 4.9). These changes were also reversed when the control bath Ringers was reintroduced.

	n	Control	Treatment	Control	P<
Furosemide	7	$-2.67 \pm 3.7^*$	$2.07 \pm 4.05^{*+}$	$-4.76 \pm 1.29^+$	0.027* and 0.04+
Bumetanide	5	$-4.7 \pm 1.3^{**}$	$-1.14 \pm 2.1^{**}$	-3.16 ± 1.34	0.0034**

Table 4.4: Effects of furosemide and bumetanide on V_t are summarized. Values are given in means (mV) \pm SD, and *P* values represent the comparison determined using paired T-test. In the bumetanide treated tubules the reintroduction of control Ringers saw a mean recovery in V_t , however, this change was not statistically significant.

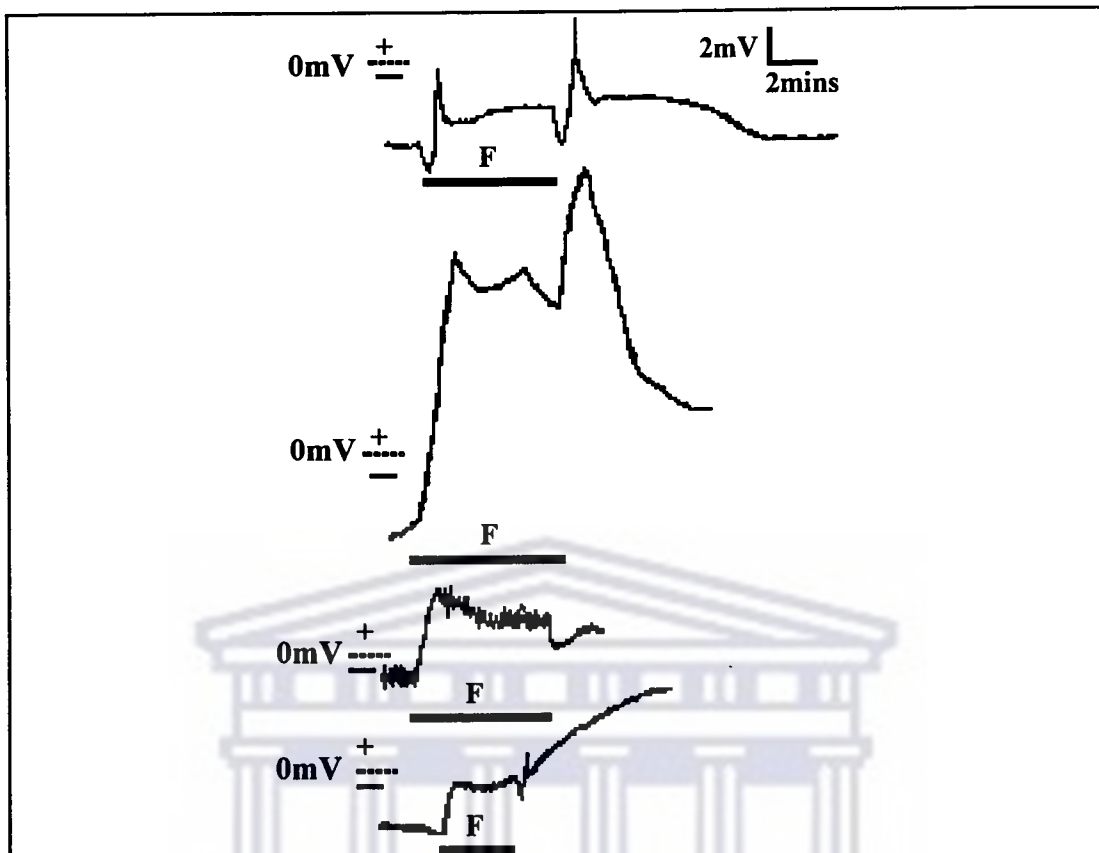


Figure 4.8: The above traces represent some of the responses of Vt to 1mM furosemide (F). The bar denotes the period during which furosemide was present in the bath Ringers.

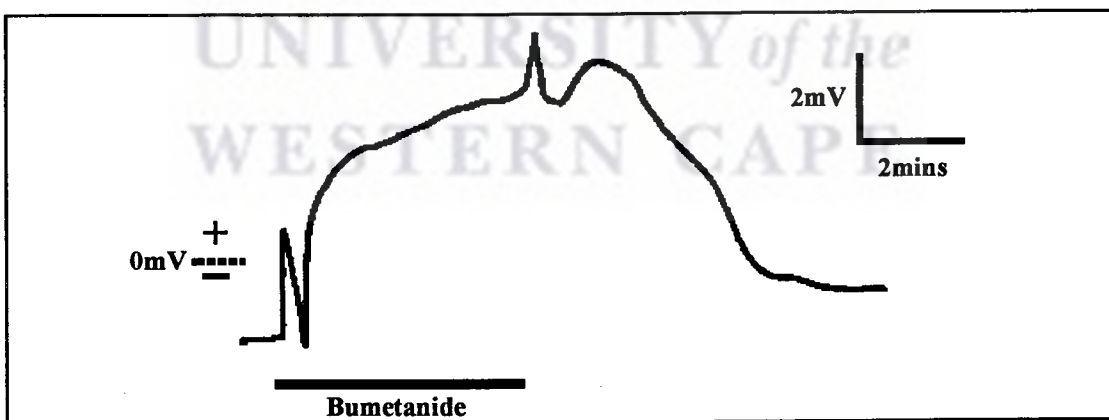


Figure 4.9: The above trace represents a typical response of Vt to bumetanide. The horizontal bar refers to the period of bumetanide exposure.

4.5.4 Effects of BaCl₂

Barium ions (2mM), known to block K⁺ channels in many tissues, resulted in a variable response so that mean V_t did not change significantly (-3.1 ± 1.5 mV to -3.13 ± 2.6 mV (n=5)) in response to 2mM BaCl₂. In two cases the response was an increase in lumen negativity, while in two other cases the response was a decrease in negativity; in the remaining case V_t did not respond (see figure 4.10). Upon returning control Ringers (bath B) V_t remained statistically unchanged (-2.67 ± 3.7 mV; $P < 0.9781$).

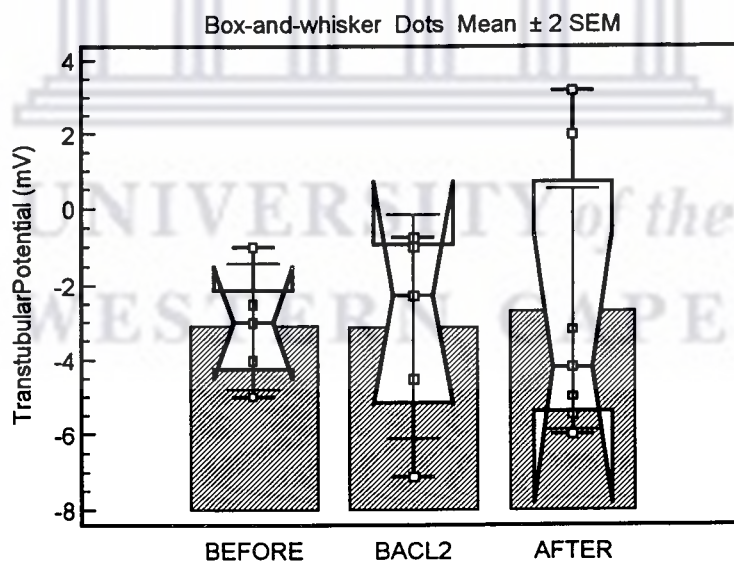


Figure 4.10: The above plot shows that BaCl₂ had no statistical effect on V_t in the oil-gap experiments. See footnote 1 on page 75 for the interpretation of box-and-whisker plot.

4.6 Agar-probe Experiments

The intraluminal agar probe was used as an alternative method to record V_t with the minimum disruption of the luminal environment from a morphological and ionic point of view. Stable V_t 's were recorded for over 180 minutes with little or no drift.

Eight tubules had a mean V_t of -5.66 ± 1.51 mV (range: -3.2 mV to -7.5 mV) and were morphologically examined at the end of the recording period (see chapter 2). The mean V_t of these tubules did not differ significantly from the oil-gap, 2.5 cm perfusate height and modified perfusion pipette groups (see section 4.2).

4.6.1 Effects of Low Chloride Ringers

The depletion of chloride from the bathing medium resulted in a decreased mean V_t negativity (from -3.43 ± 2.56 mV to -1.38 ± 2.37 mV ($P > 0.05$)). The reintroduction of chloride (111 mM) resulted in the mean V_t recovering to some degree (-2.43 ± 2.4 mV; $P > 0.05$). Figure 4.11 attempts to show a possible trend in that 5 of the 7 tubules responded by its lumen becoming more positive with respect to the bathing medium, while on returning control to the bathing Ringers (Cl^- - 111 mM) 4 of the 7 tubules recovered to a degree (these changes were not statistically different from each other (Wilcoxon test)). Figure 4.12 shows some V_t responses to a decreased chloride concentration.

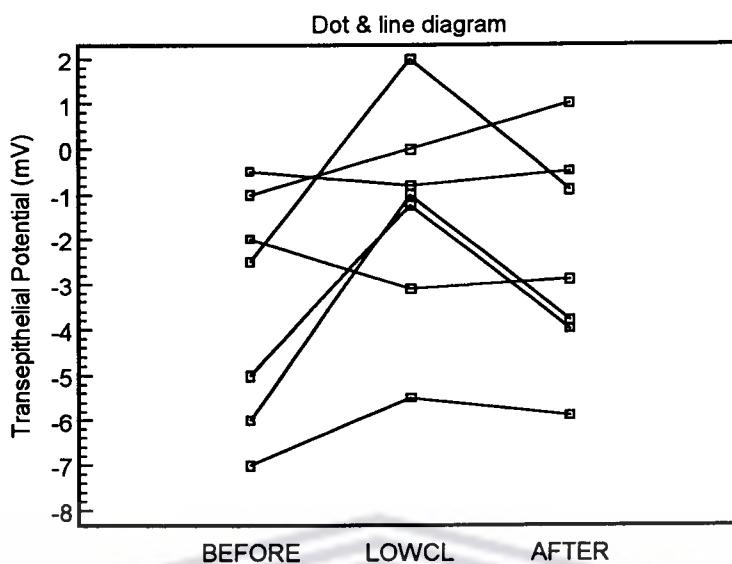


Figure 4.11: The above diagram depicts the change in V_t to a decreased chloride concentration (111 mM to 2 mM) using the agar probe technique.

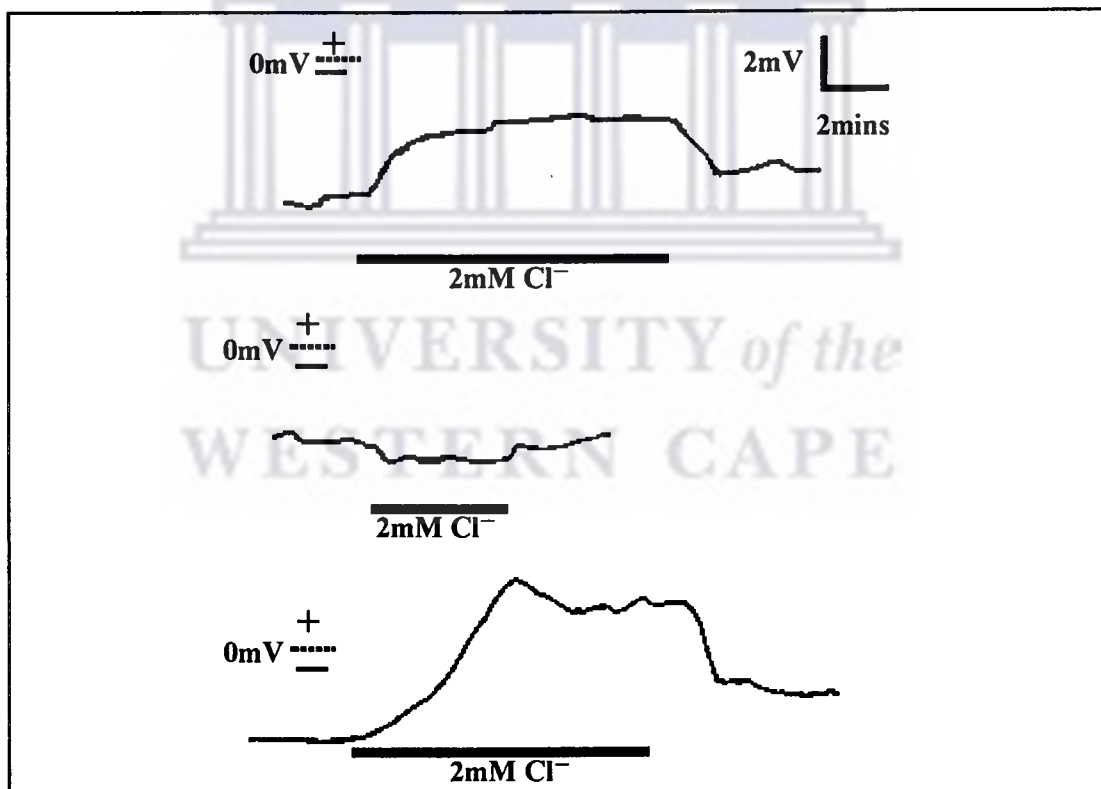


Figure 4.12: The above diagram depicts some of the V_t responses to low chloride concentration (bar). The agar probe technique was used to monitor V_t in the above cases.

4.6.2 Effects of Furosemide

Furosemide significantly changed V_t from -2.76 ± 2.9 mV to -0.93 ± 2.25 mV ($P < 0.0008$). After returning to control conditions (bath B Ringers) the mean V_t returned to -2.58 ± 1.8 mV which was just not statistically ($P = 0.07$) different from the mean V_t recorded from the furosemide V_t group. Figure 4.13 shows a diagram depicting the repetitive V_t response to furosemide treatment.

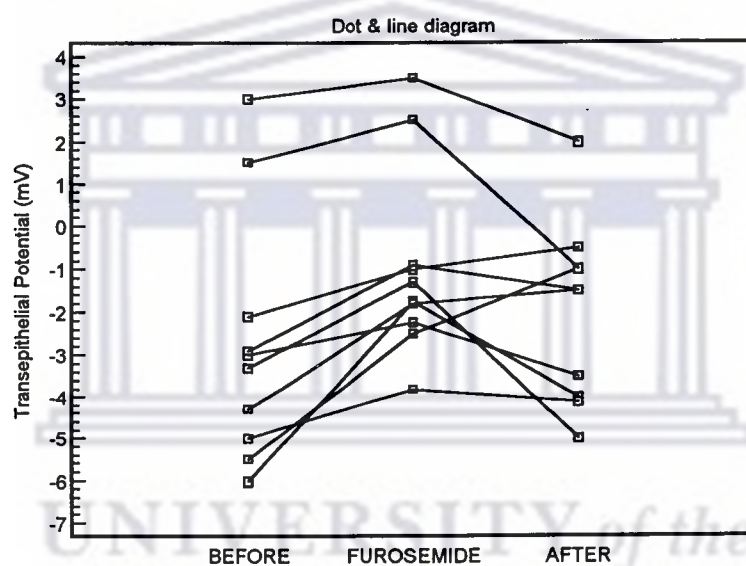


Figure 4.13: the above diagram shows a significant trend ($P < 0.0008$) in V_t 's response to furosemide recorded using the agar probe technique.

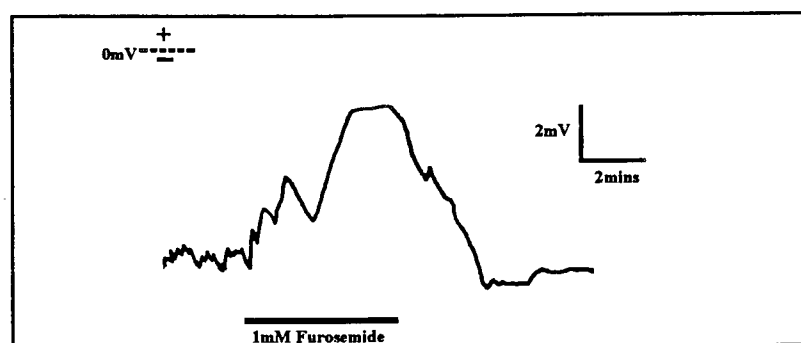


Figure 4.14: the above trace depicts the effects of 1 mM furosemide on V_t recorded via the agar probe technique. The bar denotes the period of furosemide treatment.

4.6.3 Effects of $BaCl_2$

The addition of 2mM Ba^{++} ions to the bathing medium changed V_t from -2.59 ± 2.2 mV to -1.13 ± 1.85 mV ($P < 0.02$; $n = 10$). Figure 4.16 shows some recorded V_t traces. The removal of barium ions from the bathing medium increased the mean V_t to -2.76 ± 2.9 mV. However, this recovery of V_t was not statistically different from the barium treatment group ($P = 0.08$). Figure 4.15 shows that the overall trend is an increase in the negativity of the lumen relative to the bathing medium in that 6 out of 10 tubules treated responded by an increase in luminal negativity, while 2 tubules remained unchanged and 2 tubules responded with an increased positive luminal potential.

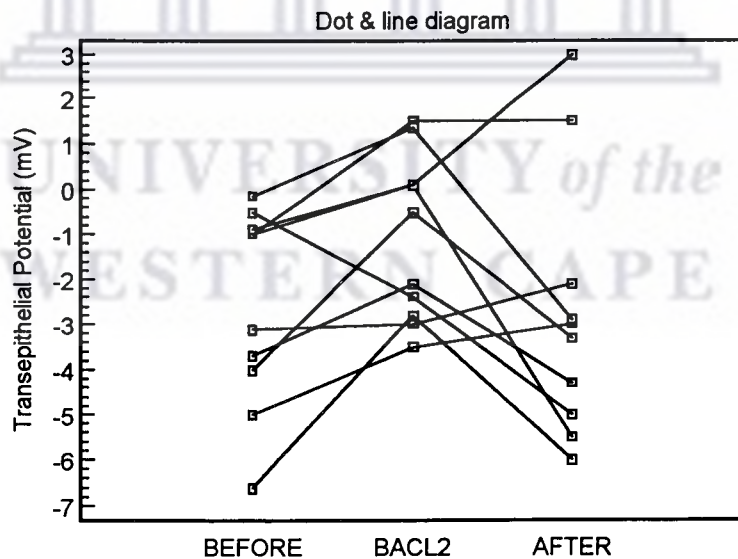


Figure 4.15: The above diagram shows recorded V_t 's before, during and after $BaCl_2$ treatment. V_t was recorded using the agar probe technique.

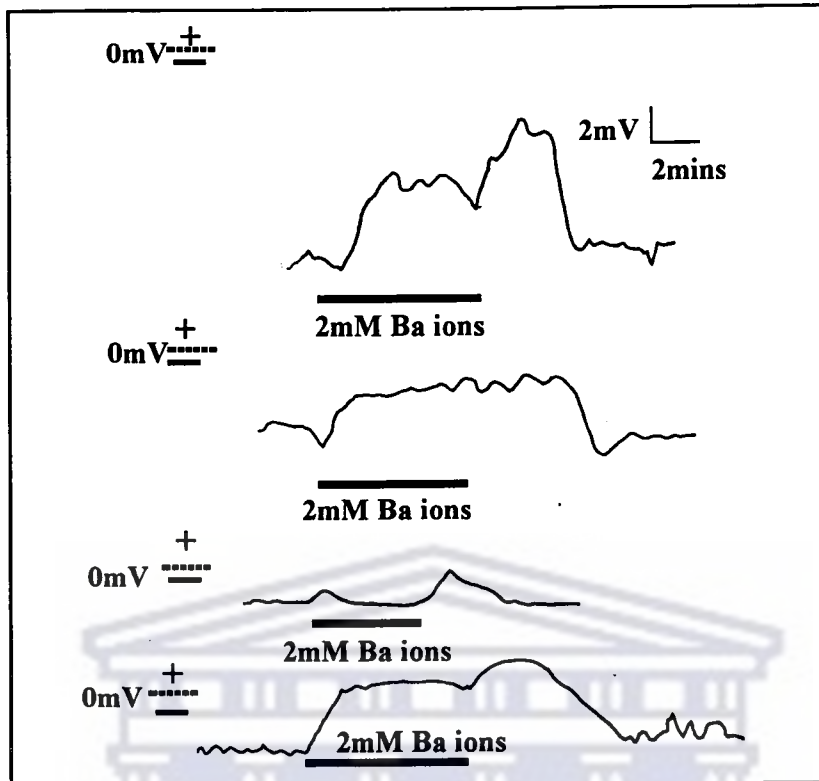


Figure 4.16: The above diagram depicts Vt traces monitored with an agar probe showing the effects of BaCl₂ (denoted with bars).

4.6.4 Effects of DNP

The effects of DNP was tested on 5 tubules which had Vt monitored via the agar probe technique. DNP had no statistically significant effects on Vt: see table 4.5. for average values before, during and after DNP treatment. Figure 4.17 uses the notched box and whisker plot to further illustrate this trend.

	Before	DNP	After
Vt (mV)	-2.01±2.1	-1.8±2.93	-3.42±2.55

Table 4.5: Although there is an average decrease in Vt in response to DNP and a return to a mean control Vt after treatment, these responses were not statistically significantly different (Wilcoxon test: $P>0.2$).

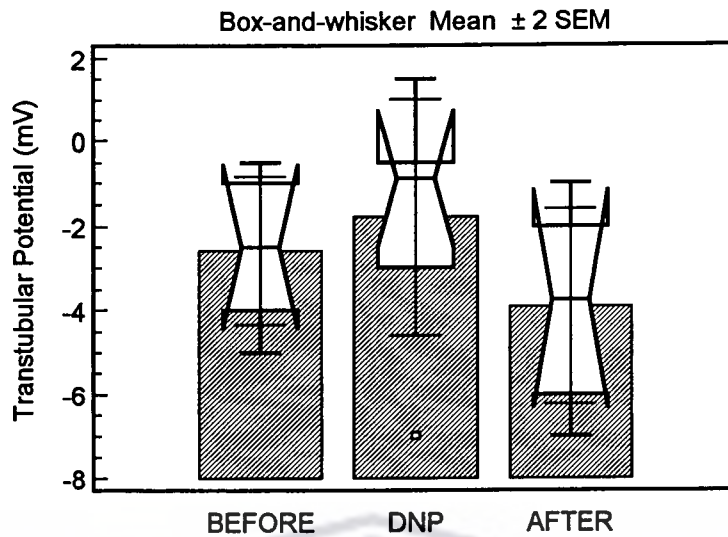


Figure 4.15: The above diagram shows the effects of DNP.

4.7 Perfusion Experiments

4.7.1 Introduction

These experiments were all carried out using the Burg, *et. al.* (1968) perfusion pipette setup with the perfusate chamber at 2.5 cm above the perfusion bath and the perfusion pipette tip narrowed to prevent damaging suction currents during the suction process of exchanging the perfusate or clearing a blocked (bubble trap) perfusion pipette. Before the start of experiments the electrical resistance of the perfusion pipettes was adjusted, using a Wheatstone bridge circuit on the Axon amplifier so that current injection resulted in no change in voltage. For a detailed description of the perfusion setup and the electrical arrangement, see chapter 2. If the bridge was found to be unbalanced by more than 3-5 mV, the cable data was discarded.

Although 25 rats were used for the current perfusion study, only the data of fourteen seminiferous tubules from 14 rats were used in this study. Once tubules were attached to the perfusion pipettes and V_t settled, control current pulses were used to obtain control cable values. Fractional resistances of the apical and basolateral membranes were not calculated as there was no means of predicting with certainty that a microelectrode was positioned in a Sertoli cell and not in a germ cell. This is also the reason for not reporting on intracellular voltages and not including the microelectrode data obtained during perfusion of the tubules in the current study.

4.7.2 Control cable parameters

Tubular length was measured from the point of the perfusion pipette tip to the Sylgard barrier of the collection pipette via a calibrated ocular micrometer. Care was taken to avoid the error of measurement (caused by the looping of the tubule between the two sets of pipettes) by measuring the length of the tubule while both sets of pipettes were close to the coverslip of the perfusion bath. The average length for tubule used to study cable parameters was $671.42 \pm 145.1 \mu\text{m}$ in length (range: 480 to 780 μm ; $n=14$).

All control cable values were taken after the 2V_o stabilized (± 10 to 15 minutes). A series of three sets of cable parameters, generated over a period of 3 minutes, was averaged to

2

V_o refers to the transepithelial potential as measured via the perfusion pipette at the proximal end of the tubule and is generally accepted in perfusion experiments to be equivalent to the transepithelial potential, V_t .

represent an individual tubule's control value for each cable parameter. The data was derived from 14 seminiferous tubules. The cable data were normally distributed ($P < 0.05$) and a paired t -test was used to establish a significant difference between groups ($P < 0.05$). Unless stated otherwise Medcalc statistical software package was used for statistical evaluation of the data. Table 4.6 tabulates the control cable parameter data.

Cable parameter	Unit	n	mean	±S.D.
V_o	mV	14	-5.16	1.45
Length constant (λ)	μm	14	296.77	70.17
Transepithelial resistance (R_t)	KOhm.cm	14	4.4	0.87
Luminal Resistance (R_c)	MOhms/cm	14	5.6	2.31
Diameter (electrical)(D_e)	μm	14	39.1	8.1
SCC	$\mu\text{Amps/cm}^2$	14	-96.2	64.87
SCCv	$\mu\text{Amps/cm}$	14	1.69	10.9
Input Resistance (R_i)	KOhms	14	152	44.87

Table 4.6: The above table summarizes the control values for the various cable parameters. SCC and SCCv is a measure of active transport and channel activity.

The diameter of the lumen was difficult to evaluate via the ocular micrometer as the lumen was not clearly visible and is as a morphological norm very irregular. It was therefore not possible to compare the diameter of the tubule measured via the ocular micrometer with the electrically determined diameter. The large difference between the values of SCC ($\mu\text{Amps/cm}^2$) and the virtual short circuit current (SCCv: $\mu\text{Amps/cm}$) is as a result of the former formula correcting for the surface area of the evaluated tubule.

Tubules were injected with currents which varied from 100 nA to 200 nA depending on the length of the tubule. Longer tubules were injected with larger currents as this improved the resolution of the voltage jumps at the distal end of the tubule. Appendix B tabulates the effects of the magnitude of the injected pulse of current on the proximal and distal voltage jumps in the perfused seminiferous tubule.

4.7.3 Induced Changes In V_o and Cable Parameters

4.7.3.1 Effects of High potassium Ringers

Control bath Ringers (K^+ : 5mM) was replaced with a high-K Ringers (bath E: 50mM). V_o did not change in response to the increased K concentration. However, there was a small but highly significant decrease in the transepithelial resistance (R_t) from 4.55 ± 0.92 to 3.95 ± 0.95 KOhm/cm ($P < 0.00001$). This was reflected in the decreased length constant (λ). The input resistance (R_{input}) also significantly decreased from 163.35 ± 33.84 to 148.21 ± 29.8 KOhms ($P < 0.00001$; paired t -test). The rest of the cable parameters did not change significantly and are tabulated in table 4.7.

4.7.3.2 Effects of $BaCl_2$

The effects of $BaCl_2$ on V_o and the cable parameters are summarized in table 4.8, while four traces illustrate typical responses (which reflects the mean response) of V_o in figure

4.19. However, the response of V_o was variable. Figure 4.18 shows the responses of all 14 tubules tested in a 'dot and line' diagram. This diagram illustrates that at times V_o did not respond, but in fact, increased the lumen's negative potential.

Effect of <i>High potassium Ringers</i>					
CABLE PARAMETERS		N	MEAN	±SD	$P \leq$
V_o (mV)	PRE	14	-2.11	1.19	0.7632
	POST	14	-2.05	1.19	
LAMBDA (μ)	PRE	14	299.74	70.78	0.0078
	POST	14	283.38	77.72	
R_t (KOhm.cm)	PRE	14	4.55	0.92	0.00001
	POST	14	3.95	0.95	
R_{core} (MOhm/cm)	PRE	14	5.86	2.54	0.479
	POST	14	5.75	2.79	
DIAMETER (μ)	PRE	14	39.46	8.39	0.207
	POST	14	39.96	8.71	
SCC _v (μ A/cm)	PRE	14	-0.49	0.29	0.269
	POST	14	-0.55	0.37	
SCC (μ A/cm ²)	PRE	14	-42.87	28.53	0.383
	POST	14	-48.1	40.1	
R_{input} (KOhm)	PRE	14	163.35	33.84	0.00001
	POST	14	148.21	29.8	

Table 4.7: $P > 0.05$ was considered not significantly different; N - number of tubules. Pre - control; Post - experimental. Cable parameters were measured before and after the potassium concentration in the perfusion bath was elevated from 5mM to 50mM. See Table 1 for abbreviations.

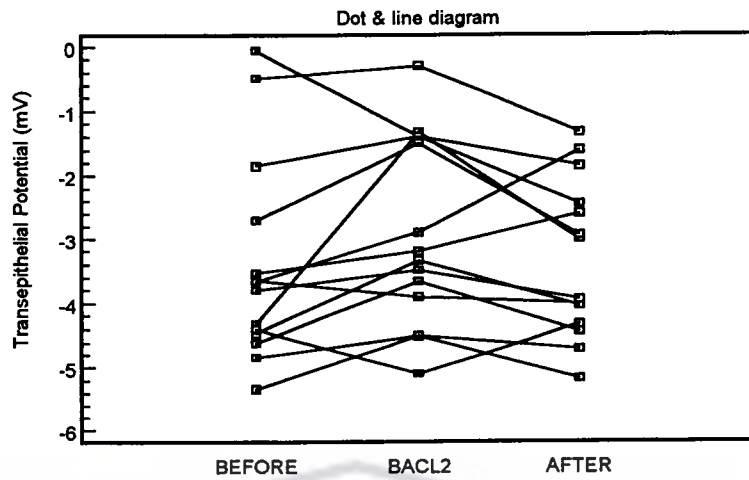


Figure 4.18: The above diagram shows the effects of 2mM BaCl₂ on transepithelial potential (V_o).

Statistically, control V_o was not different from V_o treated with 2mM BaCl₂. Removing BaCl₂ from the bathing medium also did not significantly change V_o ($P=0.09$).

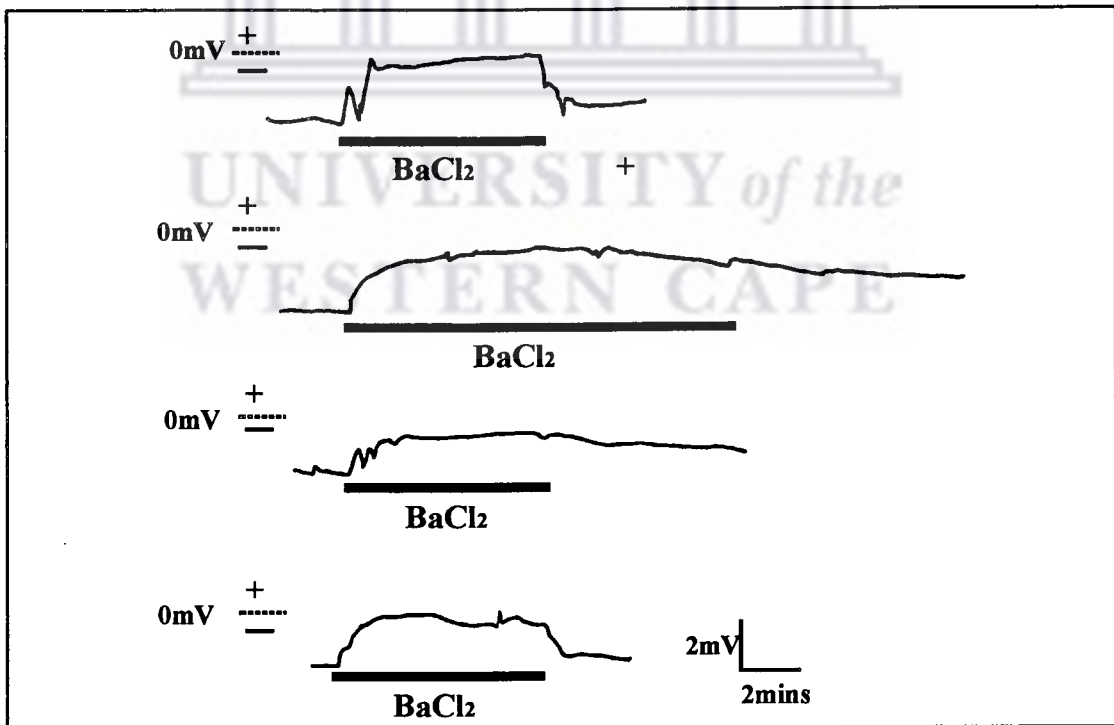


Figure 4.19: The above traces illustrates typical V_o responses to BaCl₂ when added to the perfusion bath. The dotted line represents the 0mV level.

Effect of <i>BACl₂</i> on V_o and Cable Parameters of the Rat Seminiferous tubule					
CABLE PARAMETERS		N	MEAN	\pm SD	$P \leq$
V_o (mV)	PRE	14	-3.41	1.59	0.08
	POST	14	-2.89	1.46	
LAMBDA (μ)	PRE	14	288.62	61.96	0.0004
	POST	14	324.2	62.7	
Rt (KOhm.cm)	PRE	14	4.45	0.89	0.0001
	POST	14	5.41	1.15	
Rcore (MOhm/cm)	PRE	14	5.8	2.08	0.05
	POST	14	5.5	1.73	
DIAMETER (μ)	PRE	14	38.45	6.56	0.95
	POST	14	39.3	6.42	
SCC _v (μ A/cm)	PRE	14	-0.79	0.4	0.0067
	POST	14	-0.56	0.28	
SCC (μ A/cm ²)	PRE	14	-68.22	40.98	0.0063
	POST	14	-46.88	26.9	
Rinput (KOhm)	PRE	14	162.32	28.27	0.00001
	POST	14	176.84	31.86	

Table 4.8: Differences between means were considered not significant if $P > 0.05$; N - number of tubules. Pre - control; Post - experimental. Cable parameters were measured before and after 2mM $BACl_2$ was introduced into the perfusion bath. See Table 1 for abbreviations.

Barium ions did significantly ($P < 0.0001$) increase R_t as well as the length constant ($P < 0.0004$). There was a slight but significant decrease in R_{core} . SCC and SCC_v both decreased significantly, at $P < 0.0067$ and $P < 0.0063$ respectively. All other cable values are summarized in table 4.8.

4.7.3.3 Effects of Low Chloride Concentration

The chloride concentration in the perfusion bath was decreased from 111mM (bath B Ringers) to 2mM (bath D Ringers). The effects of depleting the chloride concentration of the bathing Ringers, on V_o and the cable parameters is summarized in table 4.9, while the response of V_o to 2mM chloride is illustrated in figure 4.21.

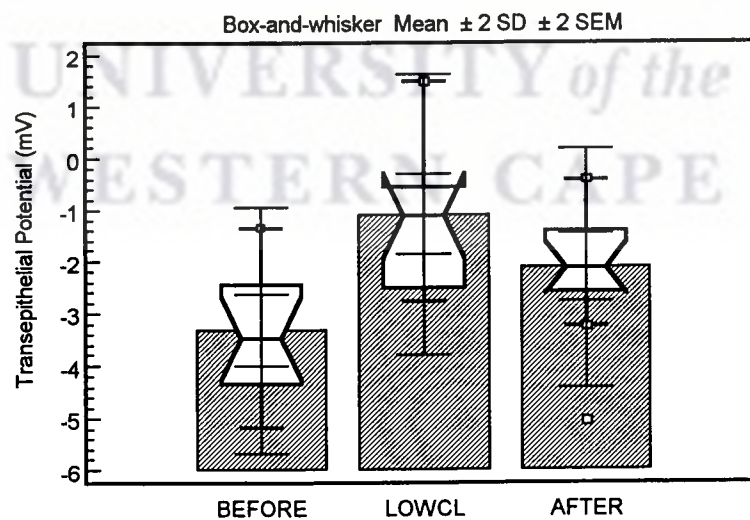


Figure 4.20: The effects of depleting the chloride concentration in the perfusion bath from 111mM to 2mM. Note the vertical bars within the notched boxes representing 95% confidence intervals clearly showing the difference between the 'before' (control) group and the 2mM chloride group.

Effect of <i>Low Chloride Ringers</i> on V_o and Cable Parameters of the Rat Seminiferous tubule					
CABLE PARAMETERS		N	MEAN	\pm SD	$P \leq$
V_o (mV)	PRE	14	-3.35	1.21	0.00001
	POST	14	-1.08	1.4	
LAMBDA (μ)	PRE	14	298.04	64.6	0.00001
	POST	14	335.54	63.4	
R_t (KOhm.cm)	PRE	14	4.38	1.03	0.00001
	POST	14	5.35	1.05	
R_{core} (MOhm/cm)	PRE	14	5.36	1.99	0.086
	POST	14	5.16	1.94	
DIAMETER (μ)	PRE	14	40.23	7.36	0.0985
	POST	14	41.1	7.96	
SCC _v (μ A/cm)	PRE	14	-0.81	0.3	0.00001
	POST	14	-0.21	0.27	
SCC (μ A/cm ²)	PRE	14	-66.57	31.14	0.00001
	POST	14	-17.66	22.84	
R_{input} (KOhm)	PRE	14	155.03	32.24	0.00001
	POST	14	171.84	36.01	

Table 4.9: The effects of a 2mM chloride concentration on V_o and cable parameters are summarized above. Means were considered not significant from each other if $P > 0.05$; N - number of tubules. Pre - control; Post - experimental. Cable parameters were measured before and after Chloride was depleted from the perfusion bath. See Table 1 for abbreviations.

V_o always responded to chloride depletion by the lumen becoming more less negative with respect to the bathing medium. The degree to which V_o changed was, however, quite varied. At times V_o would change from negative to a positive lumen potential. Figure 4.20 shows a box-and-whisker plot presenting the means and spread of data before, during and after depletion of chloride ions.

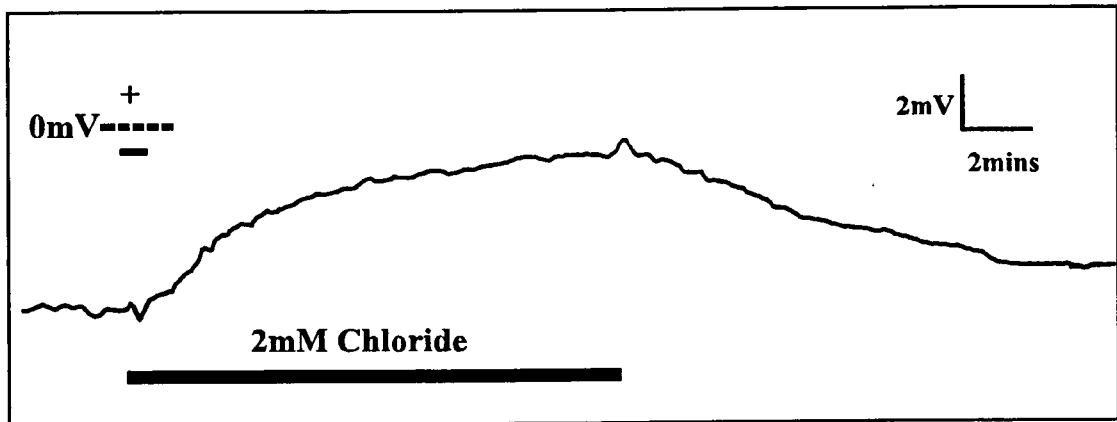


Figure 4.21: The effect of depleting perfusion bath chloride from 111 mM to 2 mM on V_o . The bar denotes the period of chloride depletion.

Transepithelial resistance (R_t) increased significantly ($P < 0.00001$) as did the length constant ($P < 0.00001$). The SCC and SCCv both significantly decreased ($P < 0.00001$).

The means and their standard deviations are summarized in table 4.9.

4.7.3.4 Effects of Furosemide

Furosemide caused a significant decrease in V_o from a control of -5.16 ± 1.45 mV to -2.80 ± 1.67 mV ($P < 0.0002$) (see figures 4.22 and 4.23). On removing furosemide from the perfusion bath Ringers the mean V_o recovered to -3.4 ± 1.6 mV ($P < 0.04$).

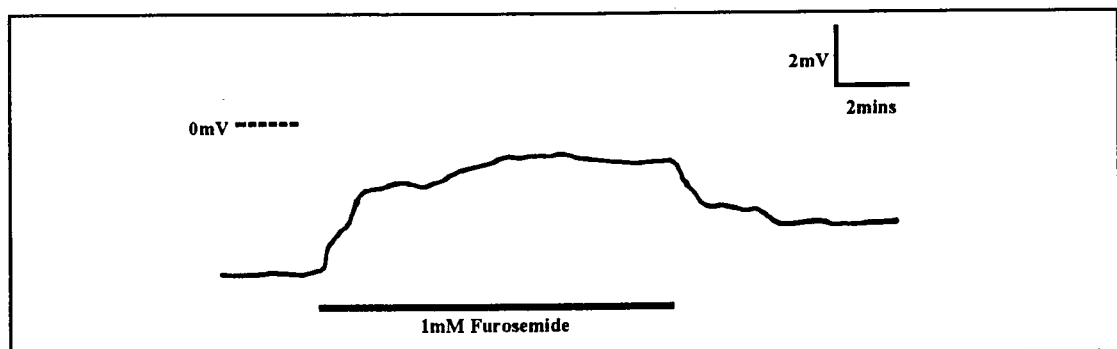


Figure 4.22: The above diagram shows a typical V_o response to furosemide.

Effect of <i>Furosemide</i> on V_o and Cable Parameters of the Rat Seminiferous tubule					
CABLE PARAMETERS		N	MEAN	\pm SD	$P \leq$
V_o (mV)	PRE	14	-5.16	1.45	0.0002
	POST	14	-2.80	1.67	
LAMBDA (μ)	PRE	14	296.77	70.17	0.427
	POST	14	288.5	60.68	
R_t (KOhm.cm)	PRE	14	4.4	0.87	0.643
	POST	14	4.33	1.13	
R_{core} (MOhm/cm)	PRE	14	5.64	2.6	0.566
	POST	14	5.47	1.82	
DIAMETER (μ)	PRE	14	39.75	8.1	0.974
	POST	14	39.72	7.5	
SCC _v (μ A/cm)	PRE	14	-1.7	10.94	0.435
	POST	14	-0.72	0.4	
SCC (μ A/cm ²)	PRE	14	-96.20	64.9	0.0424
	POST	14	-53.25	35.86	
R_{input} (KOhm)	PRE	14	152.0	44.86	0.705
	POST	14	155.59	34.89	

Table 4.10: The effects of 1mM furosemide are summarized above. Means were considered not significantly different from each other if $P > 0.05$; N - number of tubules. Pre - control; Post - experimental. Cable parameters were measured before and after furosemide was introduced into bath. See Table 1 for abbreviations.

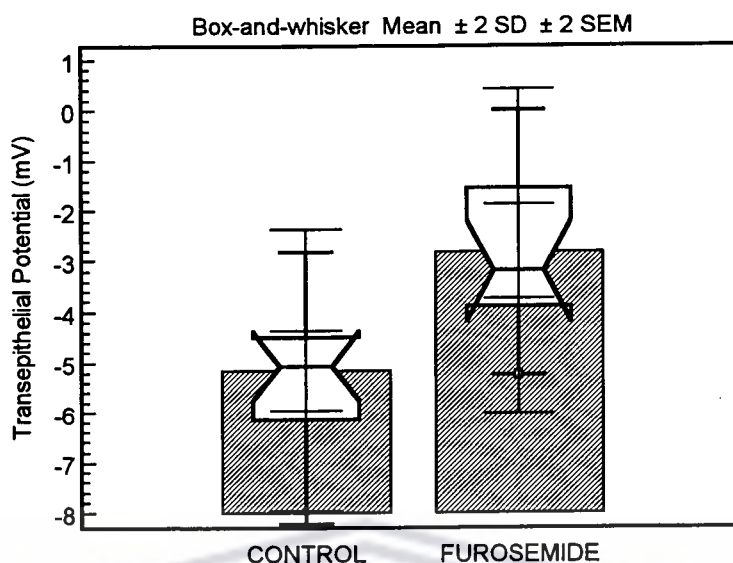


Figure 4.23: The above diagram depicts the significant differences in V_o between the control group and the furosemide treated group of tubules ($P < 0.0002$).

Furosemide also caused the SCC to decrease from $-92.2 \pm 64.9 \mu\text{A}/\text{cm}^2$ to $-53.25 \pm 35.86 \mu\text{A}/\text{cm}^2$ ($P < 0.04$). The rest of the cable parameters did not change significantly, but are summarized in table 4.10.

4.7.3.5 Effects of 2',4'-DNP

DNP (2',4'-dinitrophenol: 1mM) caused the depolarization of the transepithelial potential in that the mean V_o decreased from $-2.26 \pm 1.25 \text{ mV}$ to $-1.7 \pm 1.53 \text{ mV}$ ($P < 0.04$). However, V_o tended not to recover after the removal of DNP from the perfusion bath ($-1.69 \pm 1.5 \text{ mV}$; $P > 0.1$). Figure 4.24 shows two V_o traces which illustrates typical responses to DNP.

Cable parameters summarized in table 4.11 showed that only Rinput changed significantly in response to DNP.

Effect of <i>DNP</i> on V_o and Cable Parameters of the Rat Seminiferous tubule					
CABLE PARAMETERS		N	MEAN	\pm SD	$P \leq$
V_o (mV)	PRE	14	-2.26	1.25	0.04
	POST	14	-1.7	1.53	
LAMBDA (μ)	PRE	14	291.62	71.15	0.95
	POST	14	292.11	88.7	
Rt (kOhm.cm)	PRE	14	4.25	0.91	0.13
	POST	14	4.1	1.07	
Rcore (MOhm/cm)	PRE	14	5.67	2.5	0.51
	POST	14	5.83	3.18	
DIAMETER (μ)	PRE	14	39.6	7.62	0.32
	POST	14	40.29	9.18	
SCCv (μ A/cm)	PRE	14	-0.58	0.4	0.768
	POST	14	-0.54	0.75	
SCC (μ A/cm ²)	PRE	14	-49.16	43.62	0.829
	POST	14	-52.51	97.88	
Rinput (kOhm)	PRE	14	154.34	27.06	0.0002
	POST	14	149.76	27.20	

Table 4.11: Means were considered not significantly differ from each other if $P > 0.05$; N - number of tubules. Pre - control; Post - experimental. Cable parameters were measured before and after 2',4'-DNP was introduced into bath. See Table 1 for abbreviations.

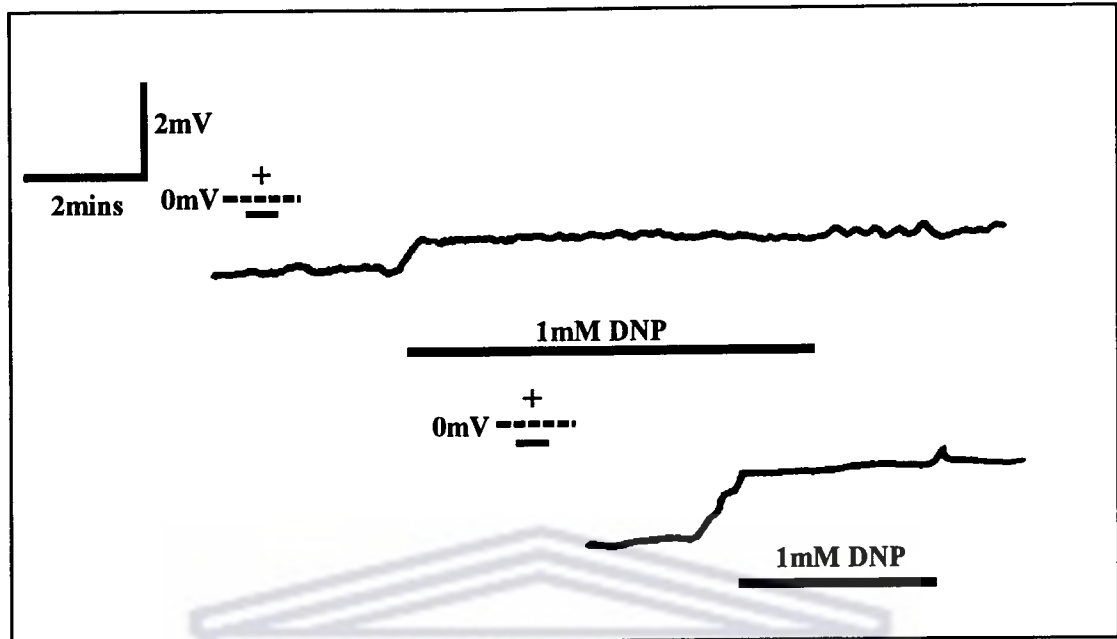


Figure 4.24: The above diagram depicts the effects of DNP on V_o . The bar denotes the period of DNP exposure.

4.8 Conclusion

All of the data presented in this chapter will be discussed in chapter 5.

CHAPTER 5

Discussion

5.1 Introduction

It appears that no previously published work on isolated seminiferous tubules, perfused according to the method of Burg and colleagues (1966) is available. Similarly, no research seems to be performed using the simple oil-gap technique (Berridge and Prince, 1972) to determine transepithelial potentials in isolated seminiferous tubules. Most of the electrophysiological data on seminiferous tubules in previously published literature were obtained using microelectrode and micropuncture techniques (see appendix A) and more recently, patch clamp techniques (e.g. Shibata, *et. al.*, 1992).

5.2 The equivalent electrical circuit

The simple equivalent electrical circuit illustrated in figure 5.1 was first proposed by Ussing (1951). This model only provides a framework in which to consider the results, and is not a complete equivalent description of the seminiferous tubule. This equivalent electrical circuit as applied to the rat seminiferous tubule has three components: a battery

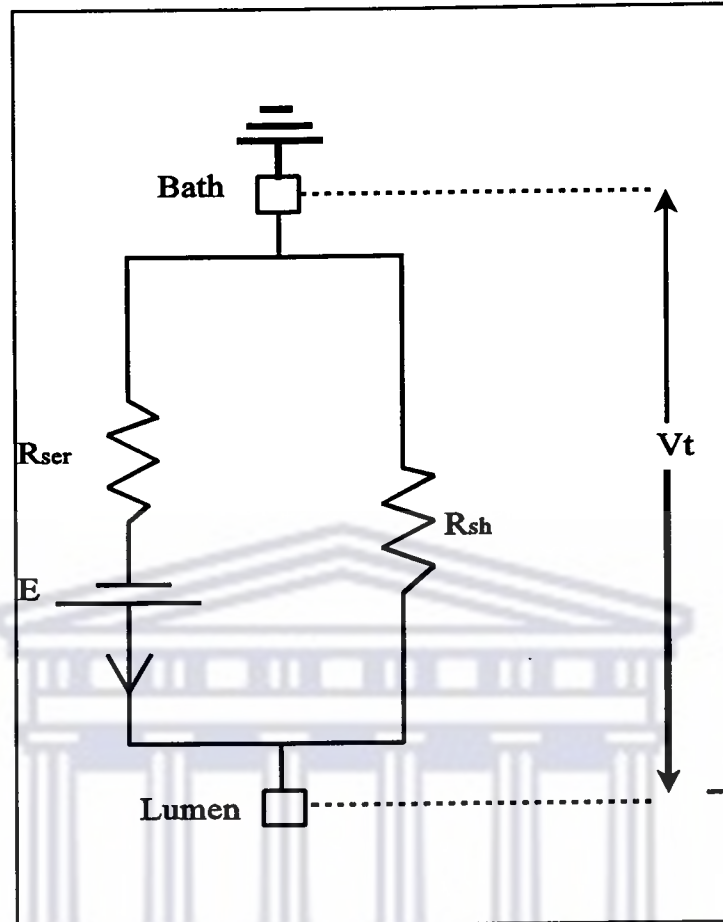


Fig. 5.1: The above electrical equivalent circuit of transepithelial transport in the seminiferous tubules of the rat considers the epithelium a 'black box' across which the transepithelial voltage and resistance are measured. E represents the e.m.f. of the transcellular pathway, R_{ser} is the resistance of the transcellular pathway, and R_{sh} is the resistance of the shunt pathway. V_t is the transepithelial voltage.

(E) representing the electromotive force (e.m.f.) of the active transport mechanism, a series resistance (R_{ser}) encountered by ions within the active transport pathway and R_{sh} representing the transepithelial leak pathways (both transcellular and paracellular) for all ions. Thus R_t , as measured by cable analysis, represents the parallel combination of R_{ser} and R_{sh} . V_o (refers to the transepithelial potential measured via the perfusion pipette and is equivalent to V_t) and SCC (short circuit current) can therefore also be expressed in terms of the following equations:

$$V_o = E \left[\frac{R_{sh}}{R_{sh} + R_{ser}} \right] \quad (5.1)$$

$$SCC = \frac{E}{R_{ser}} \quad (5.2)$$

The equivalent electrical circuit was first applied to the seminiferous tubules of the rat by Cuthbert and Wong (1975). In figure 5.2 an expansion of the circuit in figure 5.1 is illustrated. This equivalent electrical circuit is appropriate when measurements of the apical and basolateral membrane voltages, V_a and V_{bl} respectively, are made with intracellular microelectrodes simultaneously with the measurement of the transepithelial potential (V_o). (Nb. These measurements are not reported in the current study). In the expanded equivalent electrical circuit (fig. 5.2) the transcellular pathway is further divided into the e.m.f.'s (E) and resistances (R) of the apical (a) and basolateral (bl) membranes. In this circuit, R_t as measured by cable analysis, represents the parallel combination R_a , R_{bl} and R_{sh} . V_o and SCC (equations 5.1 and 5.2) can now be expressed in the expanded form in equations 5.3 and 5.4:

$$V_o = E \left[\frac{R_{shunt}}{R_{shunt} + R_a + R_{bl}} \right] \quad (5.3)$$

$$SCC = \frac{E}{R_a + R_{bl}} \quad (5.4)$$

It must be emphasized that the circuit is an over simplification of the experimental situation. For example, if the shunt pathway (R_{sh}) shows selectivity, R_{sh} would need to

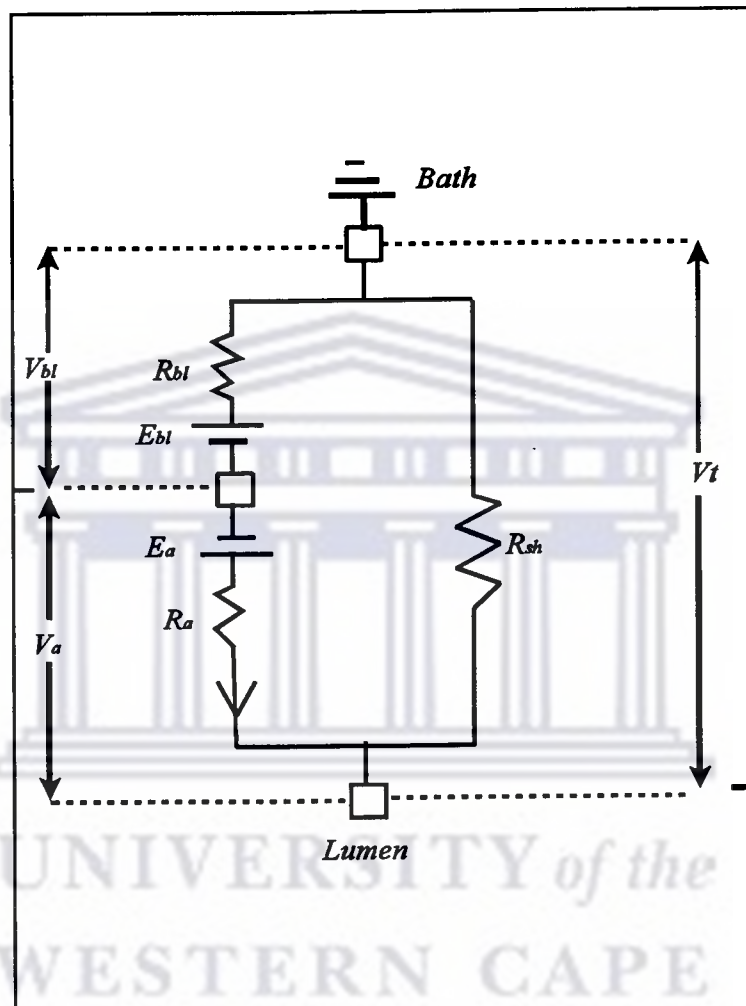


Fig. 5.2: In the above expanded electrical equivalent circuit of transepithelial transport in the seminiferous tubules of the rat the transcellular pathway is further divided into e.m.f.'s, E_a and E_{bl} , and the resistances, R_a and R_{bl} , of the apical (a) and basolateral (Bl) membranes. V_t is the transepithelial voltage, while measurements of the voltages across the apical and basolateral membranes, V_a and V_{bl} respectively, are made with intracellular microelectrodes.

be replaced by a further e.m.f and resistance network. Furthermore, since there is little information at this time about the electrical properties of the epithelium there is little purpose in making the circuit more complicated. Moreover, since only V_o and R_t are measured across the epithelium (fig. 5.2), quantification of the circuit components is not

possible unless one of the values of R_{ser} , E or R_{sh} can be determined. Although accurate determination of these values is beyond the scope of this study, the components of the expanded equivalent electrical circuit provide valuable insights into the mechanisms of transepithelial transport.

5.3 Perfusion rates, Morphology and Transepithelial Potentials

The morphological study presented in chapter 3 showed that high perfusion pressures (9.1 and 18.3 cm) resulted in fast perfusion rates (0.42 and 0.68 $\mu\text{l}/\text{min}$, respectively) which in turn developed a shear stress that caused the break down of the germinal epithelium (for an in depth discussion on the effects of perfusion rates on the morphology of the isolated seminiferous tubules, see chapter 3) . Lower perfusion rates (2.5 cm; 0.14 $\mu\text{l}/\text{min}$) prevented the breakdown of the germinal epithelium. During the current study only transepithelial potentials and cable data from perfused tubules that were not morphologically damaged were utilized.

The transepithelial potential (V_t) was also determined using essentially three different techniques: the oil-gap technique, the agar probe technique and the modified perfusion tip technique (see chapter 2). The mean V_t recorded using these different techniques did not differ significantly from each other (see table 4.1 and figure 4.1) as well as from mean V_t of the 2.5 cm perfusion height group. However, the mean V_t of all these groups differed significantly from the means of the 9.1 and 18.3 cm groups. The tubules from the latter groups also showed extensive morphological damage whereas the morphology

of the other groups did not differ significantly from their control group (see chapter 3). The V_t s of the 9.1 and 18.3 cm groups were also much closer to 0 mV than in any of the other groups. The data suggests that tubules with very low initial V_t s may not be morphologically viable and the integrity of the germinal epithelium may have been compromised. As these tubules are very fragile it is quite possible to damage them during the dissection process and/or during the transfer from the dissection bath to the perfusion bath. Therefore, V_t may pose as a valuable indicator of the integrity of the isolated perfused tubule.

Furthermore, there is considerable agreement between the mean V_t s obtained in this study and the literature. The average V_t for oil-gap, agar probe and modified perfusion techniques were -5.06, -5.66 and -5.42 mV, respectively. Levine and Marsh (1971) and Gladwell (1977), using microelectrodes, reported V_t means of approximately -4.8 mV and -5.86 mV respectively, while Tuck, *et. al.* (1970), also using microelectrodes, reported V_t of -7.4 mV for free flow fluid and -1.2 mV for primary fluid. In view of the data presented in chapter 3, this low value (-1.2 mV) for primary fluid may have arisen as a result of epithelium damage caused by the injection of oil into the tubules, prior to the formation of the primary fluid. Henning and Young (1971) reported that injection pressures of more than 300 mmHg had to be applied to move the oil along the tubular lumen. This in all probability had disrupted the apical membranes of the Sertoli cells. The tubules with high perfusion rates (9.1 and 18.3 cm groups) which showed morphologically damaged germinal epithelium also exhibited low V_t 's (-0.64 ± 1.5 mV and 0.89 ± 3.4 mV, respectively).

Furthermore, the primary fluid had a potassium concentration that appears suspiciously high (112 mEq/l: Tuck, *et. al.*, 1970) and possibly resulted as a mixture of free flow fluid (40 mEq/l: Tuck, *et. al.*, 1970; Marsh and Levine. 1971) and intracellular fluid from broken down Sertoli cells. This hypothesis is further supported by the data of Henning and Young (1971) which showed that perfusion fluid of various electrolyte composition injected so as to split the injected oil column in the lumen into two, did not resemble the ionic composition of primary fluid after 90 - 120 minutes, although equilibrium conditions prevailed within 30 to 60 minutes. Furthermore, water and electrolyte secretion decreased to zero within 30 to 60 minutes (Tuck, *et. al.*, 1970; Henning and Young, 1971). In view of this it appears that the low V_t (1.2 mV) manifested in tubules secreting primary fluid may be artifactual and probably indicative of a germinal epithelium that has been compromised.

In terms of the equivalent circuit (figure 5.2) there is a requirement that $E_{bl} > E_a$ as there is overwhelming evidence for the lumen being negative with respect to the bath. Furthermore, it must be noted that V_t is equal to the sum of the potentials across the apical and basolateral membranes (i.e. $V_t = V_a + V_{bl}$; see figure 5.2).

5.4 The Equilibration Time

Control studies showed that after 5 minutes recordings generally remained fairly stable (see figures 4.2, 4.3 and 4.4). Experiments with considerable V_t drift were discarded and not used for data collection in the current investigation. Oil-gap recordings of V_t showed

the most drift, and moreover, with this technique it was difficult to isolate the source of the drift. However, for no apparent reason recordings from subsequent tubules developed little or no drift. Experimental permutations were carried out during stable recording periods, usually between 8 to 10 minutes after the start.

Sometimes low frequency potential oscillations were superimposed on the V_t recordings. These have not been reported before in the literature and the source of these oscillations are not known. However, Cuthbert and Wong (1975), reported oscillations on their intracellular potentials recorded in isolated seminiferous tubules, which could be associated with the Ca^{++} concentration of the bathing medium. Moreover, the oscillations in the current study would sometimes arise or cease midway through an experiment. V_t oscillations were also frequently observed in the recordings of Malpighian tubules, where these V_t oscillations were shown to arise from the surrounding contractile cells (Nicolson and Isaacson, 1987). A very likely source for these oscillations, therefore, is the surrounding layer of contractile myoid cells.

5.5 Effects of Bath Temperature on V_t

Changing the temperature (range: 21- 38°C) had little to no effect on V_t , and although the average V_t decreased and increased by fractions of a millivolt to respectively decreasing or increasing temperature, these changes were not significant ($P>0.05$) when compared to the data recorded at 35°C.

These findings are supported by Setchell and Waites (1972) who reported that fluid secretion was not effected after local heating of the testis, although the testis subsequently became aspermatogenic. This is in line with current views that fluid secretion is controlled and regulated by the Sertoli cells, which also form the most important part of the blood-testis barrier, and are therefore primarily responsible for the development of a transepithelial potential. The cells most affected by temperature are the pachytene spermatocytes and young spermatids (Chowdbury and Steinberger, 1964). Furthermore, intracellular potentials of isolated tubules did not change significantly when temperature was increased from 33 to 37°C (Cuthbert and Wong, 1975). However, when the temperature was decreased to 15°C the intracellular potential fell from -28.5 mV to -10 mV (Cuthbert and Wong, 1975). The current study showed a similar trend, but with smaller increases in $V_t/^\circ\text{C}$ than that of Gladwell (1977) who showed, using the microelectrode technique, that between 25 and 35°C V_t increased in a predictable manner by 0.43 mV/°C.

The data therefore supports the current view that the Sertoli cells in the germinal epithelium which are thought to be responsible for the generation of V_t , are not susceptible to relatively large changes in temperature (also see thermoregulation of the testis in chapter 1).

5.6 Oil-gap experiments

In an attempt to minimize the inherent problems with the oil-gap technique (for critique

of the oil-gap techniques see Isaacson and Nicolson, 1989), the open end of the tubules were kept as short as possible (approximately 3-5mm from the oil gap) as a routine precaution. This was carried out to limit the potential generated in the tubule distal to the central oil bath, thereby minimizing the subtractive effects of that segment of tubule on the transepithelial potential measured across the central oil bath. Isaacson and Nicolson (1989) proved that the segments of the Malpighian tubule on either side of the oil bath acted as opposing batteries connected in series. Thus, the interelectrode potential (i.e. the potential measured across the central oil bath with only the tubule connecting the two outer Ringer baths [see chapter 2 for experiment design]) reflects only the difference in potential generated by tubule segments on either side of the oil bath. Furthermore, the standardization of the length of the open ended side of the tubule resulted in transepithelial potential data which was more uniform in its distribution.

Also, in agreement with Isaacson and Nicolson (1989), was that the removal of the ligature from the end of the longer segment of the tubule had no effect on the V_t . This is expected if the length constant of the tubule is a small fraction of a millimeter (Isaacson and Nicolson, 1989). The length constant (see cable analysis) of perfused, isolated tubules, measured in the current study for the first time, was found to be 296.77 ± 70.17 μm .

Support for the above was also found in that the average V_t for the oil-gap experiments was lower and had a greater variance than either the agar probe or the perfusion experiments. However, V_t obtained from the oil-gap experiments did not differ

significantly from the latter two groups ($P>0.5$).

5.6.1 The Effect of Increased Bath Potassium

The Sertoli cell separates the basal compartment from the adluminal compartment in the seminiferous tubule by way of tight Sertoli-Sertoli junctions (Dym and Fawcett, 1970) and produces high concentrations of potassium (40-50 mEq/l) in the lumen (Tuck, *et. al.*, 1970; Setchell and Waites, 1975). This observation raises the question of how is this high concentration of K^+ generated and maintained. In the current study the effects of raising bathing concentration of K^+ from 5 to 50 mM had a small but significant effect ($P<0.0009$) in decreasing the V_t .

It is fairly well established that the basolateral membranes of Sertoli cells have an ouabain insensitive Na^+K^+ ATPase exchange pump which is proposed to generate the gradient for transepithelial transport of K^+ into the lumen of the seminiferous tubule (Reisin and Cerejido, 1969; Muffly, *et. al.*, 1985; Muffly and Hall, 1988; Jégou, 1992). The most widely accepted explanation for transcellular ionic gradients is the two membrane hypothesis which proposes that the plasma membrane on two sides of the cell exert different influences on the transport of a given ion. This concept can be applied to the seminiferous tubule and in particular to the Sertoli cells: here the tight junctions forming the basis of the blood-testis barrier clearly divide the Sertoli cell into the apical adluminal membrane and the basolateral membrane forming the basal compartment. It is further proposed in the literature that the basolateral membrane contains a potassium pump

which pumps this ion at a rapid rate to the interior of the cell. The constant intracellular concentration is then maintained by the loss of potassium occurring via the apical membrane at a rate equal to the basolateral pump rate (Muffly and Hall, 1988). This is in agreement with the finding that increasing external K^+ resulted in a 16 mV reduction of the intracellular potential (from -28 to -12 mV) (Cuthbert and Wong, 1975).

The oil-gap data supports the above hypothesis in that increasing the external K^+ results in more K^+ being pumped across the basolateral membrane of Sertoli cells into the intracellular compartment. This results in turn in the subsequent apical membrane transport of cations (K^+) into the lumen of the seminiferous tubule which in turn causes a small decrease in the V_t .

5.6.2 Effects of $BaCl_2$

The oil-gap study failed to show a statistically significant change in V_t in response to $BaCl_2$. However, perhaps increasing the sample size would have resulted in a statistically significant change between the means of the relevant groups, as the tubules responded to barium treatment by either increasing or decreasing with only one tubule failing to respond. Furthermore, if changes in V_a and V_{bl} occurred in parallel and were equal in magnitude, resultant changes in V_t would be small. However, the current data agrees with the hypothesis that barium sensitive K^+ channels do not exist in the serosal membranes of the seminiferous tubules (Jègou, 1992).

5.6.3 Effects of Low Chloride Ringers

In order to maintain electroneutrality of cation transport into the lumen of the seminiferous tubules, chloride is thought to diffuse into the lumen in association with the cation transport (Jégou, 1992). The precise mechanisms or route (i.e. whether transcellular or paracellular transport) involved in chloride transport across the germinal epithelium are unclear.

The above hypothesis was endorsed by the data in this study. After the chloride concentration was reduced in the bathing medium the transepithelial potential became more positive. This is in agreement with the theory that with less chloride (anions) available for transport across the seminiferous epithelium into the lumen in association with cation transport, the lumen would have a decreased amount of anions relative to the cations resulting in the transepithelial potential becoming more positive.

5.6.4 The Effects of Furosemide and Bumetanide

In order to obtain more clarity on the mechanisms involved in the transport of chloride, furosemide and bumetanide, which are drugs known to inhibit NaCl co-transport in some vertebrate epithelia such as the flounder intestine (Frizzell, *et. al.*, 1983) and the rat ileum (Humphries, 1976), were used. Both these drugs had similar effects in that V_t decreased, a result similar to the effect of decreasing the external chloride concentration. Several reports have shown that the electrochemical gradient favors Na^+ entry into the lumen of

seminiferous tubules but opposes Cl^- transport into the lumen (Tuck, *et. al.*, 1970; Levine and Marsh, 1971). Thus a basal entry mechanism involving electroneutral co-transport with Na^+ would seem feasible. In this process the maintenance of the Na^+ gradient across the basal cell membrane is likely to be achieved by the activity of a Na^+/K^+ ATPase 'pump' (Jégou, 1992; Setchell and Brooks, 1988). The movement of Cl^- across the apical membrane probably occurs passively aided by the electrical gradient (approximate intracellular potential of Sertoli cells: -39mV (Eusebi, *et. al.*, 1983) although it has been suggested that bicarbonate ions might be involved in an exchange mechanism for cellular chloride ions (Jégou, 1992).

Thus the increase in the positivity of the V_t in response to treatment with furosemide and bumetanide suggest that a basal membrane mechanism for the co-transport of chloride ions and sodium ions exist. However, further research is necessary to elucidate whether K^+ transport is also involved and whether a paracellular route for transporting chloride also exists.

5.7 Agar-probe Experiments

The arrangement for these experiments were identical to the isolated perfusion method described by Burg and colleagues (1966), with the exception of replacing the inner perfusion pipettes with a similarly shaped inner pipette that had been filled with agar. The outer holding pipette was still used to attached the isolated tubule while the inner agar pipette was inserted into the lumen of the tubule. This procedure would ensure minimal

interference or damage to the germinal epithelium. This was confirmed in the current morphology study that was carried out on tubules (see chapter 3). Essentially the agar probe acts as an electrode positioned in the lumen, measuring the V_t relative to the perfusion bath.

The mean V_t (-5.66 ± 1.51 mV) recorded by the agar probe method was similar to the reported mean V_t found using the microelectrode method: -4.8 ± 0.1 mV (Levine and Marsh, 1971) and -5.86 ± 0.15 mV (Gladwell, 1977). Thus the agar-probe data endorsed the findings in the literature that the lumen was negative by approximately 5 mV relative to the bathing medium.

5.7.1 Effects of Low Chloride Ringers

The introduction of a low chloride Ringers into the bathing medium (111 mM to 2 mM) made the lumen of the tubule more positive, the response being similar to the oil-gap tubules exposed to a low chloride concentration (see section 5.6.3 for further discussion).

5.7.2 Effects of Furosemide on V_t

Furosemide produced similar V_t responses in the agar probe experiments as in the oil-gap experiments. This highly significant ($P < 0.0008$) positive change in the V_t was not unexpected and endorsed the oil-gap results. Hence the same arguments apply here.

5.7.3 Effects of BaCl₂ on V_t

Seminiferous tubules were treated with BaCl₂ in an attempt show whether or not K⁺ channels are present in the basolateral membrane. The effect of barium was unexpected in producing a small, but significant increase in the positivity of the V_t. Also, in a pilot study, the intracellular potential (V_{bl}) was shown to depolarize sharply in response to 1mM BaCl₂ (data not included in the current study). This suggests that the serosal membrane of the seminiferous tubules may be permeable to barium ions resulting in the rapid depolarization of the basolateral membrane. Furthermore, it must be noted that V_t equals the sum of the apical (V_a) and basolateral membrane potentials (V_{bl}) (i.e. $V_t = V_a + V_{bl}$) and that if V_a depolarizes less than V_{bl}, V_t will tend to become more positive, and *vice versa* (see figure 5.2). The current study also demonstrates that barium sensitive channels do not exist in the seminiferous tubule. Alternatively, BaCl₂ might not be a suitable channel blocker. Further research is needed to indicate whether other K⁺ channel blockers, e.g. tetraethylammonium (TEA) (Giebisch, 1995; Shibata, *et. al.*, 1992) may show up the existence of serosal membrane K⁺ channels. A further shortcoming in the current study is the absence of simultaneous intracellular potential measurements with those of V_t.

5.7.4 Effects of DNP on V_t

Cheung and colleagues (1976) reported that treatment of isolated seminiferous tubules with 2',4'-dinitrophenol, a metabolic inhibitor, effectively abolished fluid secretion. The

current study showed that DNP reduced the average V_t to close to zero (although not statistically significant), which suggest a trend in agreement with the previous mentioned study. The DNP depletion of cellular ATP stores is critical for the functioning of the proposed basolateral Na^+ - K^+ ATPase pumps. Decreasing or suppressing the pump rate would decrease the vectorial transport of K^+ into the tubular lumen. The sodium gradient across the basolateral membrane would be depleted, thereby decreasing the proposed sodium chloride co-transport into the Sertoli cells; this would result in a decrease of the apical gradient for chloride entry into the lumen, thereby decreasing V_t and the driving force for fluid secretion (see chapter 1).

In terms of the equivalent circuit (figure 5.1), E , the e.m.f. of the active pathway is reduced to close to zero and therefore according to equation 5.1, V_t , which is a product of E and the parallel arrangement of R_{ser} and R_{sh} , would also approach zero.

5.8 Electrophysiology of Isolated Perfused Seminiferous Tubules

5.8.1 Validation of Cable Analysis

The first test to validate cable analysis was to test the Ohmic behavior of the seminiferous tubules. This was carried out by injecting current which varied from -200 nA to +200 nA via the perfusion pipette into the lumen of the seminiferous tubules and measuring resultant V_o response. A linear relationship was found to exist between V_o and current which confirms Ohmic behavior. The validity of cable analysis was further tested by

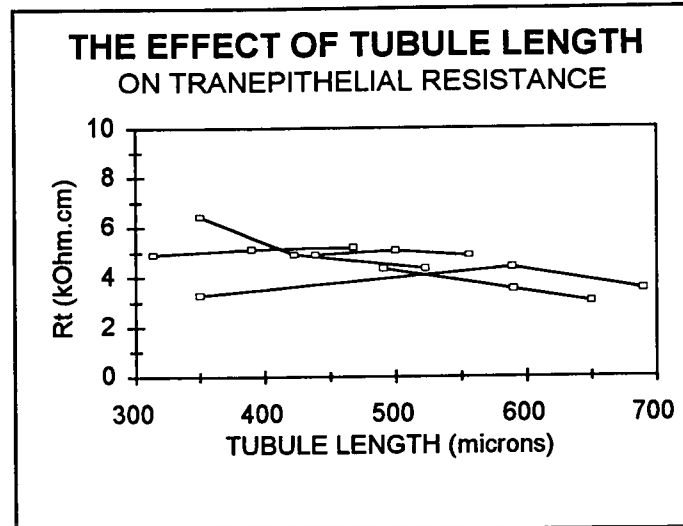


Figure 5.3: The above chart shows the effect of decreasing tubule length on Rt for 5 different seminiferous tubules.

reducing the length of the tubules in two steps, each time measuring Rt. Only small changes occurred in Rt which were unrelated to the length of the tubule, as predicted by cable analysis (see figure 5.3).

Another way of validating cable analysis is to compare the optically measured luminal diameter with the lumen diameter calculated by using cable equations (see chapter 2) which in turn uses the electrical variables obtained during luminal current injection. It was not possible to clearly visualize the lumen of the viable seminiferous tubule, and therefore also not possible to obtain an optically measured lumen diameter to compare with the diameter determined using cable formulae (see chapter 2). In the current study, the electrically determined diameter of the seminiferous tubular lumen was found to be $39 \pm 8.1 \mu\text{m}$. This finding is further endorsed by Eusebi, *et. al.* (1983) who found in a morphological study that the lumen of isolated adult rat seminiferous tubules to range between 36 to 45 μm ($n=18$). It must be noted that the electrically determined lumen

diameter represents an average of the entire seminiferous tubule and that areas of myoid contraction would contribute to an increased core resistance (R_c) and hence a decreased luminal diameter. Thus the agreement between lumen diameter (as found in the literature: Eusebi, *et. al.*, 1983) and the electrically determined luminal diameter found in the present study further endorses the validation of cable analysis.

5.8.2 Controls

The mean V_t of -5.16 ± 1.45 mV (lumen negative) measured in the current study of perfused seminiferous tubules was similar to the values reported before for the seminiferous tubules of the rat (-7.4 ± 0.5 mV, Tuck, *et. al.*, 1970; -4.8 ± 0.1 mV, Levine and Marsh, 1971; -5.86 ± 0.15 mV, Gladwell, 1977). All of the latter studies used the microelectrode technique to measure the transepithelial potential. V_t for perfused tubules was expected to have been closer to that obtained by Tuck, *et. al.* (1970) while 'primary' fluid was collected (-1.2 ± 0.3 mV (S.E.M.); lumen negative). The higher V_t found in the present study further supports the hypothesis presented earlier that there appears to be a strong case for this low V_t being indicative of a disrupted germinal epithelium (also see section 5.3).

A search of the literature failed to reveal any studies in which seminiferous tubules were isolated and perfused according to the method described by Burg, *et. al.* (1966) or any studies where cable analysis was applied to perfused tubules. This made it difficult in comparing the cable data of the current study with data of other studies.

However, some of the cable parameters, such as the transepithelial resistance and input resistance (R_i) made in the current study, could be compared with resistance measurements made across confluent sheets of cultured grown Sertoli cells and the input resistances measured using microelectrodes, respectively.

The transepithelial resistance (R_t) for the isolated perfused seminiferous tubules were found to be 4.4 ± 0.87 KOhm.cm. Transepithelial resistance has only been measured across confluent sheets of cultured grown Sertoli cells, and in these studies R_t has been expressed as specific resistance (R_{ts} : Ohm.cm²). In order to convert R_t (resistance per unit length: KOhm.cm) to specific resistance it is multiplied by πD , where D is the mean luminal diameter (39.1 μ m). Thus R_{ts} in the present study for the isolated perfused seminiferous tubule of the rat is 53.97 ± 10.7 Ohm.cm².

This differs from the much higher control values of between 85 and 145 Ohm.cm² found in studies carried out across monolayers of Sertoli cells (Onoda, *et. al.*, 1990; Janecki, *et. al.*, 1991). These studies further found that when the sheets of Sertoli cells were treated with the hormone FSH, R_{ts} decreased to 35-40 Ohm.cm². In view of this, it appears that the R_t of the seminiferous tubules can be manipulated by the chemical milieu that bathes its outside and that changes induced in these tubules were 'reluctantly' reversed (Janecki, *et. al.*, 1991). Moreover, the tubules used in the current study were dissected and studied immediately and therefore were still imbued with the long term effects of the *in vivo* conditions.

According to the definition of Frömter and Diamond (1972), the data of the current study infers that the seminiferous tubule can be classified as a 'leaky' epithelium, both in terms of transepithelial resistance (6-133 $\Omega\cdot\text{cm}^2$) and transepithelial potential (0-11 mV). In terms of these criteria the seminiferous tubule can be bracketed with the *Necturus* proximal tubule (80 $\Omega\cdot\text{cm}^2$), rabbit gall bladder (28 $\Omega\cdot\text{cm}^2$; 0 mV), rat jejunum (30 $\Omega\cdot\text{cm}^2$; 11 mV). However, Janeki (1991) showed that the transepithelial resistance in two compartment Sertoli cell cultures could be regulated by FSH and testosterone and that at temperatures of 36.5 °C the synergistic effect of these two hormones resulted in transepithelial resistances of 580-1200 $\Omega\cdot\text{cm}^2$, which would classify the seminiferous tubule as a 'tight' epithelium. Furthermore, transepithelial resistance could vary between the different spermatogenic stages of a perfused segment of seminiferous tubule, and thus the seminiferous tubule could display both 'leaky' and 'tight' characteristics. A short coming of the current study was not correlating the data with a particular spermatogenic stage.

Changes in value of R_i could act as a rough indicator of membrane permeability of the germinal epithelium to small ions (Gladwell, 1977). In the current study R_i was found to be 152 ± 44.9 KOhms, while Gladwell (1977), using a microelectrode technique found R_i to be slightly higher at 198 ± 7.8 KOhms.

The short-circuit current (SCC) measured in the current study is presented both as the 'virtual' SCC (SCC_v ; $\mu\text{Amps}/\text{cm}$) and as the SCC corrected for the surface area (SCC; $\mu\text{Amps}/\text{cm}^2$). The SCC_v is virtual because it was calculated as V_t/R_t (i.e. it was not

measured at $V_t=0$ mV). Furthermore, SCC was corrected for surface area using the electrically determined lumen diameter as a variable. Owing to the difficulty of visualizing the tubular lumen confidence in this cable parameter should be treated with scepticism. The average value for the SCC_v ($-1.69 \pm 10.1 \mu\text{Amps/cm}$) in the present study was close to that of other isolated perfused tubular epithelia (collecting ducts of the rabbit kidney: $0.28 \mu\text{Amps/cm}$: Koeppen, 1989; the Malpighian tubules of the tsetse fly in a chloride Ringer: $-0.14 \pm 0.62 \mu\text{Amps/cm}$: Isaacson and Nicolson, 1994; the proximal convoluted tubule of the rabbit: $2.48 \mu\text{Amps/cm}$: Lapointe, *et. al.*, 1984).

5.8.3 The Effects of High Potassium Ringers

It is generally believed that tubular fluid is secreted by Sertoli cells (Jégou, 1992) and that the differences between the composition of the basal and tubular fluid are maintained by Sertoli-Sertoli junctions that prevent the mixing of the two fluids (Fawcett, 1975; Tuck, *et. al.*, 1970). A striking difference between the tubular fluid and that of other body fluids is the high concentration of potassium in the former (40-50 mM in the rat) (Tuck, *et. al.*, 1970; Levine and Marsh, 1971; Setchell and Waites, 1975).

In the current study, in isolated perfused seminiferous tubules, it was surprising to find that V_t was not significantly changed by the 10 fold increase in external K^+ concentration. However, in view of the two membrane hypothesis (see section 5.6.1) proposed earlier and applied to the seminiferous epithelium, and the generally accepted view that V_t is equal to the sum of the potentials measured across the basolateral membrane (V_{bl}) and

the apical membrane (V_a) (i.e. $V_t = V_{bl} + V_a$), it is feasible to propose that if the potential changes that occurs in V_{bl} is paralleled by opposite and equal changes in V_a , that either V_t would remain unchanged or very small changes would occur. Cuthbert and Wong (1975) showed that a 10 fold increase in the potassium concentration of the bathing medium resulted in a decrease in the intracellular potential (V_{bl}) from -28 mV to -14 mV (unfortunately, V_t measurements were not made simultaneously). Also, the oil-gap experiments showed that the change in V_t in response to a 10 fold increase in bath potassium concentration was less than 1 mV. Therefore, in view of the 16 mV change in V_{bl} (Cuthbert and Wong, 1975) and the small or no changes occurring across V_t , it seems reasonable to assume that similar changes in potential are occurring at V_a to that of V_{bl} .

Furthermore, in support of the above hypothesis, a small, but significant decrease was found in R_t . As R_t is equal to the inverse of transepithelial conductance (G_t), the decrease in R_t is indicative of an increase K^+ conductance across the epithelium. However, without simultaneous intracellular recordings and the calculation of the fractional resistances of the apical and basolateral membranes, it is not possible to indicate which components of the germinal epithelium contributed to this decrease in R_t . This result is supported by the paralleled tendency for the SCC_v to increase in response to the increase in bath K^+ concentration. Further support for the increase in R_t is the parallel and highly significant decrease in R_i which indicates an increase in the permeability of the seminiferous tubule.

5.8.4 The Effects of $BaCl_2$

As in the oil-gap study, barium ions failed to change V_t significantly. As mentioned earlier, a pilot study showed that although V_t failed to change significantly, V_{bl} depolarized rapidly in response to 1 mM barium treatment (data not included in the present study). The data implies that the changes in V_{bl} were parallel and similar to potential changes at the apical membrane. The depolarization of V_{bl} suggests that the basolateral membrane may be permeable to Ba^{++} and is further supported the literature by the absence of detectable K^+ channels in the basolateral membrane (Muffly and Hall, 1988).

However, the addition of barium to the bathing medium resulted in an increased R_t , indicating a decrease in the transepithelial conductance (G_t). This was paralleled by a decrease in both SCC and SCC_v which also indicated a decrease in G_t . In terms of the equivalent circuit, where $SCC = E/R_{ser}$, it is more likely that an increase in R_{ser} occurred (as indicated with the increase in R_t) rather than a significant decrease in E , resulting in the decrease of SCC . It is reasonable to suspect that the barium ions after entering into the cytoplasm of the Sertoli cells, diffused towards the apical membrane and then blocked apical membrane K^+ channels (Muffly and Hall, 1988). This theoretical approach is supported by the V_o not changing significantly after barium was removed from the bathing medium as barium had already entered the intracellular compartment of the Sertoli cell. The above hypothesis still requires further laboratory investigation by introducing barium ions into the perfusate and simultaneously recording V_t and V_{bl} .

The resistance of the lumen to current flow, R_c , responded to barium treatment with a small but significant ($P < 0.05$) decrease, which was reflected in the increase of the electrically determined luminal diameter (see equation 4 in chapter 2). The slight increase in the luminal diameter was not statistically significant. Furthermore, due to the lumen not being clearly visible, it was not possible to verify corresponding changes in the lumen diameter with that determined electrically.

5.8.5 The Effects of Low Chloride Concentration

The literature is unclear on the precise mechanisms or route (i.e. whether transcellular or paracellular transport) involved in chloride transport across the germinal epithelium. Jégou (1992) suggests that chloride crosses the basolateral membrane via a sodium co-transport mechanism against a chloride electrochemical gradient (Levine and Marsh, 1971; Tuck, *et. al.*, 1970).

In the current study V_t decreased in response to a low bath chloride concentration. Similar effects were produced in the oil-gap study and the agar probe study. The decrease in the availability of chloride in the bathing medium results in a decreased transepithelial conductance of chloride. This is in agreement with the literature.

Furthermore, the above hypothesis is supported by the highly significant increase in R_t , which is simply a reflection of the decreased chloride transepithelial conductance (G_t). The increase in R_i which indicates a decrease in transepithelial permeability further

endorses the above theory. In addition, the parallel decreases in both SCCv (75%) and SCC (74%) also suggest that chloride plays an important role in total ionic transepithelial transport.

5.8.6 Effects of Furosemide

Although the response of V_o to furosemide treatment was similar to the effects of chloride depletion of the bathing medium, only SCC, of the cable parameter, showed a parallel and significant decrease. R_t and SCCv were not significantly different from control values. Furthermore, SCC only changed by 45% compared to 74% in response to chloride depletion from the bathing medium. This suggests that furosemide which inhibits $\text{Na}^+\text{-Cl}^-$ co-transport, may have only affected one of the mechanisms whereby chloride enters across the basolateral membrane of the Sertoli cell. Further research will be required to uncover possible alternative transcellular or/and paracellular mechanisms for transepithelial chloride transport.

5.8.7 Effects of 2',4'-DNP

The metabolic inhibitor, DNP, has been reported to depolarize the intracellular potential (V_{bl}) by 16 mV from a resting potential of -28 mV (Cuthbert and Wong, 1975). DNP was also reported to abolish secretion in isolated seminiferous tubules (Cheung, *et. al.*, 1976). The V_t in the agar probe experiments showed similar responses to DNP, although they were not significantly different.

In the current study DNP significantly decreased V_o , which suggests that some of the active transport pathways had been inhibited. On reintroducing control Ringers into the perfusion bath V_o did not recover to baseline values. Of the cable parameters only R_i showed a significant decrease in response to DNP, which indicated a slight increase in the passive permeability of the seminiferous tubule.

5.9 General Conclusion

This is the first report of the perfusion of isolated segments of seminiferous tubules as is commonly done in experiments with renal tubules. Furthermore, the agar probe technique, developed during the current study, has validated the perfusion technique by exhibiting similar V_t responses to the various experimental maneuvers. Further validation in this regard was received from the oil-gap experiments. Although all of these techniques were employed for the first time on seminiferous tubules, the transepithelial potentials (V_t) were indistinguishable from V_t values reported in the literature. The exception was the low V_t values measured in tubules which had oil injected at high pressures into the seminiferous lumen in an attempt to produce 'primary' fluid. These low V_t values were similar to V_t values obtained from tubules that had their germinal epithelia disrupted by high perfusion pressures. The oil-gap and agar probe experiments further endorsed the view that these values were artifactual as these two techniques produced V_t values in the current study that were statistically not different from V_t values obtained in tubules producing 'free-flow' fluid.

Cable analysis of the isolated perfused seminiferous tubules produced electrophysiological values such as the length constant (λ), R_t , R_{core} , R_i , SCC values, and an electrically determined luminal diameter which was verified in the literature for the first time. Some of these parameters have only been measured across monolayers of cultured Sertoli cells (or combinations of Sertoli, germ and myoid cells). Now for the first time these parameters (e.g. R_t) could be compared with parameters obtained from studies performed on the three-dimensional structure of the seminiferous tubule. Furthermore, perfusion experiments mirror the *in vivo* situation of the germinal epithelium far more closely than cell culture experiments. Moreover, in the investigation of ionic transport across the seminiferous tubule, perfusion studies provide a decided advantage, in enabling the control of both the luminal and bathing mediums, both of which could be changed at will during the course of the investigation.

The aim of this study, which was to investigate the electrophysiological properties of the isolated perfused seminiferous tubule using cable analysis, has been realized in part, and that only because intracellular potentials were not reported as it was not possible to identify the cellular source of the intracellular potentials. In future studies, seminiferous tubules from rats who have been irradiated *in utero* may provide a better model as they will contain a predominantly Sertoli cell population. However, this forms part of a future research project.

However, the study showed that the isolated perfused rat seminiferous tubule can be characterized in terms of its transepithelial potential (4-6 mV, lumen negative with

respect to the bath), its length constant (296.77 μm), its transepithelial resistance (4.4 $\text{K}\Omega\cdot\text{cm}$), its specific resistance (53.97 $\text{K}\Omega\cdot\text{cm}^2$), its electrically determined luminal diameter (39.1 μm), its SCC_v (-1.69 $\mu\text{Amps}\cdot\text{cm}$) and its input resistance (152 $\text{K}\Omega$ s). Furthermore, the study has reported on the effects of various ionic permutations, ionic channel blockers and various inhibitors on the V_t and cable parameters for the first time. This has resulted in many of the theoretical postulations in the literature either being criticized or endorsed by the current study. However, the omission of correlating the current data with a particular spermatogenic stage prevents the further discussion on its possible contribution to the variability observed in some of the responses studied. In future studies the stage of the seminiferous cycle must be correlated to the response tested in a segment of perfused seminiferous tubule.

The experimental techniques of this study provide exciting research avenues for the future testing of drugs (male contraceptives), hormones or combinations thereof on the germinal epithelium. It also provides a viable alternative to cell culture studies and allows for comparisons of the properties of germinal epithelium obtained from the different techniques.

References

1. **Bergmann, M. and Dierichs, R.** Postnatal formation of the blood-testis barrier in the rat with special reference to the initiation of meiosis. *Anat. Embryol.*, 168: 269-275; (1983).
2. **Bergmann, M. S., J. and Greven, H.** The blood-testis barrier in vertebrates having different testicular organization. *Cell Tissue Res.*, 228: 145-150; (1984).
3. **Berridge, M. J. and Prince, W. T.** Transepithelial potential changes during stimulation of isolated salivary glands with 5-hydroxytryptamine and cyclic-AMP. *J. Exp. Biol.*, 56: 139-153; (1972).
4. **Bowler, K.** The effect of repeated applications of heat on spermatogenesis in the rat: a histological study. *J. Reprod. Fertil.*, 28: 325-334; (1972).
5. **Burdzy, K., Tung, P. S. and Fritz, I. B.** High resolution scanning electron micrographs of freeze-cracked cells in testes from normal and irradiated rats at different stages of gonadal development. *J. Electron Microsc. Tech.*, 19:189-202; (1991).

6. **Burg, M. B., Grantham, J. Amramow, M. A. and Orloff, J.** Preparation and study of fragments of single rabbit nephrons. *Am. J. Physiol.*, 210: 1293-1298; (1966).
7. **Burg, M. B., Isaacson, L., Grantham, J. and Orloff, J.** Electrical properties of isolated perfused rabbit renal tubules. *Am. J. Physiol.*, 215: 788-794; (1968).
8. **Byers, S. W., Hadley, M. A., Djarkiew, D. and Dym, M.** Growth and characterization of polarized monolayers of epididymal epithelial cells and Sertoli cells in a dual environment culture chambers. *J. Androl.*, 7: 59-68; (1986).
9. **Cafilisch, C. R. and DuBose, T. D.** Direct evaluation of acidification by rat testis and epididymis: role of carbonic anhydrase. *Am. J. Physiol.*, 258: E143-E150; (1990b).
10. **Cafilisch, C. R. and DuBose, D. Jr** Effect of vasectomy on *in situ* pH in rat testis and epididymis. *Contraception*, 42:589-595; (1990a).
11. **Camatini, M., Franchi, E. and de Curtis, I.** Lack of correlation between "Sertoli tight junction" morphology and permeability properties in human germinal aplasia. *Electron. Microscopy*, 2: 438-439; (1980).
12. **Camatini, M., Franchi, E. and de Curtis, I.** Permeability to lanthanum of the blood testis barrier in human germinal aplasia. *Anat. Rec.*, 200: 293-297; (1981).

13. **Cavicchia, J. C. and Sacerdote, F. L.** Correlation between blood-testis barrier development and onset of the first spermatogenic wave in normal and in busulfan-treated rats: A lanthanum and freeze-fracture study. *Anat. Rec.*, 230:361-368; (1991).
14. **Cheung, Y. M., Hwang, J. C. and Wong, P. Y. D.** *In vitro* measurement of the secretory rate in isolated seminiferous tubules of rats. *J. Physiol.*, 254:17-19; ((1976).
15. **Chowdhury, A. K. and Steinberger, E.** A quantitative study on the effect of heat on the germinal epithelium of the rat testes. *Am. J. Anat.*, 115: 509; (1964).
16. **Clermont, Y.** Contractile elements in the limiting membrane of the seminiferous tubules of the rat. *Exp. Cell. Res.*, 15: 438-440; (1958).
17. **Clermont, Y. and Huckins, C.** Microscopic anatomy of the sex cords and the seminiferous tubules in growing and adult male albino rats. *Am. J. Anat.*, 108: 79-97; (1961).
18. **Cowles, R. B.** Hyperthermia, aspermia, mutation rates and evolution. *Quart. Rev. Biol.* 40: 341-67; (1965).
19. **Cuthbert, A. W. and Wong, P. Y. D.** Intracellular potentials in cells of the seminiferous tubules of rats. *J. Physiol.*, 248:173-191; (1975).

20. **Davidoff, M. S., Breuker, H., Holstein, A. F. and Siedl, K.** Cellular architecture of the lamina propria of human seminiferous tubules. *Cell Tissue Res.*, 262:253-261; (1990).
21. **De Bruyn, P. P. H., Robertson, R. C. and Farr, R. S.** *In vivo* affinity of deaminoacridine dyes for nuclei. *Anat. Rec.*, 108: 279-308; (1950).
22. **de Kretser, D. M. and Kerr, J. B.** The cytology of the testis. In: *The physiology of reproduction*. Edited by E. Knobil and J. Neill. Raven Press, New York, pp. 837-932; (1988).
23. **Djakiew, D. and Dym, M.** Pachytene spermatocytes influence Sertoli cell function. *Biol. Reprod.*, 39: 1193-1205; (1988).
24. **Djakiew, D., Hadley, M. A., Byers, S. W. and Dym, M.** Transferrin-mediated transcellular transport of ^{59}Fe across confluent sheets of Sertoli cells grown in bicameral culture chambers. *J. Androl.*, 7: 355-366; (1986).
25. **Dym, M. and Fawcett, D. W.** The blood-testis barrier in the rat and the physiological compartmentation of the seminiferous epithelium. *Biol. Reprod.*, 3:308-326; (1970).

26. **Dym, M., Hadley, M. A., Djakiew, D. and Byers, S. W.** The blood-testis barrier *in vitro*. In: *Development and function of the reproductive organs*. Edited by M. Parvinem, I. Huhtaniemi and L. J. Pelliniemi, *Serono Symposia, Review No 14*. Rome, pp. 113-126; (1988).
27. **Ehrenberg, L., Ehrenstein, G. von and Hedgram, A.** Gonad temperature and spontaneous mutation-rate in man. *Nature*, 180: 1433-4; (1957).
28. **Eusebi, F., Ziparo, E., Fratamico, G., Russo, M. A. and Stefanini, M.** Intercellular communication in rat seminiferous tubules. *Dev. Biol.*, 100:249-255; (1983).
29. **Faller, L. D., Smolka, A. and Sachs, G.** The gastric H⁺, and K⁺-ATPase. In: *The Enzymes of Biological Membranes*. Edited by A. N. Martonosi. Plenum Press, New York, vol. 3: 431-438; (1985).
30. **Fawcett, D. W.** Ultrastructure and function of the Sertoli cell. In *Handbook of Physiology, Male Reproductive System*, eds. D. W. Hamilton and R. O. Greep. American Physiology Society, Washington, D.C., section 7, vol.V, pp. 21-55; (1975).
31. **Fawcett, D. W., Leak, L. V. and Heidger, P. M.** Electron microscopic observations on the structural components of the blood-testis barrier. *J. Reprod. Fertil., Suppl.*, 10: 105-119; (1970).

32. **Fritz, I. B.** Sites of action of androgens and follicle stimulating hormone on cells of the seminiferous tubule. In: *Biochemical action of hormones*. Edited by G. Litwack. Academic Press, New York, vol. 5: 249; (1978).
33. **Frizzell, R. A., Smith, P. L., Vosburgh, E. and Field, M.** Coupled sodium-chloride influx across brush border of flounder intestine. *J. Membr. Biol.*, 46: 27-39; (1979).
34. **Fromter, E. and Diamond, J. M.** Route of passive ion permeation in epithelia. *Nature, Lond.*, 235, 9-13; (1972).
35. **Giebisch, G.** Renal potassium channels: An overview. *Kidney Int.*, 48:1004-1009; (1995).
36. **Gilula, N. B., Fawcett, D. W. and Aoki, A.** The Sertoli cell occluding junctions and gap junctions in mature and developing testes. *Dev. Biol.*, 50: 142-168; (1976).
37. **Gladwell, R. T.** The effect of temperature on the potential difference and input resistance of rat seminiferous tubules. *J. Physiol.*, 268: 111-121; (1977).
38. **Grasso, P. and Reichert, L. E.** Follicle-stimulating hormone receptor-mediated uptake of $^{45}\text{Ca}^{2+}$ by proteoliposomes and cultured rat Sertoli cells: evidence for involvement of voltage-dependent and voltage independent calcium channels.

- Endocrinology*, 125: 3029-3036; (1989).
39. **Gunsalus, G. L., Musto, N. A. and Bardin, C. W.** Bidirectional release of a Sertoli cell product, androgen binding protein, into the blood and seminiferous tubule. In: *Testicular Development, Structure and Function*, edited by A. Steinberger and E. Steinberger. Raven Press, New York, pp. 2291-2297; (1980).
40. **Gunsalus, G. L., Musto, N. A. and Bardin, C. W.** Factors affecting blood levels of androgen binding protein in the rat. *Int. J. Androl. (Suppl.)*, 2: 482-493; (1978).
41. **Hadley, M. A., Byers, S. W., Suarez-Quian, C. A., Kleineman, H. K. and Dym, M.** Extracellular matrix regulates Sertoli cell differentiation, testicular cord formation and germ cell development *in vitro*. *Cell Biol.*, 101: 1511-1522; (1985).
42. **Hagen, E. O.** The effect of subsequent fertility of temporary cryptorchidization in Swiss white mice. *Can. J. Zool.*, 49: 587-590; (1971).
43. **Harris, G. C. and Nicholson, H. D.** Stage differences in rat seminiferous tubule contractility *in vitro* and their response to oxytocin. *J. Endocrinol.*, 157(2) :251-257; (1998).

44. **Henning, R. D. and Young, J. A.** Electrolyte transport in the seminiferous tubules of the rat studied by the stopped-flow micro-perfusion technique. *Specialia*, 27: 1037-1039; (1971).
45. **Hinton, B. T., and Howards, S. S.** Rat testis and epididymis can transport [³H]3-O-methyl-D-glucose, [³H]inositol and [³H]α-aminoisobutyric acid across its epithelia *in vivo*. *Biol. Reprod.*, 27, 1181-1189; (1982).
46. **Hinton, B. T., White, R. W. and Setchell, B. P.** Concentrations of myo-inositol in the luminal fluid of mammalian testes and epididymis. *J. Reprod. Fertil.*, 58, 395-399; 1980.
47. **Hinton, B. T.** The testicular and epididymal luminal amino acid microenvironment in the rat. *J. Androl.*, 11:498-505; (1990).
48. **Humphries, M. H.** Inhibition of sodium chloride absorption from perfused rat ileum by furosemide. *Am. J. Physiol.*, 230: 1517-1523; (1976).
49. **Isaacson, L. and Nicolson, S.** A reappraisal of the oil-gap technique for the measurement of transtubular potentials in insect epithelia. *J. Exp. Biol.*, 141:429-440; (1989).

50. **Isaacson, L. C., Nicolson, S. W. and Fisher, D. W.** Electrophysiological and cable parameters of perfused beetle Malpighian tubules. *Am. J. Physiol.*, 257: R1190-R1198; (1989).
51. **Isaacson, L. C. and Nicolson, S. W.** Concealed transepithelial potentials and current rectification in tsetse fly Malpighian tubules. *J. Exp. Biol.*, 186:199-213; (1994).
52. **Janecki, A. Jakubowiak, A. and Steinberger, A.** Regulation of transepithelial electrical resistance in two-compartment Sertoli cell cultures: *In vitro* model of the blood-testis barrier. *Endocrinol.*, 129:1489-1496; (1991).
53. **Jégou, B.** The Sertoli cell. *Bailliere's Clinical Endocrinol. Metab.*, 6:273-311; (1992).
54. **Jégou, B., Le Gac, F. and De Kretser, D. M.** Seminiferous tubule fluid and interstitial fluid production. 1. Effects of age and hormonal regulation in immature rats. *Biol. Reprod.*, 27, 590-95; 1982.
55. **Jégou, B., Le Gac, F., Irby, D. C. and De Kretser, D. M.** Studies on seminiferous tubule fluid production in the adult rat: Effect of hypophysectomy and treatment with LH, FSH and testosterone. *Int. J. Androl.*, 6, 249-60; 1983.

56. **Jenkins, A. D., Lechene, C. P. and Howard, S. S.** Concentration of seven elements in the intraluminal fluids of the rat seminiferous tubules, rete testis, and epididymis. *Biol. Reprod.*, 23: 981-987; (1980).
57. **Jocelyn, H. D. And Setchell, B. P.** Regnier de Graaf on the human reproductive organs. An annotated translation of Tractatus de Virorum Organis Generationi Inservientibus (1668) and De mulierub Organis Generitioni Inservientibus Tractus Novus (1962). *J. Reprod. Fertil. (Suppl.)*, 17: 1-222; (1972).
58. **Kew, D. A., Muffly, K. E. and Hall, P. F.** Plasma membranes from rat Sertoli cells: purification and properties. *Biol. Reprod.*, 35: 1235-1247; (1986).
59. **Koeppen, B. M.** Electrophysiology of collecting duct H⁺ secretion: effect of inhibitors. *Am. J. Physiol.*, 246:F79-F84; (1989).
60. **Kormano, M.** Dye permeability and alkaline phosphatase activity of testicular capillaries in the postnatal rat. *Histochemie*, 9, 327-338; 1967.
61. **Kormano, M.** Penetration of intravenous trypan blue into the rat testis and epididymis. *Acta. Histochem.*, 30: 133-136; (1968).
62. **Kormano, M. and Hovatta, O.** Contractility and histochemistry of the myoid cell layer of the rat seminiferous tubules during postnatal development. *Z. Anat. Entwickl.*, 137: 239-248; (1972).

63. **Lapointe, J-Y., Laprade, R. and Cardinal, J.** Transepithelial and cell membrane electrical resistances of the rabbit proximal convoluted tubule. *Am. J. Physiol.*, 247: F637-F649; (1984).
64. **Leblond, C. P. and Clermont, Y.** Definition of the stages of the cycle of the seminiferous epithelium in the rat. *Ann. N.Y. acad. Sci.*, 55:548-573.; (1952).
65. **Levine, N. and Marsh, D. J.** Micropuncture study of the fluid composition of 'Sertoli cell-only' seminiferous tubules in rats. *J. Reprod. Fertil.*, 43(3): 547-49; (1975).
66. **Levine, N. and Marsh, D. J.** Micropuncture studies of the electrochemical aspects of fluid and electrolyte transport in individual seminiferous tubules, the epidymis and the vas deferens in rats. *J. Physiol.*, 213:557-570; (1971).
67. **Lian, G. and Enders, G. C.** Entactin ultrastructural immunolocalization in the basal laminae of mouse seminiferous tubules and with only subtle changes following hypophysectomy. *J. Androl.*, 15:52-60; (1994).
68. **Lindner, H. R.** Partition of androgen between the lymph and venous blood of the testis in the ram. *J. Endocr.*, 25: 483-494; (1963).
69. **Liptrap, R. M. and Raeside, J. I.** Urinary steroid excretion in cryptorchidism in the pig. *J. Reprod. Fertil.* 21, 293-301; 1970.

70. **Lutz, M. D., Cardinal, J. and Burg, M. B.** Electrical resistance of renal proximal tubule perfused *in vitro*. *Am. J. Physiol.*, 225: 729-734; (1973).
71. **Maekawa, M. Ngano, T. and Murakami, T.** Comparison of actin-filament bundles in myoid cells and Sertoli cells of the rat, golden hamster and mouse. *Cell Tissue Res.*, 275: 395-398; (1994).
72. **Mattmueller, D. R. and Hinton, B. T.** *In vivo* secretion and association of clusterin (SGP-2) in luminal fluid with spermatozoa in the rat testis and epididymis. *Mol. Reprod. Development*, 30:62-69; (1991).
73. **Meyer, R. Posalaky, Z. and McGinley, D.** Intercellular junction development in maturing rat seminiferous tubules. *J. Ultrastr. Res.*, 61: 271-283; (1977).
74. **Muffly, K. E. and Hall, P. F.** Vectorial (transcellular) transport of potassium ($^{86}\text{Rb}^+$) by cultured Sertoli cells. *Endocrinol.*, 123: 2083-2088; (1988).
75. **Muffly, K. E., Turner, T. T., Brown, M. and Hall, P. F.** Content of K^+ and Na^+ in seminiferous tubule and rete testis fluids from Sertoli cell-enriched testes. *Biol.Reprod.*, 33: 1245-1251; (1985).
76. **Nicander, L.** An electron microscopical study of cell contacts in the seminiferous tubules of some animals. *Z. Zellforsch. Mikroskop. Anat.*, 83: 375-97; (1967).

77. **Nicolson, S. W. and Isaacson, L. C.** Transepithelial and intracellular potentials in isolated Malpighian tubules of tenebrionid beetle. *Am. J. Physiol.*, 252: F1-F9; (1987).
78. **Niemi, M. and Kormanio, M.** Contractility of the seminiferous tubule of the postnatal rat testis and its response to oxytocin. *Ann. Med. Exp. Fenn.*, 43: 40-2; (1965).
79. **O'Donnell, M. J. and Maddrell, H. P.** Secretion by the Malpighian tubules of *rhodius prolixus stal*: Electrical events. *J. Exp. Biol.*, 110: 275-290; (1984).
80. **Onada, M., Suarez-Quain, C. A., Djakiew, D. and Dym, M.** Characterization of Sertoli cells cultured in bicameral chamber system: relationship between formation of permeability barriers and polarized secretion of transferrin. *Biol. Reprod.*, 43: 672-683; (1990).
81. **Orth, J. and Christensen, A. K.** Localization of ¹²⁵I-labelled FSH in the testis of hypophysectomized rats by autoradiography at the light and electron microscope levels. *Endocrinology*, 101: 262-278; (1977).
82. **Palfrey, H. C. and Rao, M. C.** Na/K/Cl co-transport and its regulation. *J. Exp. Biol.*, 106: 43-54; (1983).

83. **Parker, J. C.** Dog red cells: adjustment of salt and water content *in vitro*. *J. Gen. Physiol.*, 62: 147-156; (1973).
84. **Parvinen, M., Hurme, P. and Niemi, M.** Penetration of exogenous testosterone, pregnenolone, progesterone and cholesterol into the seminiferous tubules of the rat. *Endocrinol.*, 87: 1082-1084; (1970).
85. **Pelletier, R-M and Byers, S. W.** The blood-testis barrier and Sertoli cell junctions: Structural considerations. *Micrsc. Res. Tec.*, 20:3-33; (1992).
86. **Piana, G. P. and Savarese, G.** Su Alcuni studii anatomo-patologici. *La Clinica Veterinaria*, 14: 50-51; (1891).
87. **Ramsay, J. A.** Active transport of water by the Malpighian tubules of the stick insect, *Dixippus morosus* (*Orthoptera, Phasmidae*). *J. Exp. Biol.*, 31: 104-113; (1954).
88. **Raychoudhury, S. S. ,Blackshaw, A. W. and Irving, M. G.** Hormonal modulation of the interactions of cultured rat testicular Sertoli and peritubular myoid cells. *J. Androl.*, 14:9-16; (1993).
89. **Reisen, I. and Cereijido, M.** Na fluxes in single, isolated seminal tubules of the rat. *Biophysical J.*, 9:164; (1969).

90. **Ritzen, E. M., Boitani, C., Parvinen, M., French, F. C. and Feldman, M.** Stage-dependent secretion of ABP by rat seminiferous tubules. *Mol. Cell Endocrinol.*, 25(1): 25-33, (1982).
91. **Roche, A. and Joffre, M.** Effect of uncoupling treatments on FSH-induced hyperpolarization of immature rat Sertoli cells from Sertoli cell-enriched cultures. *J. Reprod.*, 85:343-354; (1989).
92. **Roosen-Runge, E. C.** Motions of the seminiferous tubules of rat and dog. *Anat. Rec.*, 109, 413; (1951).
93. **Russel, L. D., Bartke, A., Goh, J. C.** Postnatal development of the Sertoli cell barrier, tubular lumen, and cytoskeleton of Sertoli and myoid cells in the rat, and their relationship to tubular fluid secretion. *American J. Anat.*, 184: 179-189; (1989).
94. **Russell, L. D. and Steinberger, A.** Sertoli cells in culture: Views from the perspectives of an vivoist and an in vitroist. *Biol. Reprod.*, 41:571-577; (1989).
95. **Setchel, B. P.** The secretion of fluid by the testis of rats, rams, and goats with some observations on the effect of age, cryptorchidism and hypophysectomy. *J. Reprod. Fertil.*, 23: 79-85; (1970).

96. **Setchell, B. P. and Main, S. J.** The blood-testis barrier and steroids. *Curr. Top Molec. Endocrinol.*, 2: 223-233.; (1975).
97. **Setchell, B. P. and Waites, G. M. H.** The effects of local heating of the testis on the flow and composition of the rete testis fluid in the rat, with some observations on the effects of age and unilateral castration. *J. Reprod. Fertil.*, 20, 225-233; (1972).
98. **Setchell, B. P., Davies, R. V., Gladwell, R. T., Hinton, B. T., Main, S. J., Pilsworth, L. and Waites, G. M. H.** The movement of fluid in the seminiferous tubules and rete testis. *Ann. Biol. Anim. Biochim. Biophys.*, 18: 623-632; (1978).
99. **Setchell, B. P., Duggan, M. C. and Evans, R. W.** The effects of gonadotrophins on fluid secretion and production of spermatozoa by the rat and hamster testis. *J. Endocrin.*, 56: 27-36; (1973).
100. **Setchell, B. P., Hinton, B. T., Jacks, F. and Davies, R. V.** Restricted penetration of iodinated follicle-stimulated and luteinizing hormone into the seminiferous tubules of the rat testis. *Mol. Cell. Endocrinol.*, 6: 59-69; (1976).
101. **Setchell, B. P., Pollanen, P. and Zupp, J. L.** Development of the blood testis barrier and changes in the vascular permeability at puberty in rats. *Int. J. Androl.*, 11: 225-233; (1988).

102. **Setchell, B. P.** The functional significance of the blood-testis barrier. *J. Androl.*, 1:3-10; (1979).
103. **Setchell, B. P.** The Mammalian Testis *Reprod. Biol. Handbooks*, Edited by C. A. Finn, pp. 1-379; (1978).
104. **Setchell, B. P. and Brookes, D. E.** Anatomy, vasculature, innervation and fluids of the male reproductive tract. *Physiol.Reprod.*, 753-836; (1988).
105. **Setchell, B. P. and Waites, G. M. H.** The blood-testis barrier. *Handbook of physiology - Endocrinol. V*, 143-159; (1975).
106. **Setchell, B. P., Hinks, N T., Voglmayr, J K., Scott, T W.** Amino acids in ram testicular fluid and semen and their metabolism by spermatozoa. *Biochem.J.*, 106: 1061-1065; (1967).
107. **Sharpe, R. M., Maddocks, S., Millar, M., Kerr, J. B., Saunders, P. T. K. and Mckinnell, C.** Testosterone and spermatogenesis. Identification of stage-specific, androgen-regulated proteins secreted by adult rat seminiferous tubules. *J. Androl.*, 13:172-184; (1992).
108. **Shibata, E. F., Matsuda, J. J., Volk, K. A., Collison, K. A. and Segaloff, D. L.** Evidence that the FSH receptor itself is not a calcium channel. *Endocrinol.*, 131: 979-981; (1992).

109. **Skinner, M. K. and Fritz, I. B.** Testicular peritubular cells secrete a protein under androgen control that modulates Sertoli cell function. *Proc. Natl. Acad. Sci. USA*, 82: 114-118; (1985).
110. **Slyvester, S. R. and Griswold, M. D.** Localization of transferrin and transferrin receptors in the rat testes. *Biol. Reprod.*, 31: 195-203; (1984).
111. **Sun, E. L. and Gondos, B.** Formation of the blood-testis barrier in the rabbit. *Cell Tissue Res.*, 243: 575-578; (1986).
112. **Szollosi, A. and Marcaillou, C.** Electron microscope study of the blood-testis barrier in an insect *locusta migratoria*. *J. Ultrastruct. Res.*, 59: 158-172; (1977).
113. **Tindale, D. J., Vitale, R. and Means, A. R.** Androgen binding protein as a biochemical marker of formation of the blood-testis barrier. *Endocrinology*, 97: 636-648; (1975).
114. **Tuck, R. R., Setchell, B. P. and Waites, G. M. H.** The composition of fluid collected by micropuncture and catheterization from the seminiferous tubules and rete testis of rats. *Pflugers Arch.*, 318:225-243; (1970).
115. **Tung, P. S. and Fritz, I. B.** Sertoli cells in culture secrete paracrine factor(s) that inhibit peritubular myoid cell Proliferation: Identification of heparinoids as likely candidates. *J. Cell. Physiol.*, 147:470-478; (1991).

116. **Turner, T. T.** Transepithelial movement of ^3H -Androgen in seminiferous and epididymal tubules: a study using *in vivo* micropuncture and *in vivo* microperfusion. *Biol. Reprod.*, 39:399-408; (1988).
117. **Turner, T. T., Jones, C. E., Howards, S. S., Ewing, L. L., Zegeye, B. and Gunsalus, G. L.** On the androgen microenvironment of maturing spermatozoa. *Endocrinol.*, 115:1925-1932; (1984).
118. **Ussing, H. H. and Zerahn, K.** Active transport of sodium as the source of electric current in the short-circuited isolated frog skin. *Acta Phys. Scandinav.*, 23: 110-127; (1951).
119. **Vitale, R., Fawcett, D. W. and Dym, M.** The normal development of the blood-testis barrier and the effects of clomiphene and estrogen treatment. *Anat. Rec.*, 176: 333-344; (1973).
120. **Vogl, A. W. and Soucy, L. J.** Arrangement and possible function of actin filament bundles in ectoplasmic specializations of ground squirrel Sertoli cells. *J. Cell. Biol.*, 100: 814-825; (1985).
121. **Waites, G. M. H.** Temperature regulation and the testis. *In: The Testis. Edited by A. D. Johnson, W. R. Gnomes and N. L. Van Demark, London: Academic Press, vol. 1: 241-279; (1970).*

122. **Waites, G. M. H.** Temperature regulation and fertility in male and female mammals. *Israel J. Med. Sci.*, 9: 982-93; (1976).
123. **Waites, G. M. H. and Gladwell, R. T.** Physiological significance of fluid secretion in the testis and the blood-testis barrier. *Physiol. Rev.*, 62, 624-671; (1982).
124. **Waites, G. M. H. and Setchell, B. P.** Some physiological aspects of the function of the testis. In: *The Gonads, edited by K.W. McKerns. Appleton-Century-Crofts, New York, pp. 649-714; (1969).*
125. **Wassermann, G. F., Monti Bloch, L., Grillo, M. L., Silva, F. R. M. B. Loss, E. S. and McConnell, L. L.** Electrophysiological changes of Sertoli cells produced by the acute administration of amino acid and FSH. *Horm. Metab. Res.*, 24: 326-328; (1992).
126. **Weisbren, S. J., Geibel, J., Boron, W. F. and Modlin, I. M.** Luminal perfusion of isolated gastric glands. *Am. J. Physiol.*, 266: C1013-C1027; (1994).
127. **Wing, T-Y. and Christensen, A. K.** Morphometric studies on the rat seminiferous tubules. *Am. J. Anat.*, 165: 13-25; (1982).
128. **Wooley, P.** The seminiferous tubules in Dasyurid marsupials. *J. Reprod. Fertil.*, 45, 255-261; (1975).

129. **Yamamoto, M., Nagai, T. and Miyake, K.** Different mechanisms are involved in ^3H hydrogen uptake by the rat seminiferous and epididymal tubules *in vivo*. *Nagoya J. Med. Sci.*, 53: 33-41; (1991).
130. **Zwain, I. H., Grima, J., Stahler, M. S., Saso, L., Cailleau, J., Verhoeven, G., Bardin, C. W. and Cheng, C. Y.** Regulation of Sertoli cell α -2-Macroglobulin and clusterin (SGP-2) secretion by peritubular myoid cells. *Biol. Reprod.*, 48: 180-187; (1993).



UNIVERSITY *of the*
WESTERN CAPE

Appendix A

The information in this appendix has been included in this dissertation solely to clarify the procedures of the micropuncture technique, which has been widely used to obtain information pertaining to the functioning of the seminiferous tubules. For an in-depth discussion and criticism of the micropuncture and microperfusion techniques see Hinton and Howards, 1982.

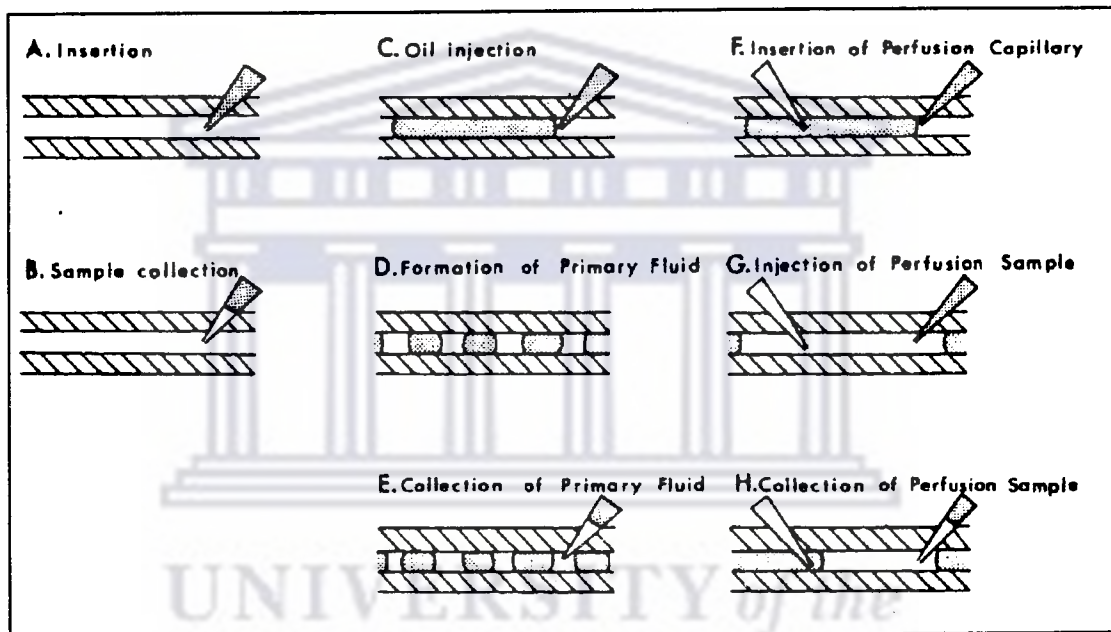


Figure A1: A diagram of the techniques used in the micropuncture of the seminiferous tubules. A. Insertion of oil-filled micropipette into seminiferous tubule. B. Withdrawal of sample. C. Injection of column of oil into seminiferous tubule. D. Formation of primary fluid by the cells lining the tubule, so that the oil column is broken up by droplets of aqueous fluid. E. This primary fluid can be sampled by introducing another micropipette into a droplet. F, G and H. Microperfusion of a length of seminiferous tubule: this is first filled with oil, which is then broken by a length of injected aqueous fluid of any chosen composition. At various times, portions of this fluid can be withdrawn for analysis. (See Tuck *et. al.*, 1970; Henning and Young, 1971). Taken from Setchell, 1978.

Appendix B

The data in the table below has been included to supplement the cable data reported in the current study. These current pulses have injected in control perfused tubules. Furthermore, if the changes in voltage at the distal end of the tubule was too small, increasing the magnitude of the current pulse improved the resolution.

Effects of current injection (nAmps)			
Current pulse injected	n	Proximal voltage jump (mV)	Distal voltage jump (mV)
100	4	17.1±4.8	4.4±1.5
120	1	25.5	2.5
150	2	22.45±1.9	3.3±2.2
200	7	29.7±3.5	6.9±4.1

Table A1: The above table shows the effects of 200 ms pulses of current (nAmps) on the voltage jumps (mV) at the proximal and distal ends of the perfused tubule. These changes in potential are used in cable formulae to calculate the transepithelial resistance of the seminiferous tubule.

UNIVERSITY of the
WESTERN CAPE